

On Residual Minimization for PDEs: Failure of PINN, Modified Equation, and Implicit Biase

Tao Luo^{1,2}, Qixuan Zhou^{1,*}

¹ *School of Mathematical Sciences, Shanghai Jiao Tong University, Shanghai, 200240, China.*

² *Institute of Natural Sciences, CMA-Shanghai, MOE-LSC and Qing Yuan Research Institute, Shanghai Jiao Tong University, Shanghai, 200240, China*

Received 12 August 2025

Abstract. As a popular and easy-to-implement machine learning method for solving differential equations, the physics-informed neural network (PINN) sometimes may fail and find poor solutions which bias against the exact ones. In this paper, we establish a framework of modified equation to explain the failure phenomenon and characterize the implicit bias of a general residual minimization (RM) method. We provide a simple way to derive the modified equation which models the numerical solution obtained by RM methods. Next, we show the modified solution deviates from the original exact solution. The proof uses a by-product of this paper, that is, a necessary and sufficient condition on characterizing the singularity of the coefficients. This equivalent condition can be extended to other types of equations in the future. Finally, we prove, as a complete characterization of the implicit bias, that RM method implicitly biases the numerical solution against the exact solution and towards a modified solution. In this work, we focus on elliptic equations with discontinuous coefficients, but our approach can be extended to other types of equations and our understanding of the implicit bias may shed light on further development of deep learning based methods for solving equations.

AMS subject classifications: 35D30, 35D35, 35R05, 35R06, 65N15

Key words: residual minimization, PINN, implicit bias, modified equation.

*Corresponding author.

Emails: luotao41@sjtu.edu.cn (T. Luo), zhouqixuan@sjtu.edu.cn (Q. Zhou)

1 Introduction

The application of machine learning, particularly deep neural networks (DNNs), has gained significant attention in recent years for solving partial differential equations (PDEs) [1–7]. Compared with traditional numerical schemes, such as finite difference, finite element methods, and spectral methods, which are often limited by the “curse of dimensionality,” DNNs have demonstrated success in solving many high-dimensional problems [8]. Although the traditional numerical methods are powerful for low-dimensional problems, it can be challenging to design a proper scheme to solve low-dimensional problems with low-regularity solutions or boundaries [9–14]. Therefore, DNNs are also promising in solving low-dimensional problems with low-regularity solutions or complex boundaries, such as problems with discontinuous elastic or dielectric constants in composite materials.

A widely used approach to solving PDEs is to utilize DNNs to parameterize the solution and optimize the parameters in an objective function, which is usually formulated as a least-squares or variational loss function (also known as a risk function). The physics-informed neural network (PINN) method was first proposed in the 1990s [15], later studied by Sirignano and Spiliopoulos under the name Deep Galerkin Method (DGM) [16], and popularized as PINN by Raissi et al. [6]. In this method, a DNN is trained to minimize the sum of the residuals of the PDE and the boundary condition. The Deep Ritz Method (DRM) [1] instead adopts a variational formulation, minimizing an energy functional. Many other approaches have also been proposed for solving PDEs with neural networks [17–19]. For further advances in PINN, we refer readers to the review articles [20, 21] and the references therein.

For completeness, we also mention that operator learning has shown promise in solving both forward and inverse PDE problems [22–25]. Despite this growing diversity, PINN has received particular attention due to its simplicity and ease of implementation: its risk function is merely the residual of the PDE and boundary conditions, without requiring the variational form needed in DRM, which is often unavailable in practical applications.

A theoretical study of DNNs is crucial for understanding and improving PDE solvers based on neural networks. For instance, the universal approximation theorem [26] guarantees the ability of wide networks to approximate continuous functions. Subsequent works have extended this by quantifying approximation rates [49], and analyzing PINN approximation errors in the case of smooth elliptic problems [27]. Several studies have derived generalization bounds under strong regularity assumptions [28–31], supporting convergence results when the solution is smooth and the network is sufficiently expressive.

However, many real-world PDEs involve solutions of low regularity, due to discontinuities in coefficients or domain geometry, etc. Several recent studies have investigated

the failure modes of physics-informed neural networks (PINNs) from a numerical optimization perspective. For example, Basir [32] identifies challenges such as gradient contamination due to high-order derivatives, sensitivity to regularization parameters, and data scarcity in forward problems, which together contribute to poor trainability and instability in classical PINNs. To mitigate these issues, the author proposes a dual unconstrained formulation that avoids higher-order derivatives and enhances convergence. Similarly, Krishnapriyan et al. [33] systematically categorized potential failure modes in PINNs, highlighting the non-convexity of the loss landscape and the complexities in optimization paths. They proposed strategies like curriculum regularization and sequence-to-sequence learning to improve training stability and accuracy.

In contrast, our work investigates a distinct but equally fundamental issue: can residual minimization (RM)-based methods fail to approximate the correct solution even when training succeeds? We establish a theoretical framework showing that, for PDEs with discontinuous or low-regularity coefficients, RM-based methods are structurally biased toward solving a *modified equation*. This phenomenon arises not from numerical instability, but from an inherent limitation in the RM formulation itself.

As low-regularity problems offer a potential application for DNNs, we focus on the use of neural networks with least-squares risk functions to solve linear PDEs whose solutions exhibit low regularity. This is a challenging regime due to several factors. First, the true solution is often less regular because of discontinuous coefficients. Second, the function space represented by neural networks is typically more regular than the true solution, owing to the derivatives involved in training. Third, the risk function is only defined via discrete sampling, which further complicates the analysis.

We begin with 1D numerical experiments using PINNs and then develop a continuum model to explain the observed behaviors. Empirically, for elliptic equations with discontinuous coefficients, the learned solution consistently deviates from the exact one. With strong numerical evidence, we model this output as a solution to a modified PDE, which we derive heuristically. We then rigorously prove that such deviation is not an artifact of training, but a generic outcome under mild assumptions. Moreover, we derive necessary and sufficient conditions for this discrepancy to occur, and prove that even starting from an excellent initialization, training drives the solution toward the biased one.

This form of failure is independent of neural network architecture and applies to any residual-minimization (RM) method, including but not limited to PINNs. In this regard, our results fundamentally differ from earlier works that rely on high regularity to prove convergence as network size and sample number increase [28–30, 34]. We emphasize that even under perfect optimization, a gap persists between the true solution and the limit of RM training. This reveals a theoretical obstruction—distinct from trainability issues—and demonstrates that residual minimization can *structurally bias* the solution.

While several PINN variants (e.g., curriculum-training-based strategy [35], adaptive

sampling [36]) aim to improve empirical performance, they remain within the RM paradigm. Our findings suggest that these improvements, while useful, cannot overcome the fundamental bias present when dealing with low-regularity PDEs.

We believe this failure phenomenon is known to some extent among practitioners and has motivated partial solutions. For example, the first-order system least-squares (FOSLS) formulation [37] recasts elliptic PDEs into equivalent systems that may avoid this bias; alternatively, DRM can yield accurate results when a variational structure is available. However, the mechanisms behind this failure remain poorly understood. Our primary contribution is to build a rigorous theoretical foundation that identifies conditions under which RM fails, quantifies the error, and characterizes the function space of “bad” residuals that induce this behavior.

In summary, while prior works aim to improve the *trainability* of RM methods by addressing numerical and algorithmic challenges, our study addresses their *representational correctness* by identifying structural limitations in the learning objective. Both perspectives are essential: one highlights practical barriers to convergence, and the other reveals theoretical obstructions to correctness—even under perfect optimization. Together, they form a unified picture of the challenges inherent to residual minimization frameworks.

The remainder of this paper is organized as follows. Section 2 provides a brief introduction to PINNs and illustrates the failure phenomenon with numerical examples. In Section 3, we summarize our main theoretical contributions and provide a roadmap for the reader. Section 4 develops a theory of removable singularities in BV-type equations. Section 5 proves that deviation from the true solution is generic and rooted in the RM formulation. In Section 6, we provide a numerical method by relaxation on the regularity constraint to mitigate the known issue. The appendix contains standard definitions and references for elliptic equations. While we focus on linear problems here, the ideas can naturally extend to quasilinear cases [38].

2 Preliminaries

We begin this preliminary section by introducing basic concepts of deep neural networks and deep learning based methods for solving PDEs, in particular, the method of physics-informed neural networks (PINN). Next, by a one-dimensional example, we illustrate that PINN can fail even in an extremely simple situation. The last subsection is left to depict the general setting, namely the linear elliptic equations and systems with BV coefficients, under which we will derive a continuum model for the numerical solution and thus prove theorems based on this model.

2.1 Deep neural networks (DNN)

An L -layer fully-connected neural network function $u_\theta : \mathbb{R}^d \rightarrow \mathbb{R}^{d'}$ is defined as for each $x \in \mathbb{R}^d$

$$u_\theta(x) = W^{[L-1]} \sigma(W^{[L-2]} \sigma(\dots (W^{[1]} \sigma(W^{[0]}x + b^{[0]} + b^{[1]}) \dots) + b^{[L-2]}) + b^{[L-1]}, \quad (2.1)$$

where the matrix $W^{[l]} \in \mathbb{R}^{m_{l+1} \times m_l}$ and the vector $b^{[l]} \in \mathbb{R}^{m_{l+1}}$ are called parameters, $m_l \in \mathbb{N}^+$ is the width of the l -th layer, and the (nonlinear) function $\sigma : \mathbb{R} \rightarrow \mathbb{R}$ is known as the activation function. With a little bit abuse of notation, σ applied on a vector means entry-wise operation, namely $(\sigma(z))_i = \sigma(z_i)$ for any subscript i . The matrices are usually reshaped and concatenated into a column vector θ , that is, $\theta = \text{vec}(\{W^{[l]}\}_{l=0}^{L-1}, \{b^{[l]}\}_{l=0}^{L-1})$. Note that the input dimension $d = m_0$ and the output dimension $d' = m_L$.

2.2 Residual minimization (RM) and physics-informed neural networks (PINN)

In our numerical experiments to be presented in the next subsection, the PINN is used to solve a given boundary value problem (BVP) of a PDE. We emphasize that the phenomenon recognized and analyzed in this work will remain the same if we replace the PINN by any other residual minimization method. Here the residual of an equation refers to the difference between the left-hand-side and the right-hand-side, and we say residual minimization because these PINN type methods follow a common approach, that is, minimizing the residual risk of both the PDE and boundary conditions. The term residual minimization is also used by other researchers, for example, [39]. Besides, some works refer the PINN to the least-squares method, for example, [37].

For a given function w , a residual minimization method for solving (the BVP of) an equation is to minimize the following population risk

$$R(w) = \int_{\Omega} (Lw - f)^2 dx + \gamma \int_{\partial\Omega} (Bw - g)^2 dx. \quad (2.2)$$

Here L is the differential operator, B is the boundary condition operator, and f (respectively, g) is a given function defined in the interior (respectively, on the boundary) of the domain Ω . The factor γ is the weight for adjusting the importance of the boundary constraints versus the one in the interior of the domain. But in practical applications, one

often uses the empirical risk (also known as the objective function in optimization) as:

$$R_S(w) = R_{S,\text{int}}(w) + \gamma R_{S,\text{bd}}(w) \quad (2.3)$$

$$R_{S,\text{int}}(w) = \frac{|\Omega|}{n_{\text{int}}} \sum_{x \in S_{\text{int}}} (Lw(x) - f(x))^2 \quad (2.4)$$

$$R_{S,\text{bd}}(w) = \frac{|\partial\Omega|}{n_{\text{bd}}} \sum_{x \in S_{\text{bd}}} (Bw(x) - g(x))^2, \quad (2.5)$$

where $R_{S,\text{int}}(w)$ is the interior empirical risk, $R_{S,\text{bd}}(w)$ is the boundary empirical risk, $n_{\text{int}} \in \mathbb{N}^+$ and $n_{\text{bd}} \in \mathbb{N}^+$ are the numbers of samples in the interior dataset S_{int} and the boundary dataset S_{bd} , respectively; $|\Omega|$ and $|\partial\Omega|$ are the Lebesgue measure \mathcal{L}^d of Ω and Hausdorff measure \mathcal{H}^{d-1} of $\partial\Omega$, respectively.

In general, it is recognized that the physics loss and boundary loss typically operate at different scales, and thus selecting an appropriate weighting parameter γ in the objective function (Equation (2.3)) is indeed meaningful. In our numerical experiments, we set $\gamma = 1$ for simplicity. Nevertheless, as demonstrated in the following numerical results, the boundary conditions are approximated very well with negligible errors.

It is important to emphasize that the main focus of this work lies in investigating the structural bias inherent to the residual minimization (RM) formulation itself. To clearly isolate and highlight this intrinsic issue, our theoretical analysis explicitly assumes a perfect fit on the boundary, meaning that the numerical solution coincides exactly with the true solution at boundary points (zero boundary residual). Even under this ideal scenario of perfect boundary fitting, a deviation between the numerical and exact solutions is still observed, further underscoring the inherent limitation of the RM formulation.

In the method of PINN, the output is a neural network and denoted by $u_\theta(x)$. Thus we usually abuse notation and write

$$R(\theta) = R(u_\theta) = \int_{\Omega} (Lu_\theta(x) - f(x))^2 dx + \gamma \int_{\partial\Omega} (Bu_\theta(x) - g(x))^2 dx. \quad (2.6)$$

Similarly, for empirical risks, we write $R_S(\theta) = R_S(u_\theta)$, $R_{S,\text{int}}(\theta) = R_{S,\text{int}}(u_\theta)$, and $R_{S,\text{bd}}(\theta) = R_{S,\text{bd}}(u_\theta)$.

Given an initial parameter θ_0 , then the parameters will be updated by first order optimization methods such as the gradient descent which is the forward Euler scheme of the (negative) gradient flow with step size Δt (also known as the learning rate) as follows

$$\theta_{k+1} = \theta_k - \Delta t D_\theta R_S(\theta_k). \quad (2.7)$$

The samples S can be chosen as quadrature method in low dimensions, say no larger than three, while it can be chosen randomly as Monte Carlo sampling method in any dimensions including very high-dimension cases. In implementation, the sample S can vary from one iteration to another.

2.3 Numerical example: failure of PINN

In this subsection, we demonstrate that using PINN to solve PDEs which has no strong (or classical) solutions could be problematic and cause a non-infinitesimal error. This is illustrated by a one-dimensional example via numerical experiments. Although the example is simple, it provides us correct and insightful intuition. Throughout this work, we will revisit this example several times and explain new understanding with our theorems to be proved in later sections. We also emphasize that this kind of failure of PINN in learning the solution to certain PDE is essential and usually can not be resolved by merely selecting the network architecture, adjusting the optimization algorithm, or tuning hyperparameters of the network.

Let us first briefly mention the setup of the experiment.

Problem setup. The considered equation is one-dimensional and reads as

$$\begin{cases} Lu = -D_x(AD_xu) = f & \text{in } \Omega = (-1, 1), \\ u = 0 & \text{on } \partial\Omega = \{-1, 1\}, \end{cases} \quad (2.8)$$

where the coefficient function A and the interior data f in (2.8) are both piece-wise continuous and read as

$$A(x) = \begin{cases} \frac{1}{2}, & x \in (-1, 0), \\ 1, & x \in [0, 1), \end{cases} \quad f(x) = \begin{cases} 0, & x \in (-1, 0), \\ -2, & x \in [0, 1). \end{cases} \quad (2.9)$$

Exact solution. Clearly, there is no strong (or classical) solution, while the weak solution $u \in H^1((-1, 1))$ to this equation is

$$u(x) = \begin{cases} -\frac{2}{3}x - \frac{2}{3}, & x \in (-1, 0), \\ x^2 - \frac{1}{3}x - \frac{2}{3}, & x \in [0, 1). \end{cases} \quad (2.10)$$

Neural network setup. In the series of numerical experiments, we use a 1-256-256-256-1 residual network (ResNet) [40]. The empirical risk, interior empirical risk, and boundary empirical risk for a given function w read as

$$\begin{aligned} R_S(w) &= R_{S,\text{int}}(w) + \gamma R_{S,\text{bd}}(w), \\ R_{S,\text{int}}(w) &= \frac{|\Omega|}{n_{\text{int}}} \sum_{x \in \mathcal{S}_{\text{int}}} [D_x(A(x)D_xw(x)) + f(x)]^2, \\ R_{S,\text{bd}}(w) &= \frac{|\partial\Omega|}{n_{\text{bd}}} [(w(-1))^2 + (w(1))^2], \end{aligned}$$

where we use $|\Omega| = 2$, $|\partial\Omega| = 2$, $n_{\text{bd}} = 2$, and $\gamma = 1$ in the experiments. We choose 1000 uniformly-sampled points in the interior of the region (namely $n_{\text{int}} = 1000$). We use “tanh” activation function, Adam optimizer, and the Xavier initialization, where the variance of each entry of $W^{[l]}$ is $\frac{2}{m_{l-1}+m_l}$ and m_l represents the width of l -th layer.

Under the above setting, we obtain the network function u_θ numerically via the PINN (or more generally the RM method) after training process. This solution u_θ will be called the RM solution to the original equation. We stress that the PINN as one realization of the RM method, is not essential and can be replaced by any other RM method. In practice, u_θ is obtained when the risk function R_S is small and does not decay anymore along the training. We plot the RM solution u_θ and compare it with u in Figure 1 (a). Obviously, the RM method fails to find the exact solution u . The gap between u and u_θ is as large as magnitude of u . Thus we call this phenomenon the failure of RM method (or failure of PINN). By the way, we also notice that the first order derivative of u_θ seems to be piecewisely parallel to that of u (see Figure 1 (b)). This suggests us to focus on the derivatives and regularity of the solutions.

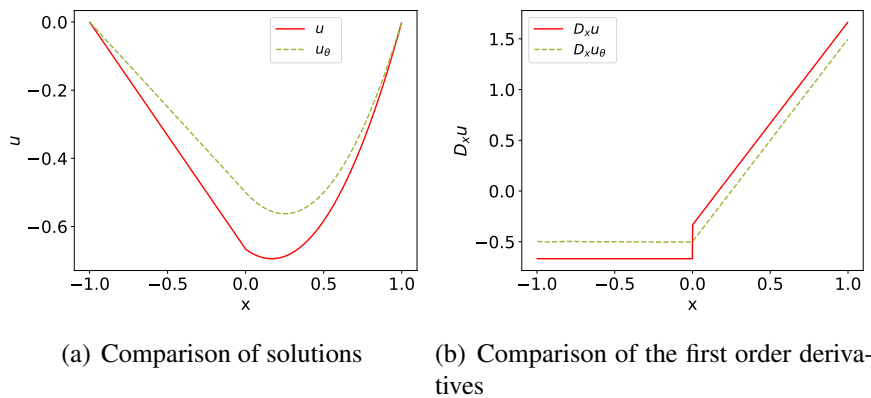


Figure 1: PINN cannot find the exact solution to equation (2.8) with the coefficient function given by (2.9).

The solution u at all points except for $x = 0$ is smooth (even in C^∞ locally), while the first order derivative of the solution u at $x = 0$ has a jump. Therefore, whether $x = 0$ contributes in the numerical method is decisive. Here comes the key observation that in practical experiments the $x = 0$ point can only be sampled with nearly zero probability as long as the distribution for sampling is absolutely continuous with respect to the Lebesgue measure. Hence the point $x = 0$ almost never contributes to numerical experiments! By the product rule, it holds that $D_x(AD_x u) = AD_x^2 u + (D_x A)D_x u$ on $(-1, 1) \setminus \{0\}$. Since the derivative $D_x A(x) = 0$ for the piece-wise constant function A and for all $x \in (-1, 1) \setminus \{0\}$, the left-hand-side of the PDE is effectively equal to $AD_x^2 u$ on the whole interval $(-1, 1)$. Therefore, in the numerical experiments, the empirical risk function equals to an effective

empirical risk function with probability nearly one, namely

$$R_S(u_\theta) = \tilde{R}_S(u_\theta), \tag{2.11}$$

where the latter at a given function w reads as

$$\tilde{R}_S(w) = \frac{2}{n_{\text{int}}} \sum_{x \in \mathcal{S}_{\text{int}}} (A(x)D_x^2 w(x) + f(x))^2 + \gamma[(w(-1))^2 + (w(1))^2]. \tag{2.12}$$

This effective empirical risk function is in turn the empirical risk function of the RM method for the modified equation

$$\begin{cases} \tilde{L}\tilde{u} = -AD_x^2\tilde{u} = f & \text{in } \Omega = (-1, 1), \\ \tilde{u} = 0 & \text{on } \partial\Omega = \{-1, 1\}. \end{cases} \tag{2.13}$$

whose population risk function at a given function w reads as

$$\tilde{R}(w) = \int_{-1}^1 (A(x)D_x^2 w(x) + f(x))^2 dx + \gamma(w^2(-1) + w^2(1)). \tag{2.14}$$

In other words, the risk (2.12) is the discretization of (2.14).

The exact solution to the modified equation (2.13) is denoted by \tilde{u} and explicitly reads as

$$\tilde{u} = \begin{cases} -\frac{1}{2}x - \frac{1}{2}, & x \in (-1, 0), \\ x^2 - \frac{1}{2}x - \frac{1}{2}, & x \in [0, 1). \end{cases}$$

To sum up, now we have altogether three solutions: u (the exact solution to the original equation eq:1dEq), u_θ (the RM solution to the original equation (2.8)) and \tilde{u} (the exact solution to the modified equation (2.13)). For completeness, we can also consider the RM solution to the modified equation (2.13), and we denote it as \tilde{u}_θ .

Figure 2 and Table 1 show a detailed and quantitative comparison between all these four solutions. Throughout the paper, a Banach space Y equipped with the norm $\|\cdot\|_Y$ will be written as an ordered pair $(Y, \|\cdot\|_Y)$ when it is needed to emphasize the norm. If the norm is obvious from the context, we will simply denote it as Y . In this work, we mainly focus on Hilbert spaces such as $L^2(\Omega)$, $H^1(\Omega)$, and $H^2(\Omega)$. However, to verify our intuition, we also add one row of the $L^\infty(\Omega)$ (relative) deviation to Table 1.

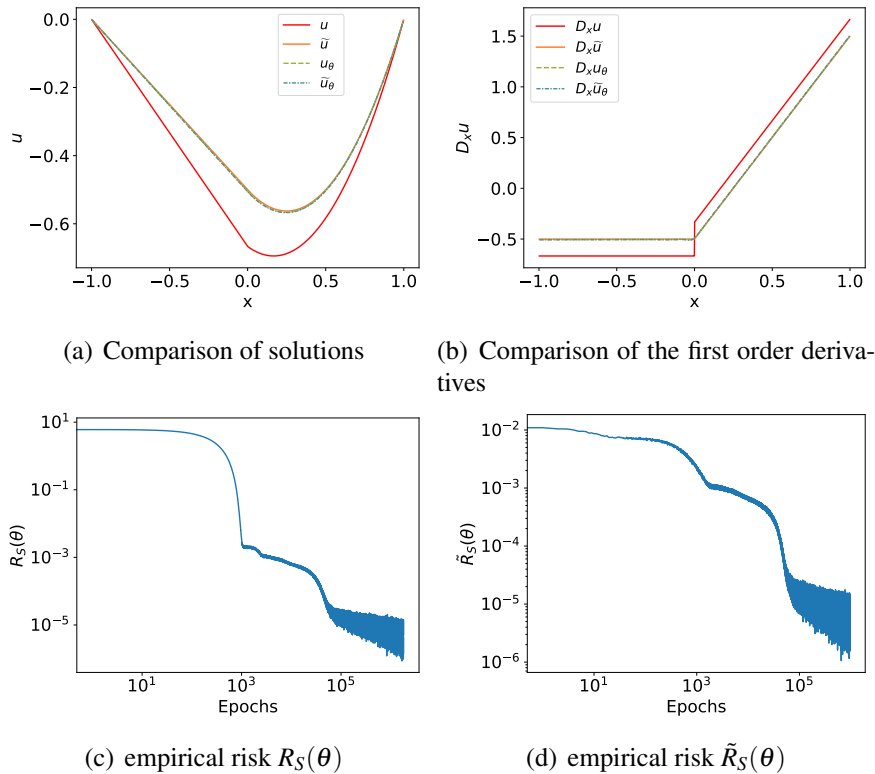


Figure 2: PINN can fit the exact solution to the equation (2.8) with coefficients as (5.4).

Notice that u and u_θ can both access very small empirical risk, while they have a finite gap in terms of $L^\infty(\Omega)$ norm as well as $H^1(\Omega)$ (and hence $L^2(\Omega)$) norm. In some sense, it indicates the non-uniqueness of the solutions as the local/global minima of the empirical risk function. It seems that the method bias to a special solution in some implicit way. This leads to one of the central problems, the implicit bias problem, of deep learning methods for solving PDEs — why a method find such a particular solution from the infinitely many minima. This implicit bias is obviously connected to the success or failure of the methods, and hence it will be the central object of this research work.

A take-away-message is the relation $u_\theta \approx \tilde{u}_\theta \approx \tilde{u} \neq u$ and the smallness $R_S(u_\theta) \ll 1$ and $\tilde{R}_S(\tilde{u}_\theta) \ll 1$. Roughly speaking, the failure of RM method occurs and the RM solution can be modelled by the modified equation. Looking more carefully at Figure 2 (b), we observe that the first-order derivative of the RM solution u_θ (as well as \tilde{u}_θ) is piece-wisely parallel to the one of the exact solution u . Therefore, except for finitely many points, that is, the only point $x = 0$ in this case, the second-order derivatives of the RM solution and the exact solution are the same. Since the point $x = 0$ can not be sampled with nearly probability one, it is expected that the RM solution have the

possibility to achieve very small empirical risk. This is validated in practical experiments. Figure 2 (c) (or (d), respectively) shows the evolution of the empirical risk R_S (or \tilde{R}_S , respectively) along training dynamics of the RM method applied to the problem (2.8) (or (2.13), respectively) with the coefficient function given by (2.9). At the initial stage of the training, the empirical risk is of order one, while at the final stage this risk can reduce to 10^{-5} or 10^{-6} .

Table 1: The deviation and relative deviation from one solution to another under and $L^\infty(\Omega)$, $L^2(\Omega)$ and $H^1(\Omega)$ norms. In part (a), the comparison is between two exact solutions u and \tilde{u} . In part (b) and (c), the RM solution u_θ is compared with u and \tilde{u} , respectively. In part (d), the comparison is between two RM solutions u_θ and \tilde{u}_θ .

$\ \cdot\ _Y$	$Y = L^\infty(\Omega)$	$Y = L^2(\Omega)$	$Y = H^1(\Omega)$
$\ u - \tilde{u}\ _Y$	$\frac{1}{6} \approx$ 1.667×10^{-1}	$\frac{\sqrt{6}}{18} \approx$ 1.361×10^{-1}	$\frac{\sqrt{6}}{9} \approx$ 2.722×10^{-1}
(a) $\ u - \tilde{u}\ _Y / \ \tilde{u}\ _Y$	$\frac{8}{27} \approx$ 2.963×10^{-1}	$\frac{\sqrt{170}}{51} \approx$ 2.557×10^{-1}	$\frac{2\sqrt{10}}{3\sqrt{67}} \approx$ 2.576×10^{-1}
$\ u - \tilde{u}\ _Y / \ u\ _Y$	$\frac{6}{25} \approx$ 2.400×10^{-1}	$\frac{\sqrt{5}}{\sqrt{119}} \approx$ 2.050×10^{-1}	$\frac{2\sqrt{5}}{\sqrt{449}} \approx$ 2.111×10^{-1}
(b) $\ u_\theta - u\ _Y$	1.646×10^{-1}	1.345×10^{-1}	2.691×10^{-1}
$\ u_\theta - u\ _Y / \ u\ _Y$	2.371×10^{-1}	2.026×10^{-1}	2.087×10^{-1}
(c) $\ u_\theta - \tilde{u}\ _Y$	2.880×10^{-3}	2.044×10^{-3}	2.281×10^{-3}
$\ u_\theta - \tilde{u}\ _Y / \ \tilde{u}\ _Y$	5.120×10^{-3}	3.839×10^{-3}	2.161×10^{-3}
(d) $\ u_\theta - \tilde{u}_\theta\ _Y$	1.465×10^{-3}	1.267×10^{-3}	5.702×10^{-3}
$\ u_\theta - \tilde{u}_\theta\ _Y / \ \tilde{u}_\theta\ _Y$	2.598×10^{-3}	2.372×10^{-3}	5.384×10^{-3}
$\ u_\theta - \tilde{u}_\theta\ _Y / \ u_\theta\ _Y$	2.592×10^{-3}	2.371×10^{-3}	5.374×10^{-3}

We believe that such example where u_θ fails to learn u has been seen by many researchers. But our approach is novel and we establish a complete framework to handle such problems with focus on \tilde{u} . This eventually leads to the understanding of the failure and implicit bias of the RM methods.

2.4 Heat equation example: failure of PINN in in more realistic problem

In the previous subsection, we demonstrated that physics-informed neural networks (PINNs) may fail to produce accurate approximations in certain elliptic problems with discontinuous or low-regularity coefficients. This naturally raises the question of whether

such failure is unique to elliptic PDEs or more broadly inherent to the residual minimization mechanism underlying PINNs.

To investigate whether the failure of PINNs in low-regularity PDEs is specific to elliptic problems or more generally rooted in the residual minimization mechanism, we consider a classical time-dependent PDE—the one-dimensional heat equation. This equation is not only a standard benchmark in numerical PDE literature, but also arises naturally in modeling heat conduction through bimetals system with spatially varying thermal conductivity. For instance, in layered or bonded metallic systems, the thermal diffusivity $A(x)$ may vary sharply across interfaces due to differences in material composition.

Our numerical experiments reveal that similar failure behavior also occurs in this parabolic setting, further highlighting the limitations of PINNs in practical applications. And unless otherwise stated, all experimental settings, including the neural network architecture, optimizer configuration, and residual sampling scheme, are identical to those used in Section 2.3.

Problem setup. We consider the one-dimensional heat equation defined on $(x, t) \in (-1, 1) \times (0, 2)$:

$$\begin{cases} u_t - D_x(A(x)D_x u) = f(x, t), & (x, t) \in (-1, 1) \times (0, 2), \\ u(x, 0) = 0, & x \in (-1, 1), \\ u(-1, t) = u(1, t) = 0, & t \in (0, 2), \end{cases} \quad (2.15)$$

The diffusion coefficient $A(x)$ and source term $f(x, t)$ are given by

$$A(x) = \begin{cases} \frac{1}{2}, & x < 0, \\ 1, & x > 0, \end{cases} \quad \text{and} \quad f(x, t) = \begin{cases} -\frac{2}{3}x - \frac{2}{3}, & x < 0, \\ x^2 - \frac{1}{3}x - \frac{2}{3} - 2t, & x > 0. \end{cases} \quad (2.16)$$

Exact solution and observations. This setup admits a unique exact solution given by:

$$u(x, t) = \begin{cases} \left(-\frac{2}{3}x - \frac{2}{3}\right)t, & x < 0, \\ \left(x^2 - \frac{1}{3}x - \frac{2}{3}\right)t, & x > 0. \end{cases} \quad (2.17)$$

Although the solution $u(x, t)$ is continuous and piecewise smooth, its spatial derivative $u_x(x, t)$ has a jump discontinuity at $x = 0$ along the spatial direction.

When training a PINN to learn this solution using standard residual minimization, we observe a systematic deviation near $x = 0$ across various time slices. The trained neural network solution u_θ tends to “smooth out” the singularity in derivative of u , thereby introducing a non-negligible pointwise error. This phenomenon is qualitatively similar to the failure mode we previously observed in the elliptic case, and again stems from the mismatch between the PINN’s inductive bias and the structure of the underlying PDE.

We report the corresponding quantitative errors and visualizations in Figures 3 and 4, which illustrate the persistent deviation of the PINN solution around the singular interface at $x = 0$.

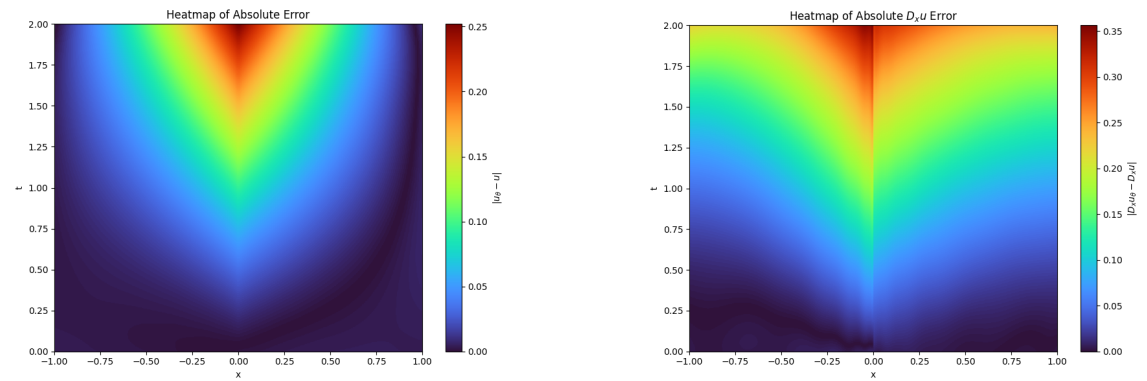


Figure 3: Heatmaps of errors. Left: Absolute error $|u_\theta - u|$. Right: Absolute derivative error $|D_x u_\theta - D_x u|$.

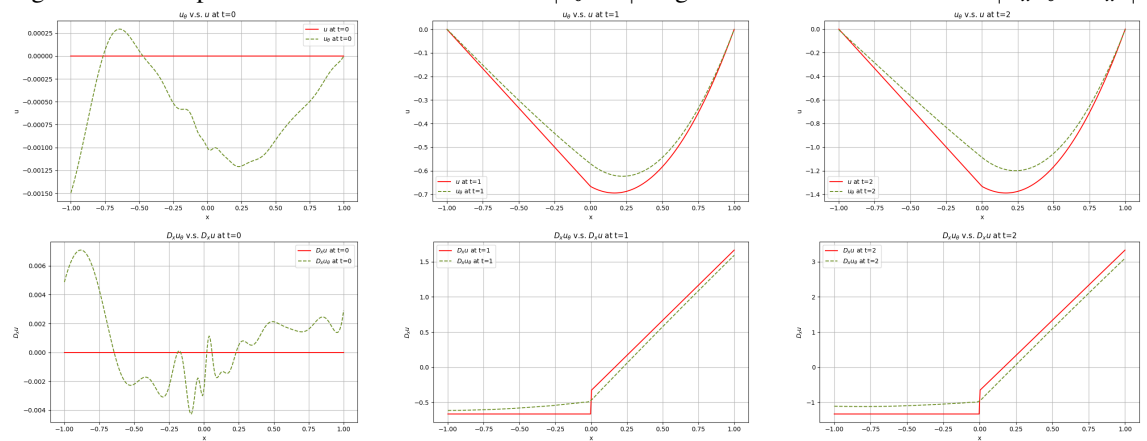


Figure 4: Comparison of solutions at $t = 0, 1, 2$. Top row: Function values u_θ, u . Bottom row: Spatial derivatives $D_x u_\theta, D_x u$.

Modified equation. Similarly as in Section 2.3, we introduce the modified equation of (2.15) as:

$$\begin{cases} u_t - A(x)D_{xx}u = f(x,t), & (x,t) \in (-1,1) \times (0,2), \\ u(x,0) = 0, & x \in (-1,1), \\ u(-1,t) = u(1,t) = 0, & t \in (0,2). \end{cases} \quad (2.18)$$

We train two separate PINNs: one using the residual form of (2.15), and another using that of (2.18), while u_θ and \tilde{u}_θ are used to represent the numerical solutions by apply-

ing PINNs to (2.15) and (2.18), respectively. The corresponding quantitative errors and comparison of u_θ , \tilde{u}_θ and u can be found in Figures 5 and 6.

Our experiments show that the two numerical solutions are nearly indistinguishable, both in terms of pointwise predictions and residual distributions. This further confirms that, in the presence of discontinuous coefficients, the PINN trained on the original form (2.15) implicitly learns the behavior of the modified equation (2.18). The consistency of these two learned solutions provides strong empirical evidence that the standard PINN approach effectively approximates the modified equation, rather than the true solution to the original PDE.

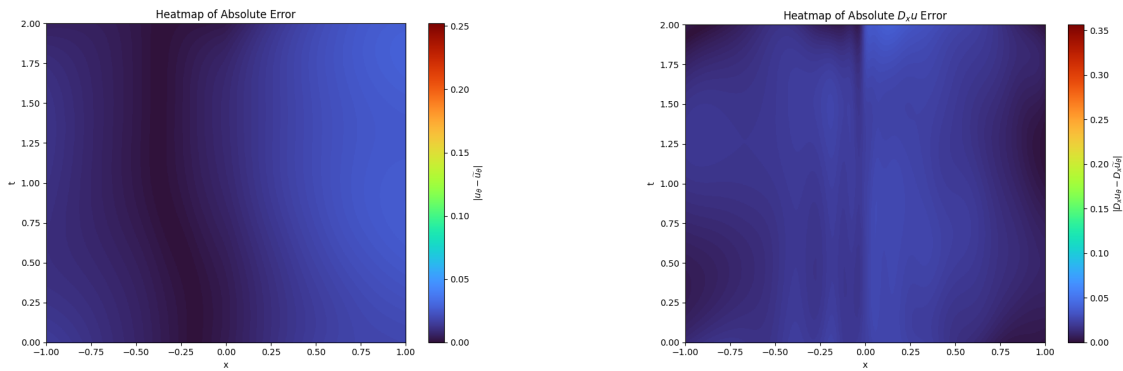


Figure 5: Heatmaps of errors Left Absolute error $|u_\theta - \tilde{u}_\theta|$ Right Absolute derivative error $|D_x u_\theta - D_x \tilde{u}_\theta|$.

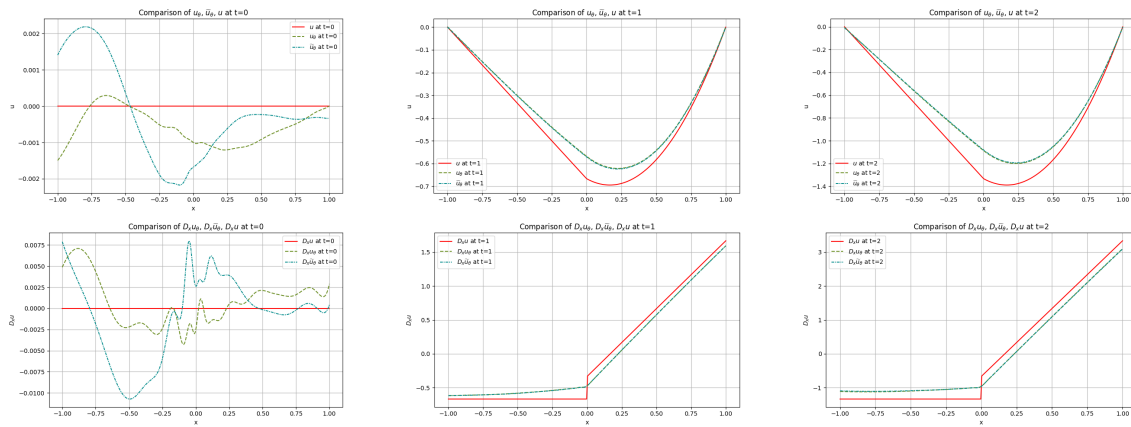


Figure 6: Comparison of solutions at time slices $t = 0, 1, 2$. Top row: Function values u_θ , \tilde{u}_θ , u . Bottom row: Spatial derivatives $D_x u_\theta$, $D_x \tilde{u}_\theta$, $D_x u$.

2.5 Linear elliptic equations with BV coefficients

In this subsection, we introduce the general setting on the (systems of) elliptic PDEs used for the main results of this work. Some assumptions are given for the linear elliptic equations and systems. Although main contributions (See detailed description in Section 3) of this work focus on these linear problems, we nevertheless stress that some key results can be extended to the quasilinear setting and hopefully it can be transferred into the case of quasilinear PDEs in the future.

We consider the system of elliptic equations written in the divergence form:

$$\begin{cases} Lu = f & \text{in } \Omega, \\ u = 0 & \text{on } \partial\Omega, \end{cases} \tag{2.19}$$

with

$$(Lu)^\alpha = - \sum_{\beta=1}^{d'} \operatorname{div} \cdot (A^{\alpha\beta}(x) Du^\beta) = - \sum_{\beta=1}^{d'} \sum_{i,j=1}^d D_i (A_{ij}^{\alpha\beta} D_j u^\beta),$$

where $\alpha, \beta \in \{1, 2, \dots, d'\}$, $i, j \in \{1, 2, \dots, d\}$, $\Omega \subseteq \mathbb{R}^d$ is a bounded domain with $C^{1,1}$ boundary, measurable functions $A^{\alpha\beta} \in S^{d \times d}$ are also symmetric in α, β , namely $A^{\alpha\beta} = A^{\beta\alpha}$, and $f \in L^2(\Omega; \mathbb{R}^{d'})$.

Now we mention the basic assumption to be used throughout the paper.

Assumption 2.1 (BV coefficients). Let L be the operator defined in (2.19). Assume that for each $\alpha, \beta \in \{1, \dots, d'\}$, there exist a scalar function $\chi^{\alpha\beta} \in SBV^\infty(\Omega)$ with $\mathcal{H}^{d-1}(J_{\chi^{\alpha\beta}}) < +\infty$ and a matrix-valued function $\bar{A}^{\alpha\beta} \in C^1(\bar{\Omega}; S^{d \times d})$ such that $A^{\alpha\beta} = \chi^{\alpha\beta} \bar{A}^{\alpha\beta}$. And there is some $\alpha_0, \beta_0 \in \{1, \dots, d'\}$ satisfying $\mathcal{H}^{d-1}(J_{\chi^{\alpha_0\beta_0}}) > 0$. Furthermore, we assume there are constants $\chi_{\min}, \chi_{\max}, \bar{\lambda}, \bar{\Lambda} > 0$ such that for each $\alpha, \beta \in \{1, \dots, d'\}$ and for all $\xi \in \mathbb{R}^d, x \in \Omega$

$$\chi_{\min} \leq \chi^{\alpha\beta}(x) \leq \chi_{\max}, \tag{2.20}$$

$$\bar{\lambda} |\xi|^2 \leq \xi^\top \bar{A}^{\alpha\beta}(x) \xi \leq \bar{\Lambda} |\xi|^2. \tag{2.21}$$

Here $\mathcal{H}^{d-1}(\cdot)$ means a $d - 1$ -dimensional Hausdorff measure of g give set and an SBV^∞ function is a **special function of bounded variation** (SBV) whose absolutely continuous part of the gradient has an L^∞ density. The precise definition and basic properties of SBV functions are given in Appendix B. Figure 7 is an illustration of a SBV function. It is no harm for the readers to think each $\chi^{\alpha\beta}$ as a piece-wise constant function throughout the paper.

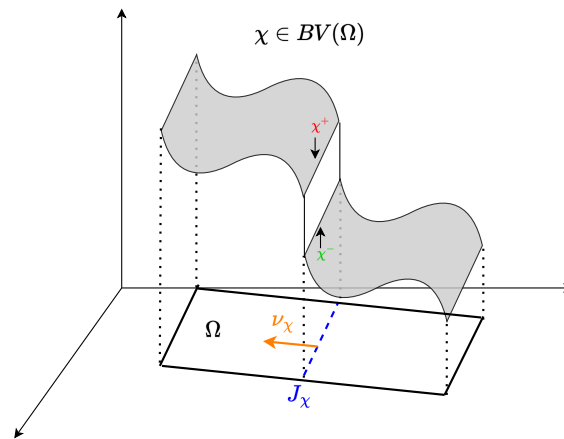


Figure 7: Illustration of a function of bounded variation χ . The set of approximate jump points J_χ is determined by the triplet $(\chi^+, \chi^-, \nu_\chi)$. See details in Appendix B.

Here we give some comments on our main assumption.

Remark 2.1 (Hadamard–Legendre condition). Assumption 2.1 implies the Hadamard–Legendre condition, which is a standard condition for the existence of solution to systems of elliptic PDEs. Let L be the operator defined in (2.19). We say that $\{A^{\alpha\beta}\}_{\alpha,\beta=1}^{d'}$ satisfy the Hadamard–Legendre condition if there exist constants $\lambda, \Lambda > 0$ such that for all $\xi^\alpha \in \mathbb{R}^d, x \in \Omega$

$$\lambda |\xi|^2 \leq \sum_{\alpha,\beta=1}^{d'} (\xi^\alpha)^\top A^{\alpha\beta}(x) \xi^\beta \leq \Lambda |\xi|^2. \quad (2.22)$$

Here $|\xi|^2 = \sum_{\alpha=1}^{d'} |\xi^\alpha|^2$.

Remark 2.2 (uniform ellipticity condition). When $d' = 1$, the superscripts α, β can only take value 1. Thus for simplicity of notation, we will drop the superscripts throughout the paper when $d' = 1$. In particular, for the case $d' = 1$, the Hadamard–Legendre condition in Remark 2.1 coincides with the uniform ellipticity condition, that is to say, there exist constants $\lambda, \Lambda > 0$ satisfying

$$\lambda |\xi|^2 \leq \xi^\top A(x) \xi \leq \Lambda |\xi|^2 \quad (2.23)$$

for all $\xi \in \mathbb{R}^d, x \in \Omega$.

We also remark that in the proofs throughout the paper, the constant C may be different from line to line, but we usually keep track of its dependence on basic constants such as χ_{\min} or $\bar{\Lambda}$ and thus make the paper more readable. In the proofs, the expression $U \prec \zeta \prec U'$ means $\zeta = 1$ in U , $\zeta = 0$ outside U' and $\zeta \in C_c^\infty(\mathbb{R}^d)$, where U, U' are bounded open sets and U is compactly contained in U' .

3 Main contributions

In this section, we describe our main contributions of this paper. After the introduction to each contribution point, several related theorems will be mentioned in an intuitive way. Most of them not only work for elliptic equations, but also work for elliptic systems, although some technical conditions may be inevitably assumed for the latter.

From now on, the term “residual minimization” (or in short “RM”) is used to replace “PINN” in the main results because these analyses provided in this and later sections work for general residual minimization methods, and are not exclusive for PINN. In particular, the DNN representation is not explicitly used in the analysis. Nevertheless, the type of the risk function (also known as loss function) is more responsible to the failure or success of the machine learning based PDE solvers.

In Section 3.1, we propose a hypothesis that \tilde{u} approximates u_θ well and derive the modified equation for \tilde{u} , in a general setting, to model the numerical solution obtained by RM method. This hypothesis serves as our starting point of the analysis and understanding of the implicit bias of RM method. In Section 3.2, we provide an if-and-only-if condition to characterize the singularity which appears naturally because of the discontinuous coefficients in the equations. In particular, this condition characterizes whether u is equal to \tilde{u} or not. Next, in Section 3.3, we introduce the RM-invariant subspace $\text{Ker}(T - I)$, defined as the set of all f which leads to $u = \tilde{u}$. This subspace $\text{Ker}(T - I)$ allow us to identify the occurrence of deviation of the numerical solution. We will show the deviation occurs generically and the relative deviation, even for the data near the RM-invariant subspace, is not small. The last contribution point is mentioned in Section 3.4, where we prove that the exact solution is unstable and hence the RM method implicit bias the exact solution towards the solution to the modified equation. In the last subsection, we present the connections of the main contributions, as well as preliminaries and by-products, by a flow chart.

3.1 Modeling numerical solution by modified equation

In any sense, it is very difficult, if not impossible, to study u_θ directly. Fortunately, as shown in Figure 2 (a), we have the key observation: $u_\theta \approx \tilde{u}_\theta \approx \tilde{u}$, that is, the RM solutions u_θ and \tilde{u}_θ both looks very close to the exact solution \tilde{u} , and they are almost indistinguishable. More precisely, part (c) and part (d) of Table 1 provide more quantitative evidences to show that the (relative) distances among u_θ , \tilde{u}_θ , and \tilde{u} are very small in either $L^\infty(\Omega)$, $L^2(\Omega)$, or $H^1(\Omega)$ norm. This closeness is already intuitively explained in Section 2.3 and it provides us a solid evidence to model u_θ by using \tilde{u} for the one-dimensional example.

We would like to extend this idea and model u_θ by using \tilde{u} to more general equations and to the case of system (that is $d' > 1$). Let us start with $d' = 1$ and a general coefficient

A. The derivation is almost the same as the one in Section 2.3. But here the coefficient A may not be piece-wise constant. Moreover, A is a $d \times d$ matrix-valued function instead of a scalar function. By the product rule, the divergence operator in (2.19) is applied to A and Du respectively. Furthermore, by the decomposition of SBV function (See Definition B.4) with $d' = 1$, we have

$$Lu = - \sum_{i,j=1}^d A_{ij} D_{ij} u - \sum_{i,j=1}^d (D_i^a A_{ij} + D_i^j A_{ij}) D_j u. \quad (3.1)$$

Here $D_i^j A_{ij}$ is supported on an \mathcal{L}^d null set J_χ . Since the number of samples is at most countable in any practical applications, the probability of selecting some points in the support of $D_i^j A_{ij}$ is zero. Unless the algorithm is specifically designed, the contribution of $D_i^j A_{ij}$ to the risk function is zero. In other words, $D_i^j A_{ij}$ will not affect the optimization process. As a result, we simply omit $D_i^j A_{ij}$ and obtain the approximate model (3.2) for studying the RM methods.

For the general setting with $d' \geq 1$ (that is including systems), we follow the same idea and thus arrive at the modified equation for (2.19) as follows

$$\begin{cases} \tilde{L}\tilde{u} = f & \text{in } \Omega, \\ \tilde{u} = 0 & \text{on } \partial\Omega, \end{cases} \quad (3.2)$$

where for each $\alpha \in \{1, \dots, d'\}$

$$(\tilde{L}\tilde{u})^\alpha = - \sum_{\beta=1}^{d'} \sum_{i,j=1}^d A_{ij}^{\alpha\beta} D_{ij} \tilde{u}^\beta - \sum_{\beta=1}^{d'} \sum_{i,j=1}^d D_i^a A_{ij}^{\alpha\beta} D_j \tilde{u}^\beta. \quad (3.3)$$

Throughout the paper, we call \tilde{L} the modified operator of L and denote u the solution to (2.19), and \tilde{u} the solution to (3.2). Also, let u_θ and \tilde{u}_θ be the RM solutions, that is, the numerical solutions under RM methods (such as PINN), to the original equation (2.19) and modified equation (3.2), respectively. When the equation is clear from the context, we call \tilde{u} the solution to the modified equation (or simply, the modified solution) and call u_θ the numerical solution (or RM solution).

The previous numerical experiments suggest us to make the following hypothesis to model the numerical solution .

Hypothesis 3.1 (modified solution approximates RM solution). The RM solution to the problem (2.19) can be approximated by the solution to its modified equation (3.2). More precisely, for any given $\varepsilon > 0$, the RM method can find a numerical solution u_θ such that $\|u_\theta - \tilde{u}\|_{H^1(\Omega)} \leq \varepsilon$ for all meaningful f .

Here we neglect the details of the neural networks such as how to design the network architecture, how to tune the hyper-parameters, and how to train the neural network parameter. These will be left to the future research. This hypothesis will be the foundation of our work, and from now on, we will focus on \tilde{u} which is more amenable because it satisfies a modified equation (3.2). We emphasize that Hypothesis 3.1 and our point of view on the modelling of the RM solution are novel. For the modified problem, we obtain a series of theorems. These with Hypothesis 3.1 lead to the understanding of the behavior and properties of the RM solution, in particular, its implicit bias.

We will work on both elliptic equations and systems. To prove the results in the case of elliptic systems, we need a further technical condition as follows.

Assumption 3.1 (*A priori estimates for linear system*). Assume that for all $\tilde{u} \in H_0^1(\Omega; \mathbb{R}^{d'}) \cap H^2(\Omega; \mathbb{R}^{d'})$, there is constant $C > 0$ such that $\|\tilde{u}\|_{H^2(\Omega; \mathbb{R}^{d'})} \leq C\|\tilde{L}\tilde{u}\|_{L^2(\Omega; \mathbb{R}^{d'})}$, where \tilde{L} is defined as in (3.2).

We remark that Assumption 2.1 with $d' = 1$ implies Assumption 3.1 (See Theorem 5.1).

3.2 Characterizing removable singularity

Intuitively, it is clear that the failure of PINN, or more generally, the RM method, is due to the singularities in the coefficients of the PDE. Moreover, whether the singularity exists is highly related to whether the exact solution coincides with the modified solution, where the later is introduced in the above subsection. In particular, if the singularity is removable then there is no such failure. In order to study the removable singularity in the coefficients, we introduce a quantity μ based on which we can establish necessary and sufficient condition. Given any \mathcal{H}^{d-1} measurable set $B \subseteq \Omega$, $\chi \in SBV^\infty(\Omega)$, $\Upsilon : H_0^1(\Omega) \rightarrow L^\infty(\Omega; S^{d \times d})$, and $\varphi \in C^1(\Omega)$, we define

$$\mu(B; \chi, \Upsilon, \varphi) = \int_{B \cap J_\chi} (\chi^+ - \chi^-) v_\chi^\top \Upsilon[\varphi] D\varphi \, d\mathcal{H}^{d-1}. \tag{3.4}$$

For example, if $B = \Omega$, $\varphi \in C_c^1(\Omega)$, and $\Upsilon[w] = \bar{A}$ for all $w \in H_0^1(\Omega)$, then we have

$$\mu(\Omega; \chi, \bar{A}, \varphi) = \int_{J_\chi} (\chi^+ - \chi^-) v_\chi^\top \bar{A} D\varphi \, d\mathcal{H}^{d-1}.$$

We thus have an essential result (Theorems 4.1 and 4.2) to characterize the removable singularity in terms of μ . Applying these theorems, we can consequently find smooth function v_δ such that

$$\mu(\Omega; \chi, \bar{A}, v_\delta) \neq 0.$$

See Theorems 4.3 and 4.4.

3.3 Identifying the occurrence of deviation

We study the occurrence of deviation $u \neq \tilde{u}$. Thanks to Theorems 4.3 and 4.4, we prove in Theorem 5.3 that for specific interior data f the deviation occurs. To step further, we ask whether this occurrence of deviation is generic and whether it is large in some sense. Affirmative answers to these questions will be obtained by studying the RM-invariant subspace $\text{Ker}(T - I)$. The $\text{Ker}(T - I)$ basically identifies the interior f where $u = \tilde{u}$.

To define $\text{Ker}(T - I)$, we should study the properties of \tilde{L} first. Let us consider the largest possible domain of \tilde{L} , which is naturally a subset of $H_0^1(\Omega; \mathbb{R}^{d'})$. In fact, it should be a subset of $H^2(\Omega; \mathbb{R}^{d'})$. Otherwise, we have $v \in H_0^1(\Omega; \mathbb{R}^{d'}) \setminus H^2(\Omega; \mathbb{R}^{d'})$, and hence $D_{ij}v^\beta \in H^{-1}(\Omega)$ and $A_{ij}^{\alpha\beta} \in SBV(\Omega)$ imply that the point-wise product $A_{ij}^{\alpha\beta} D_{ij}v^\beta$ may not be a classical function. Thus the largest possible domain of \tilde{L} is

$$\text{dom}(\tilde{L}) = H_0^1(\Omega; \mathbb{R}^{d'}) \cap H^2(\Omega; \mathbb{R}^{d'}). \quad (3.5)$$

Consequently, the image of \tilde{L} , denoted by X , is

$$X = \{\tilde{L}w : w \in H_0^1(\Omega; \mathbb{R}^{d'}) \cap H^2(\Omega; \mathbb{R}^{d'})\}. \quad (3.6)$$

Next, we introduce the RM-transformation T . Suppose that Assumptions 2.1 and 3.1 hold. Let u and \tilde{u} be solutions to (2.19) and (3.2) with data $f \in L^2(\Omega; \mathbb{R}^{d'})$, respectively. Then we can define the operator T

$$T : X \rightarrow H^{-1}(\Omega; \mathbb{R}^{d'}) \quad (3.7)$$

$$f \mapsto Tf = L\tilde{u}. \quad (3.8)$$

Clearly, \tilde{u} is the weak solution to

$$\begin{cases} L\tilde{u} = Tf & \text{in } \Omega, \\ \tilde{u} = 0 & \text{on } \partial\Omega. \end{cases} \quad (3.9)$$

In particular, when $d' = 1$, Assumption 3.1 holds automatically by Assumption 2.1. Hence, for the single elliptic equation case, namely $d' = 1$, we have $X = L^2(\Omega)$ and $T : L^2(\Omega) \rightarrow H^{-1}(\Omega)$.

Let $\sigma(T)$ be the spectrum of T . Then we will show in Theorem 5.4 that the only eigenvalue of T is 1, namely $\sigma(T) = \{1\}$. Thus to identify the occurrence of deviation $u \neq \tilde{u}$, we only need to characterize the invariant subspace of X under RM-transformation T . This naturally leads to the following kernel $\text{Ker}_X(T - I)$, that is, the eigenspace of T corresponding to the eigenvalue 1 restricted to X :

$$\text{Ker}(T - I) = \text{Ker}_X(T - I) = \{f \in X : Tf = f\} = \{\tilde{L}w \in X : \tilde{L}w = Lw\}. \quad (3.10)$$

When the X is clear from the context, we will drop it in the subscript and denote the kernel as $\text{Ker}(T - I)$. We also denote its complement with respect to the whole space $L^2(\Omega; \mathbb{R}^{d'})$ as $(\text{Ker}(T - I))^c = L^2(\Omega; \mathbb{R}^{d'}) \setminus \text{Ker}(T - I)$.

Let us explain why the space $\text{Ker}(T - I)$ can characterize the occurrence of the deviation. If there is a non-zero $f \in X \setminus \text{Ker}(T - I)$, then the unique solution \tilde{u} to (3.2) (namely $\tilde{L}\tilde{u} = f$) satisfies $\tilde{L}\tilde{u} \neq L\tilde{u}$. In other words, $f \neq L\tilde{u}$, and hence \tilde{u} deviates from u , implying there is a deviation. Therefore, to understand the implicit bias of RM method, we only need to study the properties of $\text{Ker}(T - I)$. In particular, Theorem 5.4 shows that under a mild condition that the jump is not omnipresent, the complement of the kernel $(\text{Ker}(T - I))^c$ is open and dense (see also Theorem 5.4 for the case of system). As a direct result, for almost all $f \in L^2(\Omega; \mathbb{R}^{d'})$, the deviation occurs. Furthermore, Theorem 5.5 shows the relative deviation $\|u - \tilde{u}\|_{H^1(\Omega; \mathbb{R}^{d'})} / \|\tilde{u}\|_{H^1(\Omega; \mathbb{R}^{d'})}$ can be even unbounded.

Now, with these theorems on the relation between \tilde{u} and u , we are ready to explain the phenomenon $u_\theta \neq u$ shown in the previous numerical experiments. Let us recall the phenomenon, discuss first intuitively, and then give a more quantitative explanation.

Recall that, according to Figure 2 (a), the RM solution u_θ is entirely deviated from the exact solution u . More precisely, the part (b) of Table 1 show that the (relative) numerical errors between u and u_θ are not small in both $L^\infty(\Omega)$ and $L^2(\Omega)$ (and hence $H^1(\Omega)$) norm.

We first provide an intuitive understanding on the non-zero difference between the exact solution and the RM solution. For the exact solution u , the term $AD_x u$ has to be continuous, otherwise its derivative would be a Dirac-like function. Roughly speaking, the Dirac-like function is only non-zero at a single point but its integration on the whole space is non-zero. Therefore, even in the weak sense, the effect of Dirac function can not be ignored. However, the source term f is a classical function which is defined point-wisely. In particular, it is not a Dirac-like function. Note that A is discontinuous. In order to make $AD_x u$ be continuous, $D_x u$ has to be discontinuous as shown in Figure 1(b). For the RM solution u_θ , as the isolated discontinuities of A can not be exactly sampled, any solution, whose first-order derivative is piece-wisely parallel to that of the exact solution, is a solution that minimizes the empirical loss. The frequency principle [41–44] shows that deep neural network implicitly prefers a low-frequency function to fit training data. Roughly speaking, compared with all feasible solutions, the one with continuous first-order derivative is a function has low frequency, which is learned by RM as shown in Figure 1(b). The rigorous connect between the frequency principle and the implicit bias of RM method is beyond the scope of this paper, and will be left to the future work.

Next, we conclude the contribution on the occurrence of the deviation with a more quantitative remark which explains the phenomenon $u_\theta \neq u$.

Remark 3.1 (error of RM solution). Theorem 5.3 leads to a finite error of RM solution. In fact, if we assume Hypothesis (3.1) with $\varepsilon \leq \frac{C}{2}$, then we can numerically achieve u_θ such that $\|\tilde{u} - u_\theta\|_{L^2(\Omega; \mathbb{R}^{d'})} \leq \frac{C}{2}$. Consequently, the deviation $\|u - \tilde{u}\|_{H^1(\Omega; \mathbb{R}^{d'})} \geq C$ leads

to the estimate

$$\|u - u_\theta\|_{L^2(\Omega; \mathbb{R}^{d'})} \geq \|u - \tilde{u}\|_{L^2(\Omega; \mathbb{R}^{d'})} - \|\tilde{u} - u_\theta\|_{L^2(\Omega; \mathbb{R}^{d'})} \geq \frac{C}{2},$$

which implies a finite (non-infinitesimal) numerical error when the gap $\|u - \tilde{u}\|_{L^2(\Omega; \mathbb{R}^{d'})}$ takes a non-infinitesimal value.

3.4 Understanding the implicit bias

Compared to the above results on the deviation, it is more important to understand the implicit bias of the RM method. The latter has to be more dynamical. One may ask whether the dynamics (and more precisely the initialization of the dynamics) matters. In particular, shall we still expect the failure of RM method for the previous example, if we take the initial output function $u_{\theta(0)}$ being sufficiently close to the exact solution u ? We should study this in both numerical and theoretical way, and eventually this leads to the understanding of the implicit bias of RM methods.

Thanks to the well-known universal approximation theorem, the exact solution u from the above failure example can be approximated well by, for example, a two-layer neural network. Thus we can first use supervised learning to find sufficiently good parameter and then apply RM methods with such good initialization.

In numerical experiments, we still take the example (2.8) and the results are shown in Figure 8. We use supervised learning to find neural network function u_θ^{SV} with parameter θ^{SV} , where the empirical risk function reads as

$$R_S^{\text{SV}}(u_\theta^{\text{SV}}) = \frac{|\Omega|}{n_{\text{int}}} \sum_{x \in S_{\text{int}}} ((u_\theta^{\text{SV}}(x) - u(x))^2 + (D_x u_\theta^{\text{SV}}(x) - D_x u(x))^2) + \gamma R_{S, \text{bd}}(u_\theta^{\text{SV}}).$$

By Figure 8 (a), u_θ^{SV} almost overlaps u as is expected. Next, let θ^{SV} be the initial parameter and apply the RM method to the original equation (2.8) and the modified equation (2.13), respectively. In other words, we train the neural network with R_S and \tilde{R}_S , respectively, until the risk is small and does not decay anymore. After training, the output functions are denoted as $u_\theta^{\text{SV} \rightarrow \text{RM}}$ and $\tilde{u}_\theta^{\text{SV} \rightarrow \text{RM}}$, respectively. We observe that both output functions are very close to \tilde{u} , as shown in Figure 8 (b). For a comprehensive comparison, we also plot u_θ and \tilde{u}_θ and their derivatives in Figure 8. Roughly speaking, we have $u \approx u_\theta^{\text{SV}}$ and $u_\theta \approx \tilde{u}_\theta \approx \tilde{u} \approx u_\theta^{\text{SV} \rightarrow \text{RM}} \approx \tilde{u}_\theta^{\text{SV} \rightarrow \text{RM}}$. Therefore, even given a sufficiently good initialization, the RM method implicitly biases the numerical solution against the exact solution u and towards the solution \tilde{u} to the modified equation.

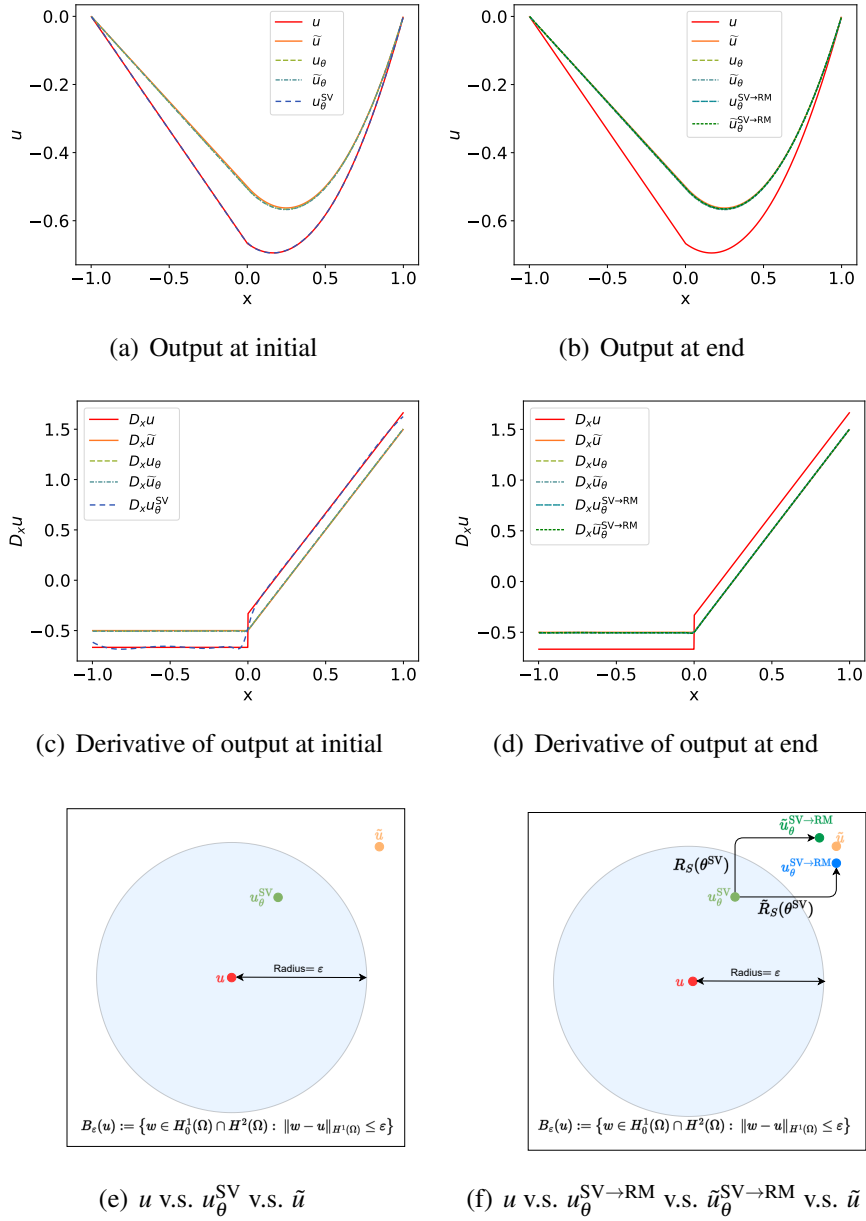


Figure 8: evolution of modified solution with supervised initialization.

We prove Theorems 5.7 and Proposition 5.1 which essentially explains the implicit bias. In the following remark, we provide such theoretical explanation to the implicit bias phenomenon shown in Figure 8.

Remark 3.2 (implicit bias of RM method). (i) The effective risk is large at u_θ^{SV} . More precisely, $\tilde{R}_S(u_\theta^{\text{SV}}) \approx \tilde{R}(u_\theta^{\text{SV}}) \geq C_0$ for some finite $C_0 > 0$. Hence the risk is very likely to be decreased along the training dynamics. This explains the RM method implicitly biases against u_θ^{SV} .

(ii) Suppose that the RM method achieves a very small (effective) empirical risk after training. That is $\tilde{R}_S(u_\theta^{\text{SV} \rightarrow \text{RM}}) \leq \varepsilon$ for very small $\varepsilon > 0$. Then

$$\|u_\theta^{\text{SV} \rightarrow \text{RM}} - \tilde{u}\|_{H^1(\Omega; \mathbb{R}^{d'})} \leq C \sqrt{\tilde{R}(u_\theta^{\text{SV} \rightarrow \text{RM}})} \approx C \sqrt{\tilde{R}_S(u_\theta^{\text{SV} \rightarrow \text{RM}})} \leq C \sqrt{\varepsilon}.$$

This explains the RM method implicitly biases towards \tilde{u} .

This contribution can also be understood as follows. From the Observation (ii), we have the commonly-seen phenomenon that $R(u_\theta) \ll 1$ while $\|u - u_\theta\| \geq C$ for some finite $C > 0$. Now these experiments and phenomenon answers the reverse statement is also true: if $\|u - u_\theta\| \ll 1$, then $R(u_\theta) \geq C_0$ for some constant C_0 . It shows that the exact solution is unstable in the sense of RM method and implicitly biases towards the solution to the modified equation.

3.5 Connection of the contributions

We conclude the main contribution section by presenting in Figure 9 within which the readers may find the connections between our main results mentioned above as well as more preliminary lemmas, propositions, etc. The arrows show the logic flow and various colors correspond to different types of the results.

4 Removability of singularity

Let us explain the title of this section. For $\chi \in \text{SBV}(\Omega)$, we say the set of singularity J_χ is removable if $\mathcal{H}^{d-1}(J_\chi) = 0$ (definition of J_χ can refer to Definition B.3). In this section, we obtain the equivalence between the removability of singularity and the condition $\mu = 0$. The quantity μ is essentially an integral and defined by (3.4) in Section 3.2. The advantage of using μ , as what we do in latter sections, is that it allows us to estimate the pairing $\langle Lu - L\tilde{u}, \Phi \rangle_{H^{-1}(\Omega), H_0^1(\Omega)}$ in a quantitative way, and hence we can estimate the difference $\|u - \tilde{u}\|_{H^1(\Omega)}$.

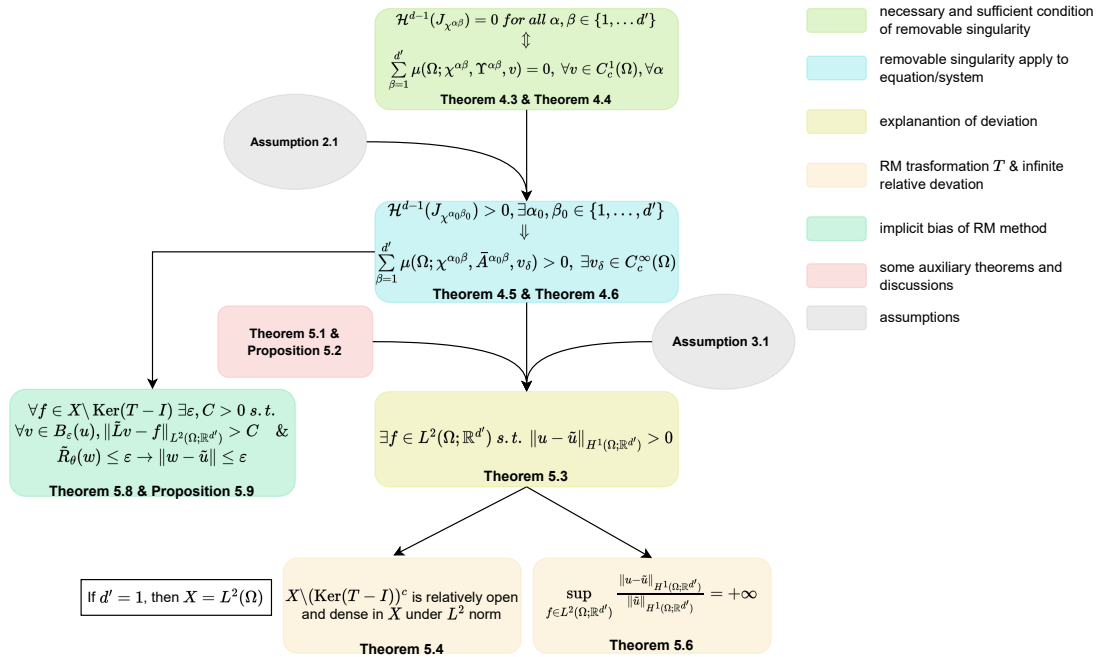


Figure 9: The schematic proof of linear elliptic equation/system

4.1 Necessary and sufficient condition of removable singularity

We begin with two simple lemmas: one to bound χ^\pm (defined in Definition B.3) and the other to construct a smooth cutoff function. The latter one (namely Lemma 4.2) is standard, but we provide the proof for completeness.

Lemma 4.1 (boundedness of χ^\pm on jump set). *If $\chi \in L^\infty(\Omega) \cap SBV(\Omega)$ with $\mathcal{H}^{d-1}(J_\chi) > 0$, then $|\chi^\pm(x)| \leq \|\chi\|_{L^\infty(\Omega)}$ for all $x \in J_\chi$.*

Proof. We prove by contradiction. Suppose there is an $x_0 \in J_\chi$ satisfying $|\chi^\pm(x_0)| > \|\chi\|_{L^\infty(\Omega)}$. Denote $B_\rho^\pm(x_0, \nu) = \{x \in B_\rho(x_0) : \pm(x_0 - x)^\top \nu > 0\}$. Thus we have

$$\lim_{\rho \rightarrow 0} \frac{1}{|B_\rho^\pm(x_0, \nu)|} \int_{B_\rho^\pm(x_0, \nu)} |\chi(y) - \chi^\pm(x_0)| \, dy > 0,$$

which contradicts the definition of χ^\pm . □

Lemma 4.2 (smooth cutoff function with controlled derivative). *Suppose that bounded open sets $U \subseteq U' \subseteq \mathbb{R}^d$ satisfy $\text{dist}(U, \partial U') > 2\delta > 0$. Then there is a cutoff function $\zeta \in C_c^\infty(U')$ such that $U \prec \zeta \prec U'$ and $\|D\zeta\|_{L^\infty(U')} \leq \frac{C}{\delta}$, where C depends only on d .*

Proof. Define $\rho(x) = \frac{1}{C} \exp(\frac{1}{|x|^2-1})$ for $x \in B_1(0)$ and $\rho(x) = 0$ for $x \in \mathbb{R}^d \setminus B_1(0)$, where the constant $C = \int_{B_1(0)} \exp(\frac{1}{|x|^2-1}) dx$ only depends on d . Thus $\int_{\mathbb{R}^d} \rho(x) dx = 1$ and $\rho \in C_c^\infty(\mathbb{R}^d)$ with compact support $\overline{B_1(0)}$. For each $\delta > 0$, define $\rho_\delta(x) = \delta^{-d} \rho(\delta^{-1}x)$ and $\mathbb{1}_{U_\delta}$ the characteristic function of U_δ , where $U_\delta = \{x \in \mathbb{R}^d : \text{dist}(x, U) < \delta\}$. Let $\zeta = \rho_\delta * \mathbb{1}_{U_\delta}$. It is clear that $U \prec \zeta \prec U'$. Therefore, we have for all $x \in U'$

$$|D\zeta(x)| = |(\mathbb{1}_{U_\delta} * D\rho_\delta)(x)| = \left| \int_{B_\delta(0)} \mathbb{1}_{U_\delta}(x-y) \delta^{-d-1} D\rho(\delta^{-1}y) dy \right| \leq \delta^{-1} \int_{B_1(0)} |D\rho(y)| dy \leq \frac{C}{\delta},$$

where C only depends on d . □

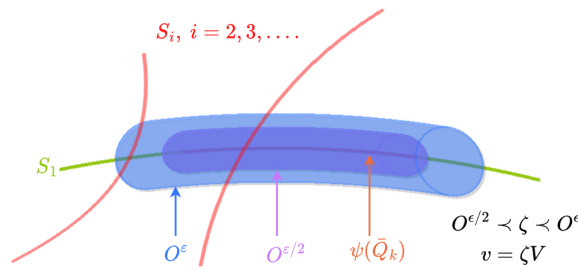


Figure 10: Schematic diagram of the proof of Theorem 4.1

Now we are ready to obtain the first important result in this work. That is a necessary and sufficient condition for the removable singularities of SBV functions. Some key quantities and sets constructed in the proof of Theorem 4.1 are illustrated with various colors in the schematic diagram, namely Figure 10. To clarify our ideas, we also make three claims which play the roles as milestones on the road of our proof.

Theorem 4.1 (necessary and sufficient condition of removable singularity). *Let $\Upsilon : H_0^1(\Omega) \rightarrow L^\infty(\Omega; S^{d \times d})$ and $\chi \in L^\infty(\Omega) \cap SBV(\Omega)$ with $\mathcal{H}^{d-1}(J_\chi) < +\infty$. Suppose there exist constants $\lambda_0, \Lambda_0 > 0$ satisfying*

$$\lambda_0 |\xi|^2 \leq \xi^\top \Upsilon[w](x) \xi \leq \Lambda_0 |\xi|^2$$

for all $w \in H_0^1(\Omega)$, $\xi \in \mathbb{R}^d$, and $x \in \Omega$. We have $\mathcal{H}^{d-1}(J_\chi) = 0$ if and only if

$$\mu(\Omega; \chi, \Upsilon, v) = 0, \quad \forall v \in C_c^1(\Omega). \tag{4.1}$$

Before we prove this theorem, we would like to stress that the sufficient part of this theorem is non-trivial. Even for a special case where $\Upsilon[w] = \bar{A}$ holds for all $w \in H_0^1(\Omega)$, the result of Theorem 4.1 is not standard. By the definition of μ in (3.4), the quantity in (4.1) with $\Upsilon[w] = \bar{A}$ reads as

$$\mu(\Omega; \chi, \bar{A}, \nu) = \int_{J_\chi} (\chi^+ - \chi^-) \nu_\chi^\top \bar{A} D\nu \, d\mathcal{H}^{d-1} = \bar{\mu}(D\nu),$$

where $\bar{\mu}$ is a Radon measure on Ω such that for all $\bar{\varphi} \in C(\Omega; \mathbb{R}^d)$

$$\bar{\mu}(\bar{\varphi}) = \int_{J_\chi} (\chi^+ - \chi^-) \nu_\chi^\top \bar{A} \bar{\varphi} \, d\mathcal{H}^{d-1}.$$

At first glance, it looks like a version of the fundamental lemma of the calculus of variation (sometimes also known as the Du Bois-Reymond lemma), which says that if a Radon measure $\hat{\mu}$ satisfying $\hat{\mu}(\hat{\varphi}) = 0$ for all $\hat{\varphi} \in C_c^\infty(\Omega)$, then $\hat{\mu} = 0$ on Ω . However, the setting in Theorem 4.1 is quite different. In fact $D\nu$ is in the form of a gradient. Therefore, what we have is not the fact that $\bar{\mu}(\bar{\varphi}) = 0$ for all $\bar{\varphi} \in C_c^\infty(\Omega; \mathbb{R}^d)$, but only the condition that $\bar{\mu}(D\nu) = 0$ for all $\nu \in C_c^1(\Omega)$. In general, such condition will not imply $\bar{\mu} = 0$. In our proof of Theorem 4.1, we essentially make use of the geometric structure of the jump part of BV function.

Besides, Υ takes a quite general form depending on ν and not necessarily being constant \bar{A} . This general form is necessary to develop our theory into the quasilinear case.

Proof. The necessary part of the statement is easy. In fact, by Corollary B.1, $\mathcal{H}^{d-1}(J_\chi) = 0$ implies $\chi \in W^{1,1}(\Omega)$, and hence $\mu(\Omega; \chi, \Upsilon, \nu) = 0$ holds. In the rest of the proof, we show by the method of contradiction that the condition (4.1) is also sufficient. Suppose that $\mu(\Omega; \chi, \Upsilon, \nu) = 0$ for all $\nu \in C_c^1(\Omega)$ and $\mathcal{H}^{d-1}(J_\chi) > 0$.

Claim 1. There exist an \mathcal{H}^{d-1} measurable set Σ , a C^1 -hypersurfaces S , and a function V such that $\Sigma \subseteq J_\chi \cap S$ and

$$\mu(\Sigma; \chi, \Upsilon, V) > 0.$$

Let $J_\chi^\pm = \{x \in J_\chi : \chi^+(x) - \chi^-(x) \gtrless 0\}$. Clearly, J_χ^\pm are \mathcal{H}^{d-1} measurable sets. Noticing $\mathcal{H}^{d-1}(J_\chi) = \mathcal{H}^{d-1}(J_\chi^+) + \mathcal{H}^{d-1}(J_\chi^-) > 0$, without loss of generality, we suppose that $\mathcal{H}^{d-1}(J_\chi^+) > 0$. By the structure theorem of J_χ , namely Theorem B.2, there is a countable sequence of C^1 -hypersurfaces $\{S_i\}_{i=1}^\infty$ satisfying $\mathcal{H}^{d-1}(J_\chi \setminus (\bigcup_{i=1}^\infty S_i)) = 0$. Thus we can pick an S from $\{S_i\}_{i=1}^\infty$ satisfying $\mathcal{H}^{d-1}(J_\chi^+ \cap S) > 0$.

Note that S is a C^1 -hypersurface. Thus for each $z \in S$, there exist a C^1 function h , a permutation of coordinates mapping $\tau : \mathbb{R}^d \rightarrow \mathbb{R}^d, x \mapsto \tau(x)$, and an open ball $B_{r_z}(z'_\tau) \subseteq \mathbb{R}^{d-1}$ with $r_z > 0$ such that S can locally be represented by the graph of $h: (x_\tau)_d = h(x'_\tau)$, $x'_\tau \in B_{r_z}(z'_\tau)$. Here the shorthand notation z'_τ means $((z_\tau)_1, \dots, (z_\tau)_{d-1})$. We also write

$x_\tau = \tau(x)$ for simplicity. Consider the transformation $\phi : B_{r_z}(z'_\tau) \times \mathbb{R} \rightarrow B_{r_z}(z'_\tau) \times \mathbb{R}$, $x_\tau \mapsto y = \phi(x)$ defined by

$$\begin{cases} y_i = \phi_i(x_\tau) = (x_\tau)_i, & i \in \{1, \dots, d-1\}, \\ y_d = \phi_d(x_\tau) = (x_\tau)_d - h(x'_\tau), \end{cases} \tag{4.2}$$

and its inverse transformation $\phi = \psi^{-1}$

$$\begin{cases} (x_\tau)_i = \psi_i(y) = y_i, & i \in \{1, \dots, d-1\}, \\ (x_\tau)_d = \psi_d(y) = y_d + h(y'). \end{cases} \tag{4.3}$$

In short, we write

$$y = \phi(x_\tau) = (\phi_1(x_\tau), \dots, \phi_d(x_\tau)), \tag{4.4}$$

$$x_\tau = \psi(y) = (\psi_1(x_\tau), \dots, \psi_d(x_\tau)). \tag{4.5}$$

By this construction, we have $|\det D\phi| = |\det D\psi| = 1$.

Let $B_z = B_{r_z}(z'_\tau) \times [-r_z, r_z]$. For each $y \in B_z$, define

$$\Psi(y) = \tau^{-1} \circ \psi(y) = \tau^{-1}(y_1, \dots, y_{d-1}, y_d + h(y_1, \dots, y_{d-1})).$$

Thus Ψ is a C^1 diffeomorphism between B_z . Denote $U_z = \Psi(B_z)$. If we define for $x \in U_z$

$$\begin{aligned} \Phi(x) &= \phi \circ \tau(x) \\ &= ((x_\tau)_1, \dots, (x_\tau)_{d-1}, (x_\tau)_d - h((x_\tau)_1, \dots, (x_\tau)_{d-1})), \end{aligned}$$

then $\Phi \circ \Psi = I$ on B_z and $\Psi \circ \Phi = I$ on U_z with $|\det D\Phi| = |\det D\Psi| = 1$. See Figure 11 for the relations between these transformations.

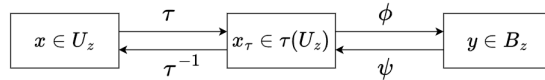


Figure 11: Sketch map of coordinate transformations between U_z and B_z .

Let $V(x) = \Phi_d(x)$ for all $x \in U_z$. Clearly, $V(x) = 0$ on $U_z \cap S$. By choosing r_z small enough, we can require that $0 < |DV(x)| < C$ on U_z , where C only depends on d and J_χ . Let us choose an appropriate U_z such that $\mathcal{H}^{d-1}(\Psi(B_{r_z/2}(z'_\tau) \times [-\frac{r_z}{2}, \frac{r_z}{2}]) \cap S) > 0$. Thanks to Lindelöf's lemma, such U_z exists because the manifold S is second countable and a countable union of such $\Psi(B_{r_z/2}(z'_\tau) \times [-\frac{r_z}{2}, \frac{r_z}{2}])$ must cover S , and hence also cover $J_\chi^+ \cap S$. Let $\Sigma = J_\chi^+ \cap \Psi(B_{r_z/2}(z'_\tau) \times \{0\}) \subseteq J_\chi \cap S$ and $\Sigma' = J_\chi^+ \cap U_z \cap S$.

Note that $DV = |DV| v_\chi$ on Σ' and $\chi^+ - \chi^- > 0$ on Σ . Therefore

$$\mu(\Sigma; \chi, \Upsilon, V) = \int_\Sigma (\chi^+ - \chi^-) v_\chi^\top \Upsilon[V] v_\chi |DV| d\mathcal{H}^{d-1} > 0,$$

where we use the uniform ellipticity of $\Upsilon[V]$.

Claim 2. There is a “ $(d - 1)$ -dimensional cube” $Q_k \subseteq B_{r_z/2}(z'_\tau)$ with $\bar{Q}_k = Q_k \times \{0\}$ satisfying

$$\mu(\Psi(\bar{Q}_k); \chi, \Upsilon, V) > 0.$$

For each $\delta > 0$, there exists countably many dyadic cubes $\{Q_k\}_{k=1}^\infty$ which are almost disjoint and satisfy $Q_k \subseteq B_{r_z/2}(z'_\tau)$, $\Sigma \subseteq \Psi(\cup_{k=1}^\infty \bar{Q}_k)$, and $\mathcal{H}^{d-1}(\Psi(\cup_{k=1}^\infty \bar{Q}_k) \setminus \Sigma) < \delta$. Thus we have

$$\begin{aligned} \sum_{k=1}^\infty \mu(\Psi(\bar{Q}_k); \chi, \Upsilon, V) &= \mu(\Psi(\cup_{k=1}^\infty \bar{Q}_k); \chi, \Upsilon, V) \\ &= \mu(\Sigma; \chi, \Upsilon, V) + \mu(\Psi(\cup_{k=1}^\infty \bar{Q}_k) \setminus \Sigma; \chi, \Upsilon, V) \\ &\geq \mu(\Sigma; \chi, \Upsilon, V) - 2\|\chi\|_{L^\infty(\Omega)} \Lambda_0 \|DV\|_{L^\infty(U_z)} \mathcal{H}^{d-1}(\Psi(\cup_{k=1}^\infty \bar{Q}_k) \setminus \Sigma) \\ &> 0, \end{aligned} \tag{4.6}$$

where the first equality is due to that $\{Q_k\}_{k=1}^\infty$ are almost disjoint, in the third inequality we use Lemma 4.1 and uniform ellipticity, and δ is taken small enough in the last line. Thus there is some Q_k satisfying $\mu(\Psi(\bar{Q}_k); \chi, \Upsilon, V) > 0$.

Claim 3. There is a function $v \in C_c^1(\Omega)$ such that

$$\mu(\Omega; \chi, \Upsilon, v) > 0.$$

This claim contradicts $\mu(\Omega; \chi, \Upsilon, v) = 0$, and hence the statement of the theorem is completed. Towards the claim, we consider the ε -neighborhood of $\Psi(\bar{Q}_k)$ as follows

$$O^\varepsilon = \{y \in \Omega: |y - x| < \varepsilon \text{ for some } x \in \Psi(\bar{Q}_k)\},$$

where $\varepsilon < \frac{1}{2} \text{dist}(\Psi(\bar{Q}_k), \partial U_z)$. This is admissible since

$$\text{dist}(\Psi(\bar{Q}_k), \partial U_z) > \text{dist}\left(\Psi(B_{r_z/2}(z'_\tau) \times [-\frac{r_z}{2}, \frac{r_z}{2}]), \partial U_z\right) \geq 0. \tag{4.7}$$

The neighborhood $O^{\varepsilon/2}$ is defined similarly. By Lemma 4.2 with $\text{dist}(O^{\varepsilon/2}, \partial O^\varepsilon) > \frac{\varepsilon}{4}$, there is a cutoff function $\zeta \in C_c^\infty(O^\varepsilon)$ such that

$$O^{\varepsilon/2} \prec \zeta \prec O^\varepsilon \text{ and } \|D\zeta\|_{L^\infty(O^\varepsilon)} \leq \frac{C}{\varepsilon}, \tag{4.8}$$

where C depends only on d . Let $v = \zeta V$. Note that $\mu(O^\varepsilon; \chi, \Upsilon, v) = \mu(\Omega; \chi, \Upsilon, v)$ due to $v \in C_c^1(O^\varepsilon)$. It is sufficient to consider the integration $\mu(O^\varepsilon; \chi, \Upsilon, v)$. Let $O_S^\varepsilon = O^\varepsilon \cap S$. Take the decomposition as shown in Figure 10:

$$\mu(O^\varepsilon; \chi, \Upsilon, v) = \mu(O_S^\varepsilon; \chi, \Upsilon, v) + \mu(O^\varepsilon \setminus O_S^\varepsilon; \chi, \Upsilon, v).$$

We will later show that the first integration has a lower bound, that is,

$$\mu(O_S^\varepsilon; \chi, \Upsilon, \nu) \geq \frac{3}{4} \mu(\Psi(\bar{Q}_k); \chi, \Upsilon, V),$$

while the second integration has a small contribution, that is,

$$|\mu(O^\varepsilon \setminus O_S^\varepsilon; \chi, \Upsilon, \nu)| \leq \frac{1}{2} \mu(\Psi(\bar{Q}_k); \chi, \Upsilon, V).$$

These estimates with the decomposition together lead to

$$\mu(O^\varepsilon; \chi, \Upsilon, \nu) \geq \frac{1}{4} \mu(\Psi(\bar{Q}_k); \chi, \Upsilon, V) > 0,$$

and therefore the proof is completed.

Notice that $V(x) = 0$ for all $x \in \Psi(B_{r_z}(z'_\tau) \times \{0\})$. Thus

$$V(x) \leq \varepsilon \|DV\|_{L^\infty(O^\varepsilon)} < C\varepsilon, \quad \forall x \in O^\varepsilon, \tag{4.9}$$

where C depends on d and J_χ . This with (4.8) leads to

$$|Dv(x)| \leq |D\zeta(x)| |V(x)| + |\zeta(x)| |DV(x)| < C, \quad \forall x \in O^\varepsilon, \tag{4.10}$$

where C depends on d and J_χ . By monotonicity of the measure \mathcal{H}^{d-1} , we have

$$\lim_{\varepsilon \rightarrow 0} \mathcal{H}^{d-1}(O_S^\varepsilon \cap J_\chi) = \mathcal{H}^{d-1}(\Psi(\bar{Q}_k) \cap J_\chi).$$

Hence for small enough constant $\varepsilon_1 > 0$, we obtain

$$\begin{aligned} \mu(O_S^\varepsilon; \chi, \Upsilon, \nu) &= \mu(\Psi(\bar{Q}_k); \chi, \Upsilon, \nu) + \mu(O_S^\varepsilon \setminus \Psi(\bar{Q}_k); \chi, \Upsilon, \nu) \\ &= \mu(\Psi(\bar{Q}_k); \chi, \Upsilon, V) + \int_{(O_S^\varepsilon \setminus \Psi(\bar{Q}_k)) \cap J_\chi} (\chi^+ - \chi^-) v_\chi^\top \Upsilon[v] Dv \, d\mathcal{H}^{d-1} \\ &\geq \mu(\Psi(\bar{Q}_k); \chi, \Upsilon, V) - 2\|\chi\|_{L^\infty(\Omega)} \Lambda_0 \|Dv\|_{L^\infty(O^\varepsilon)} \mathcal{H}^{d-1}((O_S^\varepsilon \setminus \Psi(\bar{Q}_k)) \cap J_\chi) \\ &\geq \frac{3}{4} \mu(\Psi(\bar{Q}_k); \chi, \Upsilon, V), \end{aligned}$$

where the second equality is due to $\nu = V$ on $\Psi(\bar{Q}_k) \cap J_\chi$ and the last step holds by choosing $\varepsilon < \varepsilon_1$.

Similarly, by monotonicity of the measure \mathcal{H}^{d-1} , we have

$$\lim_{\varepsilon \rightarrow 0} \mathcal{H}^{d-1}((O^\varepsilon \setminus O_S^\varepsilon) \cap J_\chi) = 0.$$

By choosing $\varepsilon < \varepsilon_2$ for small enough constant $\varepsilon_2 > 0$ and combining (4.10), we obtain

$$\begin{aligned} |\mu(O^\varepsilon \setminus O_S^\varepsilon; \chi, \Upsilon, \nu)| &\leq 2\|\chi\|_{L^\infty(\Omega)}\Lambda_0\|D\nu\|_{L^\infty(O^\varepsilon)}\mathcal{H}^{d-1}((O^\varepsilon \setminus O_S^\varepsilon) \cap J_\chi) \\ &\leq \frac{1}{2}\mu(\Psi(\bar{Q}_k); \chi, \Upsilon, V). \end{aligned}$$

As discussed above, this completes the whole proof. □

Now we extend this result to the case of systems.

Theorem 4.2 (necessary and sufficient condition of removable singularity for system). *Let $\Upsilon^{\alpha\beta} : H_0^1(\Omega) \rightarrow L^\infty(\Omega; S^{d \times d})$ and $\chi^{\alpha\beta} \in L^\infty(\Omega) \cap SBV(\Omega)$ with $\mathcal{H}^{d-1}(J_{\chi^{\alpha\beta}}) < +\infty$ for each $\alpha, \beta \in \{1, \dots, d'\}$ with $d' \geq 1$. Suppose that there exist $\lambda_0, \Lambda_0 > 0$ such that for all $\alpha, \beta \in \{1, \dots, d'\}$, $w \in H_0^1(\Omega)$, $\xi \in \mathbb{R}^d$, $x \in \Omega$*

$$\lambda_0|\xi|^2 \leq \xi^\top \Upsilon^{\alpha\beta}[w]\xi \leq \Lambda_0|\xi|^2.$$

Then $\mathcal{H}^{d-1}(J_{\chi^{\alpha\beta}}) = 0$ for all $\alpha, \beta \in \{1, \dots, d'\}$ if and only if

$$\sum_{\beta=1}^{d'} \mu(\Omega; \chi^{\alpha\beta}, \Upsilon^{\alpha\beta}, \nu^\beta) = 0, \quad \forall \nu \in C_c^1(\Omega; \mathbb{R}^{d'}), \forall \alpha \in \{1, 2, \dots, d'\}. \quad (4.11)$$

Proof. The proof is a standard adaptation of proof of Theorem 4.1. We highlight some key modification, omit the details, and outline the proof by just stating three claims which are counterpart of those in Theorem 4.1. The necessary part is clear. As above, we show by the method of contradiction that the condition (4.11) is also sufficient still by dividing this proof into three parts. Suppose that for some $\alpha_0, \beta_0 \in \{1, \dots, d'\}$, $\sum_{\beta=1}^{d'} \mu(\Omega; \chi^{\alpha_0\beta}, \Upsilon^{\alpha_0\beta}, \nu^\beta) = 0$ for all $\nu \in C_c^1(\Omega; \mathbb{R}^{d'})$ and $\mathcal{H}^{d-1}(J_{\chi^{\alpha_0\beta_0}}) > 0$.

Claim 1. There are $\alpha_0, \beta_0 \in \{1, \dots, d'\}$, an \mathcal{H}^{d-1} measurable set Σ , a C^1 -hypersurface S and a function $V \in C^1(\Omega; \mathbb{R}^{d'})$ such that $\Sigma \subseteq J_{\chi^{\alpha_0\beta_0}} \cap S$ and

$$\mu(\Sigma; \chi^{\alpha_0\beta_0}, \Upsilon^{\alpha_0\beta_0}, V^{\beta_0}) > 0$$

Following the proof of Claim 1 in Theorem 4.1 with J_χ replaced by $J_{\chi^{\alpha_0\beta_0}}$, we can construct $V^{\beta_0}(x) = \Phi_d(x)$ for all $x \in U_z$. Thus by defining $V = (0, \dots, V^{\beta_0}, \dots, 0)^\top \in C^1(U_z; \mathbb{R}^{d'})$, it is easy to check that

$$\mu(\Sigma; \chi^{\alpha_0\beta_0}, \Upsilon^{\alpha_0\beta_0}, V^{\beta_0}) > 0.$$

Comparing with the proof of Theorem 4.1, we emphasize that the new ingredient the definition of V which is a vector valued function with only one non-zero entry. By this construction of V , we further see that for all \mathcal{H}^{d-1} measurable set B ,

$$\sum_{\beta=1}^{d'} \mu(B; \chi^{\alpha_0\beta}, \Upsilon^{\alpha_0\beta}, V^\beta) = \mu(B; \chi^{\alpha_0\beta_0}, \Upsilon^{\alpha_0\beta_0}, V^{\beta_0}).$$

For the rest of the proof, we simply state the two claims and omit their proofs for which one can refer to the proof of Theorem 4.1.

Claim 2. There are $\alpha_0, \beta_0 \in \{1, \dots, d'\}$ and a “ $(d-1)$ -dimensional cube” $Q_k \subseteq B_{r_z/2}(z'_\tau)$ with $\bar{Q}_k = Q_k \times \{0\}$ such that

$$\mu(\Psi(\bar{Q}_k); \chi^{\alpha_0\beta_0}, \Upsilon^{\alpha_0\beta_0}, V^{\beta_0}) > 0.$$

Claim 3. There are $\alpha_0, \beta_0 \in \{1, \dots, d'\}$ and a function $v \in C_c^1(\Omega; \mathbb{R}^{d'})$ such that

$$\sum_{\beta=1}^{d'} \mu(\Omega; \chi^{\alpha_0\beta}, \Upsilon^{\alpha_0\beta}, v^\beta) = \mu(\Omega; \chi^{\alpha_0\beta_0}, \Upsilon^{\alpha_0\beta_0}, v^{\beta_0}) > 0.$$

□

4.2 Singularity in linear elliptic equations

Now we apply the removable singularity theorems (Theorem 4.1 and Theorem 4.2) to the case of linear elliptic equations as well as systems.

In Theorem 4.3 (as well as its counterpart for system, namely Theorem 4.4), we construct a more smooth function v_δ in $C_c^\infty(\Omega)$ instead of a function v just in $C_c^1(\Omega)$, as in the statement of Theorem 4.1. On the one hand, to guarantee the well-definedness of $\tilde{L}v_\delta$ in L^2 space, v_δ needs to be sufficiently regular, at least belonging to $W^{2,p}(\Omega)$. On the other hand, to quantify the deviation of the numerical solution, we have to achieve a particular solution v_δ to the modified equation (3.2) with a carefully chosen f . Therefore, this improvement on the regularity of v_δ is inevitable.

Theorem 4.3 (characterization of removable singularity with smooth function for equation). *Suppose that Assumption 2.1 holds with $d' = 1$. Then there exists a $v_\delta \in C_c^\infty(\Omega)$ such that*

$$\mu(\Omega; \chi, \bar{A}, v_\delta) > 0. \tag{4.12}$$

Proof. Let $\Upsilon[w] = \bar{A}$ for all $w \in H_0^1(\Omega)$. By Theorem 4.1 there is a $v \in C_c^1(\Omega)$ such that

$$\mu(\Omega; \chi, \bar{A}, v) = \int_{J_\chi} (\chi^+ - \chi^-) v_\chi^\top \bar{A} Dv \, d\mathcal{H}^{d-1} > 0.$$

To show (4.12), we approximate v by a smooth function $v_\delta \in C_c^\infty(\Omega)$. Similar to the proof of Lemma 4.2, choose a mollifier $\rho \in C_c^\infty(\mathbb{R}^d)$ with compact support $\bar{B}_1(0)$. For any $\delta > 0$, define $\rho_\delta(x) = \delta^{-d} \rho(\delta^{-1}x)$, $x \in \mathbb{R}^d$ and $v_\delta = v * \rho_\delta$ with $\delta < \frac{1}{4} \text{dist}(\Psi(\bar{Q}_k), \partial U_z)$ (See (4.7)). Thus We have $Dv_\delta \in C_c^\infty(\Omega)$ satisfying $Dv_\delta = v * D\rho_\delta$. Since $v \in C_c^1(\Omega)$, we obtain

$$\lim_{\delta \rightarrow 0} v * D\rho_\delta = Dv \text{ uniformly in } \Omega.$$

Since $\mathcal{H}^{d-1}(J_\chi) < +\infty$, we have for δ small enough

$$|\mu(\Omega; \chi, \bar{A}, v_\delta - v)| \leq 2\chi_{\max} \bar{\Lambda} \mathcal{H}^{d-1}(J_\chi) |Dv_\delta - Dv| \leq \frac{1}{2} \mu(\Omega; J_\chi, \bar{A}, v).$$

Thus we complete the proof by

$$\mu(\Omega; \chi, \bar{A}, v_\delta) = \mu(\Omega; \chi, \bar{A}, v_\delta - v) + \mu(\Omega; \chi, \bar{A}, v) \geq \frac{1}{2} \mu(\Omega; \chi, \bar{A}, v) > 0.$$

□

Theorem 4.4 (characterization of removable singularity with smooth function for system). *Suppose that Assumption 2.1 holds with $d' \geq 1$. Then there exists a $v_\delta \in C_c^\infty(\Omega; \mathbb{R}^{d'})$, such that*

$$\sum_{\beta=1}^{d'} \mu(\Omega; \chi^{\alpha_0\beta}, \bar{A}^{\alpha_0\beta}, v_\delta^\beta) > 0. \tag{4.13}$$

Proof. Apply Theorem 4.2 with $\Upsilon^{\alpha\beta}[w] = \bar{A}^{\alpha\beta}$ for all $\alpha, \beta \in \{1, \dots, d'\}$ and $w \in H_0^1(\Omega)$. Therefore, the proof is similar to that of Theorem 4.3. □

5 Deviation and implicit bias of RM methods

Based on the characterization of the singularities, we are ready to study the deviation and implicit bias of RM formulation for linear elliptic equations and systems. In Section 5.1, we state some preliminary results on the existence and *a priori* estimates of linear elliptic equations and systems which will be applied to equations (2.19) and (3.2). In Section 5.2, we show that the solution to the modified equation is deviated from the one to the original equation, which is a theoretical explanation to experiments mentioned

in Section 2.3. Consequently, we ask what kind of data f gives rise to such deviation and to what extent does such f occupy in L^2 space. We give a characterization by utilizing the RM-transformation T in Section 5.3, which gives a complete answer to the above question. In addition to the deviation in Section 5.2, we also study relative deviation in Section 5.4. Finally, in Section 5.5, we prove the implicit bias of RM method towards the solution to the modified equation. In fact, even if we choose initialization $\theta(0)$ such that the output function, $u_{\theta(0)}$, is close enough to the true solution of equation (2.19), u , after training via gradient flow with RM risk, the parameters θ will evolve and converge to some $\theta(\infty)$ with $u_{\theta(\infty)}$ which is very close to the solution to equation (3.2) \tilde{u} . This shows the RM methods at the exact solution u is unstable under small perturbation, and also the RM methods implicitly biases towards the solution to the modified equation.

5.1 Existence and *a priori* estimates

We prove the existence of solutions to the original and modified equations together with their *a priori* estimates. These results are standard, and we include them here for completeness.

Theorem 5.1 (existence and *a priori* estimates for linear elliptic equations and systems).

- (i) Suppose that Assumption 2.1 holds with $d' \geq 1$. For any $f \in L^2(\Omega; \mathbb{R}^{d'})$, system (2.19) has a unique solution $u \in H_0^1(\Omega; \mathbb{R}^{d'})$. Moreover, there exists a constant $C > 0$ such that

$$\|u\|_{H^1(\Omega; \mathbb{R}^{d'})} \leq C \|f\|_{L^2(\Omega; \mathbb{R}^{d'})}.$$

- (ii) Suppose that Assumption 2.1 holds with $d' \geq 1$. For any $f \in H^{-1}(\Omega; \mathbb{R}^{d'})$, system (2.19) has a unique solution $u \in H_0^1(\Omega; \mathbb{R}^{d'})$. Moreover, there exists a constant $C > 0$ such that

$$\frac{1}{C} \|f\|_{H^{-1}(\Omega; \mathbb{R}^{d'})} \leq \|u\|_{H^1(\Omega; \mathbb{R}^{d'})} \leq C \|f\|_{H^{-1}(\Omega; \mathbb{R}^{d'})}.$$

- (iii) Suppose that Assumption 2.1 and 3.1 hold with $d' \geq 1$. For any $f \in X$, system (3.2) has a unique solution $\tilde{u} \in H_0^1(\Omega; \mathbb{R}^{d'}) \cap H^2(\Omega; \mathbb{R}^{d'})$. Moreover, there exists a constant $C > 0$ such that

$$\frac{1}{C} \|f\|_{L^2(\Omega; \mathbb{R}^{d'})} \leq \|u\|_{H^2(\Omega; \mathbb{R}^{d'})} \leq C \|f\|_{L^2(\Omega; \mathbb{R}^{d'})}.$$

The constants C 's is independent of and f .

Proof.

- (i) See Theorem C.1 which is rephrased from standard textbook such as [45] for $d' = 1$, and Theorem C.3 which is rephrased from standard textbook such as [46] for $d' \geq 1$.
- (ii) The existence and the second inequality is also standard and can be found in Theorems C.1 and C.3. To show the first inequality, we notice for all $\varphi \in H_0^1(\Omega; \mathbb{R}^{d'})$ with $d' \geq 1$ and $\|\varphi\|_{H^1(\Omega; \mathbb{R}^{d'})} = 1$

$$\langle f, \varphi \rangle_{H^{-1}(\Omega; \mathbb{R}^{d'}), H_0^1(\Omega; \mathbb{R}^{d'})} \leq C \|D\varphi\|_{L^2(\Omega; \mathbb{R}^{d'})} \|Du\|_{L^2(\Omega; \mathbb{R}^{d'})} \leq C \|Du\|_{L^2(\Omega; \mathbb{R}^{d'})},$$

where C depends on Ω and A . Taking supremum, we obtain

$$\|f\|_{H^{-1}(\Omega; \mathbb{R}^{d'})} \leq C \|\tilde{u}\|_{H^1(\Omega; \mathbb{R}^{d'})}.$$

- (iii) For $d' = 1$, $X = L^2(\Omega)$, Theorem C.2 with $p = 2$ guarantees the existence of the solution \tilde{u} to the equation

$$-\sum_{i,j=1}^d (\bar{A}_{ij} D_{ij} \tilde{u} + \chi^{-1} D_i^a A_{ij} D_j \tilde{u}) = \chi^{-1} f.$$

Its solution \tilde{u} satisfies

$$\|\tilde{u}\|_{H^2(\Omega)} \leq C \|\chi^{-1} f\|_{L^2(\Omega)} \leq \chi_{\min}^{-1} C \|f\|_{L^2(\Omega)}, \tag{5.1}$$

where C depends on Ω , χ , and \bar{A} . Recall $A = \chi \bar{A}$. Obviously, \tilde{u} is also the solution to

$$\tilde{L}\tilde{u} = -\sum_{i,j=1}^d (A_{ij} D_{ij} \tilde{u} + D_i^a A_{ij} D_j \tilde{u}) = f.$$

Note that $\tilde{L}\tilde{u}$ is the weighted sum of $D_j \tilde{u}$ and $D_{ij} \tilde{u}$ with L^∞ coefficients A_{ij} and $D_i^a A_{ij}$, respectively. We have the following inequality

$$\|f\|_{L^2(\Omega)} = \|\tilde{L}\tilde{u}\|_{L^2(\Omega)} \leq C \|\tilde{u}\|_{H^2(\Omega)},$$

where C is independent of f .

For $d' > 1$, the set X in (3.6) is well-defined, and hence the existence to the equation (3.6) holds. And since for all $\tilde{u} \in X$, $\tilde{L}\tilde{u}$ is a linear combination of \tilde{u} up to second order and $A^{\alpha\beta} \in L^\infty(\Omega; S^{d \times d})$ and $D^a A^{\alpha\beta} \in L^\infty(\Omega; S^{d \times d})$ for all α, β . Thus for all $\tilde{u} \in X$, there is $C > 0$ such

$$\|f\|_{L^2(\Omega; \mathbb{R}^{d'})} \leq C \|\tilde{u}\|_{H^2(\Omega; \mathbb{R}^{d'})}.$$

and by Assumption 3.1, second inequality in (iii) and the uniqueness hold.

□

5.2 Deviation occurs

In this subsection, we prove that, for some specific f , the distance between the solutions to the original and modified equations is non-zero. According to our modelling in Section 3.1 and numerical simulation, the solutions u_θ and \tilde{u} are very close to each other. Therefore, in the worst case, the deviation of RM solution is not negligible for the elliptic equations. And this explains why PINN sometimes may fail as shown in Section 2.3.

The goal is clear, and essential we need to find a particular data f such that the corresponding u is not equal to \tilde{u} . In fact, as we mentioned previously, the set of f which induces a gap between u and \tilde{u} is identified by the kernel $\text{Ker}(T - I)$. Hence the transformation T is informative and required to be investigated. We will, in particular, show the compactness and the fact that it is generically not equal to identity. This is given by the following proposition.

Proposition 5.2 (properties of RM-transformation). Suppose that Assumptions 2.1 and 3.1 hold with $d' \geq 1$. Let u and \tilde{u} be solutions to the original equation/system (2.19) and modified equation/system (3.2) with data $f \in X$, respectively. Let T be the operator defined in (3.7). Then

- (i) $L: (H_0^1, \|\cdot\|_{H^1}) \rightarrow (H^{-1}, \|\cdot\|_{H^{-1}})$ is a bounded linear operator,
- (ii) $T: (X, \|\cdot\|_{L^2}) \rightarrow (H^{-1}, \|\cdot\|_{H^{-1}})$ is a bounded linear operator,
- (iii) $(Tf - f)^\alpha = (L\tilde{u} - \tilde{L}\tilde{u})^\alpha = -\sum_{\beta=1}^{d'} (\chi^{\alpha\beta+} - \chi^{\alpha\beta-}) \nu_{\chi^{\alpha\beta}} \bar{A}^{\alpha\beta} D\tilde{u}^\beta \, d\mathcal{H}^{d-1}$ for all $\alpha \in \{1, \dots, d'\}$ is a Radon measure and $Tf - f$ is in $H^{-1}(\Omega; \mathbb{R}^{d'})$
- (iv) $T \neq I$, that is, T is not the identity on $L^2(\Omega)$.

Proof. Clearly, L and T are both linear.

- (i) This is proved by Theorem 5.1 (ii).
- (ii) Estimate the H^{-1} norm of Tf by Theorem 5.2 (i)

$$\|Tf\|_{H^{-1}(\Omega; \mathbb{R}^{d'})} = \|L\tilde{u}\|_{H^{-1}(\Omega; \mathbb{R}^{d'})} \leq C\|\tilde{u}\|_{H^1(\Omega; \mathbb{R}^{d'})}, \quad (5.2)$$

where C depends on Ω and A . The natural embedding $H^1(\Omega) \hookrightarrow H^2(\Omega)$ with estimates (5.1) and (5.2) leads to the boundedness of T , that is,

$$\|Tf\|_{H^{-1}(\Omega; \mathbb{R}^{d'})} \leq C\|\tilde{u}\|_{H^1(\Omega; \mathbb{R}^{d'})} \leq C\|\tilde{u}\|_{H^2(\Omega; \mathbb{R}^{d'})} \leq C\|f\|_{L^2(\Omega; \mathbb{R}^{d'})},$$

where C 's are different from one inequality to another and depending on Ω , χ , \bar{A} .

(iii) By direct calculation with the structure theorem (Theorem B.1), $Tf - f$ satisfies for all $\alpha \in \{1, \dots, d'\}$

$$(Tf - f)^\alpha = (L\tilde{u} - \tilde{L}\tilde{u})^\alpha = - \sum_{\beta=1}^{d'} (\chi^{\alpha\beta+} - \chi^{\alpha\beta-}) v_{\chi^{\alpha\beta}} \bar{A}^{\alpha\beta} D\tilde{u}^\beta \, d\mathcal{H}^{d-1}$$

in the sense of Radon measure. Moreover, $Tf - f \in H^{-1}(\Omega; \mathbb{R}^{d'})$ as a consequence of the Theorem 5.2 (i) and (ii). In fact, we have with some C depending on Ω, χ, \bar{A} :

$$\|Tf - f\|_{H^{-1}(\Omega; \mathbb{R}^{d'})} \leq \|Tf\|_{H^{-1}(\Omega; \mathbb{R}^{d'})} + \|f\|_{H^{-1}(\Omega; \mathbb{R}^{d'})} \leq C\|f\|_{L^2(\Omega; \mathbb{R}^{d'})}.$$

(iv) By Theorem 4.3 and 4.4, there are $\alpha_0 \in \{1, \dots, d'\}$ and $v_\delta \in C_c^\infty(\Omega; \mathbb{R}^{d'})$ such that

$$\sum_{\beta=1}^{d'} \mu(\Omega; \chi^{\alpha_0\beta}, \bar{A}^{\alpha_0\beta}, v_\delta^\beta) > 0.$$

By setting $f = \tilde{L}v_\delta \in L^2(\Omega; \mathbb{R}^{d'})$, we have

$$(Tf - f)^{\alpha_0} = - \sum_{\beta=1}^{d'} (\chi^{\alpha_0\beta+} - \chi^{\alpha_0\beta-}) v_{\chi^{\alpha_0\beta}} \bar{A}^{\alpha_0\beta} Dv_\delta^\beta \, d\mathcal{H}^{d-1}$$

in the sense of Radon measure. Let $\Omega_n = \{x \in \Omega : \text{dist}(x, \partial\Omega) > \frac{1}{n}\}$ and use Lemma 4.2 to choose a cutoff function ζ_n such that $\Omega_n \prec \zeta_n \prec \Omega$. Then for sufficiently large n

$$\begin{aligned} & \langle (f - Tf)^{\alpha_0}, \zeta_n \rangle_{H^{-1}(\Omega), H_0^1(\Omega)} \\ &= \sum_{\beta=1}^{d'} \mu(\Omega; \chi^{\alpha_0\beta}, \zeta_n \bar{A}^{\alpha_0\beta}, v_\delta^\beta) \\ &= \sum_{\beta=1}^{d'} \mu(\Omega; \chi^{\alpha_0\beta}, \bar{A}^{\alpha_0\beta}, v_\delta^\beta) - \sum_{\beta=1}^{d'} \mu(\Omega; \chi^{\alpha_0\beta}, (1 - \zeta_n) \bar{A}^{\alpha_0\beta}, v_\delta^\beta) \\ &\geq \sum_{\beta=1}^{d'} \mu(\Omega; \chi, \bar{A}, v_\delta) - 2d' \chi_{\max} \bar{\Lambda} \|Dv_\delta\|_{L^\infty(\Omega)} \mathcal{H}^{d-1}((\Omega \setminus \Omega_n) \cap J_\chi) \\ &> 0, \end{aligned}$$

which implies $Tf \neq f$.

□

The last statement immediately implies that for specific f , the deviation of solution \tilde{u} from u occurs as follows.

Theorem 5.3 (deviation occurs for linear elliptic equations). *Suppose that Assumptions 2.1 and 3.1 hold with $d' \geq 1$. Then there exists $f \in L^2(\Omega; \mathbb{R}^{d'})$ such that $\|u - \tilde{u}\|_{H^1(\Omega; \mathbb{R}^{d'})} > 0$, where u and \tilde{u} are solutions to the original equation/system (2.19) and modified equation/system (3.2), respectively.*

Proof. By Proposition 5.2 (iv), there is $f \in L^2(\Omega; \mathbb{R}^{d'})$ such that $\|Tf - f\|_{H^{-1}(\Omega; \mathbb{R}^{d'})} > 0$, combining Theorem 5.1 (ii), there is $C > 0$ such that

$$\|u - \tilde{u}\|_{H^1(\Omega; \mathbb{R}^{d'})} \geq \frac{1}{C} \|Tf - f\|_{H^{-1}(\Omega; \mathbb{R}^{d'})} > 0,$$

and this completes the proof. \square

Remark 5.1. We have to note that for all theorems in Section 5, when $d' = 1$, only Assumption 2.1 is required. And Assumption 3.1 is needed for the case $d' > 1$.

5.3 Deviation occurs generically

Based on Proposition 5.2, we further study the eigenvalue and eigenspace of T in this subsection. We recall that an eigenvalue could be a complex number in general. Hence, for the full consideration of the eigenvalue problem, we would like to enlarge the space of f from X to the complex-valued one, namely $\bar{X} := \{\tilde{L}w : w \in H_0^1(\Omega; \mathbb{C}^{d'}) \cap H^2(\Omega; \mathbb{C}^{d'})\}$. Meanwhile, we extend the operator T to $\bar{T} : \bar{X} \rightarrow H^{-1}(\Omega; \mathbb{C}^{d'})$. But for notational simplicity, we still write T for \bar{T} . This will not cause any ambiguity, since we only need this extension for the discussion on eigenvalues. Similar remark applies to the system case in Theorem 5.4.

No matter whether we consider the eigenvalue problem over the complex field or the real field, the only eigenvalue of T is 1, as shown in Theorem 5.4. Hence there is no harm to regard all functions to be real-valued, and it is consistent to our situation, that is, to study the real-valued PDE problems. Next, to characterize the implicit bias via RM-transformation, we only need to consider the real-valued kernel $\text{Ker}(T - I)$ which consists of all RM-invariant data f . Thus the $X \setminus \text{Ker}(T - I)$ consists of data f satisfying $u \neq \tilde{u}$. In the following theorems, we show that the latter is more generic, and hence RM method fail for almost all data f in equations considered in this paper.

Theorem 5.4 (eigenvalue and eigenspace of T for linear elliptic equation/system). *Suppose that Assumption 2.1 and 3.1 hold with $d' \geq 1$ and $\bigcup_{\alpha, \beta=1}^{d'} J_{\chi^{\alpha\beta}}$ is not dense in Ω . Then we have*

- (i) $\sigma(T) = \{1\}$;
- (ii) $\text{Ker}(T - I) = \{f \in X : \exists w \text{ such that } \tilde{L}w = f, \forall \alpha \sum_{\beta=1}^{d'} \mu(\cdot; \chi^{\alpha\beta}, \bar{A}^{\alpha\beta}, w) = 0\}$;
- (iii) $L^2(\Omega; \mathbb{R}^{d'}) \setminus \text{Ker}(T - I)$ is dense in $L^2(\Omega; \mathbb{R}^{d'})$;
- (iv) X is a closed subspace of $L^2(\Omega; \mathbb{R}^{d'})$ and $X \setminus \text{Ker}(T - I)$ is relatively open in $L^2(\Omega; \mathbb{R}^{d'})$.

As above, we also note that $\sum_{\beta=1}^{d'} \mu(\cdot; \chi^{\alpha\beta}, \bar{A}^{\alpha\beta}, w) = 0, \forall \alpha \in \{1, \dots, d'\}$ for all \mathcal{H}^{d-1} measurable set B is equivalent to $\sum_{\beta=1}^{d'} \bar{A}^{\alpha\beta} D w^\beta \cdot D^j \chi^{\alpha\beta} = 0, \forall \alpha \in \{1, \dots, d'\}$ as Radon measures.

Proof.

- (i) For any $f \in \bar{X}$, let \tilde{u} be the solution to (3.2) with data f .

For $z \in \mathbb{C} \setminus \{1\}$, we have for all $\alpha \in \{1, \dots, d'\}$

$$T f^\alpha - z f^\alpha = (1 - z) f^\alpha + \sum_{\beta=1}^{d'} \bar{A}^{\alpha\beta} D \tilde{u}^\alpha \cdot D^j \chi^{\alpha\beta} \quad \text{in the sense of Radon measure.}$$

Notice that the measures $(1 - z) f^\alpha$ and $\sum_{\beta=1}^{d'} \bar{A}^{\alpha\beta} D \tilde{u}^\alpha \cdot D^j \chi^{\alpha\beta}$ are mutually singular to

each other. Hence

$$T f - z f = 0 \text{ is equivalent to } (1 - z) f^\alpha = 0 \text{ and } \sum_{\beta=1}^{d'} \bar{A}^{\alpha\beta} D \tilde{u}^\alpha \cdot D^j \chi^{\alpha\beta} = 0, \quad \forall \alpha \in \{1, \dots, d'\}.$$

Therefore for all $\alpha, f^\alpha = 0$. By Assumption 3.1, we have $\tilde{u} = 0$.

For $z = 1$, we obtain for all $\alpha \in \{1, \dots, d'\}$

$$T f^\alpha - f^\alpha = \sum_{\beta=1}^{d'} \bar{A}^{\alpha\beta} D \tilde{u}^\beta \cdot D^j \chi^{\alpha\beta}.$$

Since $\cup_{\alpha,\beta=1}^{d'} J_{\chi^{\alpha\beta}}$ is not dense in Ω , there is a open ball $B_r(x)$ such that $B_r(x) \cap (\cup_{\alpha,\beta=1}^{d'} J_{\chi^{\alpha\beta}}) = \emptyset$. By choosing $B_{\frac{r}{2}}(x) \prec \tilde{u} \prec B_r(x)$ and $f = \tilde{L}\tilde{u}$, we obtain

$$Tf - f = 0.$$

Hence $\sigma(T) = \{1\}$.

(ii) This is obvious.

(iii) By Theorem 4.2, there are α_0 and $v_\delta \in C_c^\infty(\Omega; \mathbb{R}^{d'})$ such that

$$\sum_{\beta=1}^{d'} \mu(\Omega; \chi^{\alpha_0\beta}, \bar{A}^{\alpha_0\beta}, v_\delta^\beta) \neq 0.$$

By setting $g = \tilde{L}v_\delta$, it is easy to see that $Tg \neq g$. For each $f \in \text{Ker}(T - I)$, let $f_\varepsilon = f + \varepsilon \frac{g}{\|g\|_{L^2(\Omega; \mathbb{R}^{d'})}}$. We have $f_\varepsilon \notin \text{Ker}(T - I)$ for all $\varepsilon > 0$ and that $\lim_{\varepsilon \rightarrow 0} f_\varepsilon = f$.

Hence $X \setminus \text{Ker}(T - I)$ is dense in X . Therefore $L^2(\Omega; \mathbb{R}^{d'}) \setminus \text{Ker}(T - I)$ is dense in $L^2(\Omega; \mathbb{R}^{d'})$.

(iv) We show that X is closed under $L^2(\Omega; \mathbb{R}^{d'})$ norm. By Theorem 5.1, there is $C > 0$

$$\|\tilde{L}w\|_{L^2(\Omega; \mathbb{R}^{d'})} \leq C\|w\|_{H^2(\Omega; \mathbb{R}^{d'})}.$$

By choosing a Cauchy sequence $\{f_k\}_{k=1}^\infty \subseteq X$ with $f_k = \tilde{L}\tilde{u}_k$, there is $f \in L^2(\Omega; \mathbb{R}^{d'})$ and $\tilde{u} \in H_0^1(\Omega; \mathbb{R}^{d'}) \cap H^2(\Omega; \mathbb{R}^{d'})$ such that

$$\begin{aligned} \lim_{k \rightarrow \infty} \|f - f_k\|_{L^2(\Omega; \mathbb{R}^{d'})} &= 0, \\ \lim_{k \rightarrow \infty} \|\tilde{u} - \tilde{u}_k\|_{H^2(\Omega; \mathbb{R}^{d'})} &= 0. \end{aligned}$$

Now we show that $\tilde{L}\tilde{u} = f$, \mathcal{L}^d -a.e. and that $\|\tilde{u}\|_{H^2(\Omega; \mathbb{R}^{d'})} \leq C\|f\|_{L^2(\Omega; \mathbb{R}^{d'})}$.

Note that

$$\begin{aligned} \|\tilde{L}\tilde{u} - f\|_{L^2(\Omega; \mathbb{R}^{d'})} &\leq \|\tilde{L}\tilde{u} - \tilde{L}\tilde{u}_k\|_{L^2(\Omega; \mathbb{R}^{d'})} + \|\tilde{L}\tilde{u}_k - f\|_{L^2(\Omega; \mathbb{R}^{d'})} \\ &\leq C\|\tilde{u} - \tilde{u}_k\|_{H^2(\Omega; \mathbb{R}^{d'})} + \|f_k - f\|_{L^2(\Omega; \mathbb{R}^{d'})}. \end{aligned}$$

Taking $k \rightarrow \infty$, we obtain $\|\tilde{L}\tilde{u} - f\|_{L^2(\Omega; \mathbb{R}^{d'})} = 0$. Moreover,

$$\begin{aligned} \|\tilde{u}\|_{H^2(\Omega; \mathbb{R}^{d'})} &\leq \|\tilde{u}_k - \tilde{u}\|_{H^2(\Omega; \mathbb{R}^{d'})} + \|\tilde{u}_k\|_{H^2(\Omega; \mathbb{R}^{d'})} \\ &\leq C\|f_k\|_{L^2(\Omega; \mathbb{R}^{d'})} + \|\tilde{u}_k - \tilde{u}\|_{H^2(\Omega; \mathbb{R}^{d'})} \\ &\leq C\|f\|_{L^2(\Omega; \mathbb{R}^{d'})} + C\|f - f_k\|_{L^2(\Omega; \mathbb{R}^{d'})} + \|\tilde{u}_k - \tilde{u}\|_{H^2(\Omega; \mathbb{R}^{d'})}. \end{aligned} \tag{5.3}$$

Taking $k \rightarrow \infty$ again, we have $\|\tilde{u}\|_{H^2(\Omega; \mathbb{R}^{d'})} \leq C\|f\|_{L^2(\Omega; \mathbb{R}^{d'})}$. Hence C is a closed set.

Now by letting $\{f_k\}_{k=1}^\infty \subseteq X \cap \text{Ker}(T - I)$ be a Cauchy sequence under L^2 norm, there is an f such that

$$\lim_{k \rightarrow \infty} f_k = f \in X.$$

In the rest, we show $f \in \text{Ker}(T - I)$.

Also let u and u_k be the solution to (2.19) with data f and f_k , respectively. Since $f_k \in \text{Ker}(T - I)$ for all k , then $u_k = \tilde{u}_k$, \mathcal{L}^d -a.e..

By (5.3), we have:

$$\begin{aligned} \|u - u_k\|_{L^2(\Omega; \mathbb{R}^{d'})} &\leq C\|f - f_k\|_{L^2(\Omega; \mathbb{R}^{d'})}, \\ \|\tilde{u} - \tilde{u}_k\|_{L^2(\Omega; \mathbb{R}^{d'})} &\leq C\|f - f_k\|_{L^2(\Omega; \mathbb{R}^{d'})}, \end{aligned}$$

which indicates that $u = \tilde{u}$, \mathcal{L}^d -a.e.. Thus

$$Tf = L\tilde{u} = Lu = f,$$

which means $Tf = f$ and hence $f \in \text{Ker}(T - I)$.

□

When $d' = 1$, we have $X = L^2(\Omega)$ and when $d' > 1$, X is the largest space that makes equation (3.2) solvable. Theorem 5.4 (iii) and (iv) together claim that most of f in X make deviation occur.

To illustrate Theorem 5.4, we show in the following example that for $d' = 1$ and $f \in \text{Ker}(T - I)$, we have $u = \tilde{u}$ and the numerical solution u_θ matches them quite accurately. Of course, such f should be very rare according to Theorem 5.4.

Example 5.1 (back to 1-d). We again consider (2.8) with coefficients and right hand side as follows:

$$A(x) = \begin{cases} \frac{1}{2}, & x \in (-1, 0), \\ 1, & x \in [0, 1), \end{cases} \quad f(x) = \begin{cases} -1, & x \in (-1, 0), \\ -2, & x \in [0, 1). \end{cases} \quad (5.4)$$

For this problem, we have $u = \tilde{u} = x^2 - 1$ and hence $D_x \tilde{u} = 2x$ which satisfies $D_x \tilde{u}(0) = 0$. Thus by Theorem 5.4, $Tf = f$, which means the equalities hold: $u = \tilde{u}$. Here the numerical simulation is under the same setting as that of Section 2.3.

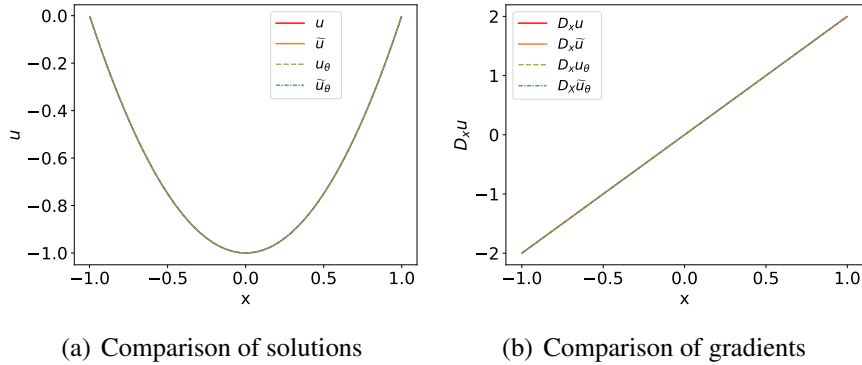


Figure 12: PINN can fit the exact solution to (2.8) with coefficients as (5.4).

The numerical simulation indicates $u = \tilde{u} \approx u_\theta$, which verifies Theorem 5.4, though only for very rare f .

The behavior of RM method solving linear PDEs satisfying Assumption 2.1 can be summarized as follows: if $\mu(\cdot; \chi, \bar{A}, \tilde{u}) = 0$, then $u_\theta \approx \tilde{u}_\theta \approx \tilde{u} = u$, if $\mu(\cdot; \chi, \bar{A}, \tilde{u}) \neq 0$, then $u_\theta \approx \tilde{u}_\theta \approx \tilde{u} \neq u$.

5.4 Deviation occurs severely

As we studied in Section 5.2, for $f \notin \text{Ker}(T - I)$, the deviation occurs, that is $\|u - \tilde{u}\|_{H^1(\Omega)} > 0$. From this, it is still unknown whether the relative deviation $\sup_{f \in L^2(\Omega)} \frac{\| \tilde{u} - u \|_{H^1(\Omega)}}{\| \tilde{u} \|_{H^1(\Omega)}}$ is bounded or not. In this section, we step further and prove that the supremum could be infinity, i.e., $\sup_{f \in L^2(\Omega)} \frac{\| \tilde{u} - u \|_{H^1(\Omega)}}{\| \tilde{u} \|_{H^1(\Omega)}} = +\infty$ (See Theorem 5.5). Furthermore, we will obtain a stronger result (See Proposition 5.6) showing that even for data f sufficiently close to the RM-invariant subspace $\text{Ker}(T - I)$, the relative deviation can still achieve have a finite value.

Theorem 5.5 (Unboundedness of relative deviation for linear elliptic equation). *Suppose that Assumptions 2.1 and 3.1 hold with $d' \geq 1$. For the countably many $(d - 1)$ -dimensional C^1 manifolds $\{S_i^{\alpha\beta}\}_{i=1}^\infty$ such that $\mathcal{H}^{d-1} \left(\bigcup_{\alpha,\beta=1}^{d'} \left(J_{\chi^{\alpha\beta}} - \bigcup_{i=1}^\infty S_i^{\alpha\beta} \right) \right) = 0$ (see in Theorem B.2), suppose that there is a constant $r_0 > 0$ such that for $(i, \alpha_1, \beta_1) \neq (j, \alpha_2, \beta_2)$, $\text{dist}(S_i^{\alpha_1\beta_1}, S_j^{\alpha_2\beta_2}) = \inf_{x \in S_i^{\alpha_1\beta_1}, y \in S_j^{\alpha_2\beta_2}} |x - y| \geq r_0$. Then*

$$\sup_{f \in L^2(\Omega; \mathbb{R}^{d'})} \frac{\| \tilde{u} - u \|_{H^1(\Omega; \mathbb{R}^{d'})}}{\| \tilde{u} \|_{H^1(\Omega; \mathbb{R}^{d'})}} = +\infty. \tag{5.5}$$

where u and \tilde{u} are solutions to the original system (2.19) and modified system (3.2) with data $f \in L^2(\Omega; \mathbb{R}^{d'})$, respectively.

Proof. Let's start with the case $d' = 1$: By Theorem 5.1, we have

$$\frac{\|\tilde{u} - u\|_{H^1(\Omega)}}{\|\tilde{u}\|_{H^1(\Omega)}} \geq C \frac{\|Tf - f\|_{H^{-1}(\Omega)}}{\|\tilde{u}\|_{H^1(\Omega)}} = C \frac{\|(\chi^+ - \chi^-)v_\chi \bar{A} D \tilde{u} d_{\mathcal{H}^{d-1}}\|_{H^{-1}(\Omega)}}{\|\tilde{u}\|_{H^1(\Omega)}}, \quad (5.6)$$

where for the last equality, we refer readers to Proposition 5.2. Combining Theorems 4.1 and 4.3, there is a $v_\delta = \rho_\delta * v \in C_c^\infty(\Omega)$ with $v = \zeta V \in C_c^1(\Omega)$, where ρ_δ , ζ and V are defined according to the proofs of Theorems 4.1 and 4.3. Since $\|v\|_{H^1(\Omega)} > 0$ and $\mu(\Omega; \chi, \bar{A}, v) > 0$, we have

$$\|(\chi^+ - \chi^-)v_\chi \bar{A} D v d_{\mathcal{H}^{d-1}}\|_{H^{-1}(\Omega)} > 0. \quad (5.7)$$

Case 1. Proof of the theorem when $\|(\chi^+ - \chi^-)v_\chi \bar{A} D v d_{\mathcal{H}^{d-1}}\|_{H^{-1}(\Omega)} = +\infty$.

For each $k \in \mathbb{N}^+$, there is a $\varphi_k \in C_c^\infty(\Omega)$ such that

$$\mu(\Omega; \chi, \varphi_k \bar{A}, v) \geq k \|\varphi_k\|_{H^1(\Omega)}.$$

We can choose sufficiently small δ such that

$$\mu(\Omega; \chi, \varphi_k \bar{A}, v_\delta - v) \leq \|\varphi_k\|_{H^1(\Omega)},$$

because $v_\delta = \rho_\delta * v \rightarrow v$ uniformly and $\|\varphi_k\|_{L^\infty(\Omega)} < +\infty$. Hence

$$\mu(\Omega; \chi, \varphi_k \bar{A}, v_\delta) \geq (k - 1) \|\varphi_k\|_{H^1(\Omega)}.$$

Therefore

$$\|(\chi^+ - \chi^-)v_\chi \bar{A} D v_\delta d_{\mathcal{H}^{d-1}}\|_{H^{-1}(\Omega)} \geq k - 1. \quad (5.8)$$

Moreover $\lim_{\delta \rightarrow 0} \|v_\delta\|_{H^1(\Omega)} = \|v\|_{H^1(\Omega)}$, which indicates that

$$\lim_{\delta \rightarrow 0} \frac{\|\tilde{u} - u\|_{H^1(\Omega)}}{\|\tilde{u}\|_{H^1(\Omega)}} = +\infty,$$

where u, \tilde{u} are solutions to equation (2.19) and (3.2) respectively with the data $f = \tilde{L}v_\delta$.

Case 2. Proof of the theorem when $\|(\chi^+ - \chi^-)v_\chi \bar{A} D v d_{\mathcal{H}^{d-1}}\|_{H^{-1}(\Omega)} < +\infty$.

Recall that

$$V(x) = (x_\tau)_d - h(x'_\tau), \quad (5.9)$$

where $x'_\tau = ((x_\tau)_1, \dots, (x_\tau)_{d-1})$, h is a C^1 function, and for all $x \in S \cap U_z$, $V(x) = 0$, and the unit normal vector at $x \in S \cap U_z$ is $v_\chi = \frac{DV}{|DV|}$ by proof of Theorem 4.1.

Claim 1. For each $r \in (0, 1]$, there is a function v such that

$$Dv = \frac{1}{r}Dv, \text{ for all } x \in S \cap U_z.$$

By our construction in the proof of Theorems 4.1 and 4.3, $v = \zeta V$ is supported in O^ε and v_δ is supported in $O^{2\varepsilon}$ with

$$\varepsilon = \delta < \frac{1}{4} \min(\text{dist}(\Psi(\bar{Q}_k), \partial U_z), r_0).$$

Since $V(x) = 0, x \in S \cap U_z$ and $\|DV\|_{L^\infty(O^\varepsilon)} \leq C$ according to (4.9), then $|V(x)| \leq 2C\varepsilon, x \in O^{2\varepsilon}$. By choosing $\varepsilon \leq \varepsilon_1$ with a sufficiently small $\varepsilon_1 > 0$, we can define for $0 < r \leq 1$

$$\begin{aligned} C_r &= \{(y', y_d) : \exists \omega \in \mathbb{R} \text{ such that } \Psi(y', \omega) \in O^{2\varepsilon}, |y_d| \leq 2Cr\varepsilon\} \\ &= B \times [-2Cr\varepsilon, 2Cr\varepsilon], \end{aligned}$$

where $B = \{y' : \exists \omega \in \mathbb{R} \text{ such that } \Psi(y', \omega) \in O^{2\varepsilon}\}$ and $O^{2\varepsilon} \subseteq \Psi(C_1) \subseteq U_z$. Thus we have $\|v_\delta\|_{H^1(\Omega)} = \|v_\delta\|_{H^1(\Psi(C_1))}$.

Consider the integration over C_1

$$\begin{aligned} \int_{\Psi(C_1)} v_\delta(x) \, dx &= \int_{\Psi(C_1)} [\rho_\delta * (\zeta V)](x) \, dx \\ &= \int_B \int_{-2C\varepsilon}^{2C\varepsilon} [\rho_\delta * (\zeta V)] \circ \tau^{-1}(y', y_d + h(y')) \, dy_d \, dy'. \end{aligned}$$

Denote $Q(y) = [\rho_\delta * (\zeta V)] \circ \tau^{-1} \circ \psi(y)$ with $y = (y', y_d)$ and consider the rescaled function $F(y)$ defined on C_r and $v(x)$ defined on $x \in U_z$ respectively as

$$F(y) = F(y', y_d) = Q\left(y', \frac{1}{r}y_d\right) = [\rho_\delta * v] \circ \tau^{-1}\left(y', \frac{1}{r}y_d + h(y')\right) \tag{5.10}$$

and

$$v(x) = v \circ \tau^{-1}\left(x'_\tau, \frac{1}{r}(x_\tau)_d + \frac{r-1}{r}h(x'_\tau)\right).$$

It is easy to verify that $v \in H_0^1(\Omega)$. For simplicity, we denote

$$\begin{aligned} z(x) &= \zeta \circ \tau^{-1}\left(x'_\tau, \frac{1}{r}(x_\tau)_d + \frac{r-1}{r}h(x'_\tau)\right), \\ V(x) &= V \circ \tau^{-1}\left(x'_\tau, \frac{1}{r}(x_\tau)_d + \frac{r-1}{r}h(x'_\tau)\right). \end{aligned}$$

By the definition of V as in (5.9), we have for $x \in U_z$

$$\begin{aligned} V(x) &= V \circ \tau^{-1} \left(x'_\tau, \frac{1}{r}(x_\tau)_d + \frac{r-1}{r}h(x'_\tau) \right) \\ &= \frac{1}{r}(x_\tau)_d + \frac{r-1}{r}h(x'_\tau) - h(x'_\tau) = \frac{1}{r}((x_\tau)_d - h(x'_\tau)) = \frac{1}{r}V(x). \end{aligned}$$

Hence $V(x) = V(x) = 0$ and $DV(x) = \frac{1}{r}DV(x)$ for all $x \in S \cap U_z$. For $x \in S \cap U_z$, $(x_\tau)_d = h(x'_\tau)$ implies that for each $x \in S \cap U_z$,

$$z(x) = \zeta \circ \tau^{-1} \left(x'_\tau, \frac{1}{r}(x_\tau)_d + \frac{r-1}{r}h(x'_\tau) \right) = \zeta \circ \tau^{-1}(x_\tau) = \zeta(x). \tag{5.11}$$

Thus by the product rule, we have for $x \in S \cap U_z$

$$Dv = VDz + zDV = zDV = \frac{1}{r}\zeta DV = \frac{1}{r}Dv(x). \tag{5.12}$$

Claim 2. For $r \in (0, 1]$, $\|v\|_{H^1(\Omega)} \leq \frac{C}{\sqrt{r}}$ for some constant $C > 0$ independent of r .

For all $x \in O^{2\varepsilon}$, we have

$$|zDV| = \frac{1}{r}|zDV| \leq \frac{1}{r} \sup_{x \in U_z} |DV(x)| \leq \frac{C}{r}. \tag{5.13}$$

With a little bit abuse of notation, we use $\tau(i)$ to denote the i -th entry of $\tau((1, \dots, d)^\top)$. For $i \in \{1, \dots, d-1\}$

$$\begin{aligned} D_{\tau(i)}z &= D_{\tau(i)}[\zeta] \left(\tau^{-1} \left(x'_\tau, \frac{1}{r}(x_\tau)_d + \frac{r-1}{r}h(x'_\tau) \right) \right) \\ &\quad + \frac{r-1}{r}D_{\tau(d)}[\zeta] \left(\tau^{-1} \left(x'_\tau, \frac{1}{r}(x_\tau)_d + \frac{r-1}{r}h(x'_\tau) \right) \right) D_i[h](x'_\tau), \\ D_{\tau(d)}z &= \frac{1}{r}D_{\tau(d)}[\zeta] \left(\tau^{-1} \left(x'_\tau, \frac{1}{r}(x_\tau)_d + \frac{r-1}{r}h(x'_\tau) \right) \right). \end{aligned}$$

Since h is C^1 function in U_z and $\tau^{-1} \left(x'_\tau, \frac{1}{r}(x_\tau)_d + \frac{r-1}{r}h(x'_\tau) \right) \in O^{2\varepsilon} \subseteq U_z$, combining (4.8), we have for all $x \in C_r$,

$$|Dz| \leq \frac{dC}{r\varepsilon}. \tag{5.14}$$

Thus

$$|VDz| = \left| \frac{1}{r}VDz \right| \leq \frac{1}{r}2Cr\varepsilon \frac{dC}{r\varepsilon} \leq \frac{C}{r}. \tag{5.15}$$

Combining (5.13) and (5.15), we obtain $|Dv(x)| \leq \frac{2C}{r}$ for all $x \in C_r$. Therefore

$$\|v\|_{H^1(\Omega)}^2 = \|v\|_{L^2(\Omega)}^2 + \|Dv\|_{L^2(\Omega)}^2 \leq r \int_{\Psi(C_r)} v^2 dx + \frac{C}{r} \leq \frac{C}{r},$$

where C is independent of r .

Claim 3. For each $r \in (0, 1]$, there is $\delta > 0$ such that the convolution $v_\delta = \rho_\delta * v \in H_0^1(\Omega) \cap H^2(\Omega)$ satisfying

$$\|(\chi^+ - \chi^-)v_\chi \bar{A} Dv_\delta d\mathcal{H}^{d-1}\|_{H^{-1}(\Omega)} > \frac{C}{\sqrt{r}}$$

for some constant $C > 0$ independent of r .

Note that

$$\|(\chi^+ - \chi^-)v_\chi \bar{A} Dv d\mathcal{H}^{d-1}\|_{H^{-1}(\Omega)} = \frac{1}{r} \|(\chi^+ - \chi^-)v_\chi \bar{A} Dv d\mathcal{H}^{d-1}\|_{H^{-1}(\Omega)} > 0.$$

Hence there is $\varphi \in C_c^\infty(\Omega)$ such that

$$\mu(\Omega; \chi, \varphi \bar{A}, v) \geq \frac{3}{4} \|(\chi^+ - \chi^-)v_\chi \bar{A} Dv d\mathcal{H}^{d-1}\|_{H^{-1}(\Omega)} \|\varphi\|_{H^1(\Omega)}.$$

Let $v_\delta = \rho_\delta * v \in H_0^1(\Omega) \cap H^2(\Omega)$, by the property of mollifier $\lim_{\delta \rightarrow 0} \|v_\delta - v\|_{H^1(\Omega)} = 0$. We thus can choose $\delta \leq \varepsilon_2$ with sufficiently small ε_2 such that

$$\frac{\|v\|_{H^1(\Omega)}}{\|v_\delta\|_{H^1(\Omega)}} \geq \frac{1}{2} \text{ and } \mu(\Omega; \chi, \varphi \bar{A}, v_\delta) \geq \frac{1}{2} \|(\chi^+ - \chi^-)v_\chi \bar{A} Dv d\mathcal{H}^{d-1}\|_{H^{-1}(\Omega)} \|\varphi\|_{H^1(\Omega)},$$

which implies

$$\|(\chi^+ - \chi^-)v_\chi \bar{A} Dv_\delta d\mathcal{H}^{d-1}\|_{H^{-1}(\Omega)} \geq \frac{1}{2} \|(\chi^+ - \chi^-)v_\chi \bar{A} Dv d\mathcal{H}^{d-1}\|_{H^{-1}(\Omega)}.$$

Hence there is $\delta = \varepsilon < \min(\frac{\text{dist}(Q_k, \partial U_z)}{4}, r_0, \varepsilon_1, \varepsilon_2)$ such that

$$\begin{aligned} & \frac{\|(\chi^+ - \chi^-)v_\chi \bar{A} Dv_\delta d\mathcal{H}^{d-1}\|_{H^{-1}(\Omega)}}{\|v_\delta\|_{H^1(\Omega)}} \\ &= \frac{\|(\chi^+ - \chi^-)v_\chi \bar{A} Dv_\delta d\mathcal{H}^{d-1}\|_{H^{-1}(\Omega)}}{\|(\chi^+ - \chi^-)v_\chi \bar{A} Dv d\mathcal{H}^{d-1}\|_{H^{-1}(\Omega)}} \times \frac{\|(\chi^+ - \chi^-)v_\chi \bar{A} Dv d\mathcal{H}^{d-1}\|_{H^{-1}(\Omega)}}{\|v\|_{H^1(\Omega)}} \times \frac{\|v\|_{H^1(\Omega)}}{\|v_\delta\|_{H^1(\Omega)}} \\ &\geq \frac{1}{4r} \frac{\|(\chi^+ - \chi^-)v_\chi \bar{A} Dv d\mathcal{H}^{d-1}\|_{H^{-1}(\Omega)}}{\|v\|_{H^1(\Omega)}} \\ &\geq \frac{C}{\sqrt{r}} \|(\chi^+ - \chi^-)v_\chi \bar{A} Dv d\mathcal{H}^{d-1}\|_{H^{-1}(\Omega)}. \end{aligned} \tag{5.16}$$

Recalling (5.7) and taking $r \rightarrow 0^+$, we obtain

$$\lim_{r \rightarrow 0^+} \frac{\|(\chi^+ - \chi^-)v_\chi \bar{A} D v_\delta \, d\mathcal{H}^{d-1}\|_{H^{-1}(\Omega)}}{\|v_\delta\|_{H^1(\Omega)}} = +\infty. \tag{5.17}$$

Let $\tilde{u} = v_\delta$ and $f = \tilde{L}v_\delta$ for sufficiently small r . Also recall the definition of u . Thus (5.6) and (5.17) leads to the desired unboundedness of $\frac{\|\tilde{u}-u\|_{H^1(\Omega)}}{\|\tilde{u}\|_{H^1(\Omega)}}$.

For the case of $d' > 1$, since Assumption 2.1 holds, by Theorem 5.1 (ii), there is constant $C > 0$ such that $\|u\|_{H^1(\Omega; \mathbb{R}^{d'})} > \frac{1}{C} \|f^\alpha\|_{H^{-1}(\Omega; \mathbb{R}^{d'})}$.

Thus we have

$$\begin{aligned} \frac{\|\tilde{u} - u\|_{H^1(\Omega; \mathbb{R}^{d'})}}{\|\tilde{u}\|_{H^1(\Omega; \mathbb{R}^{d'})}} &\geq \frac{\|(Tf)^{\alpha_0} - f^{\alpha_0}\|_{H^{-1}(\Omega; \mathbb{R}^{d'})}}{C\|\tilde{u}\|_{H^1(\Omega; \mathbb{R}^{d'})}} \\ &= \frac{\left\| \sum_{\beta=1}^{d'} (\chi^{\alpha_0\beta+} - \chi^{\alpha_0\beta-}) v_{\chi^{\alpha_0\beta}} \bar{A} D \tilde{u}^\beta \, d\mathcal{H}^{d-1} \right\|_{H^{-1}(\Omega; \mathbb{R}^{d'})}}{C\|\tilde{u}\|_{H^1(\Omega; \mathbb{R}^{d'})}}. \end{aligned} \tag{5.18}$$

Recall the Claim 1 of proof of Theorem 4.2. Let $V = (0, \dots, V^{\beta_0}(x), \dots, 0)^\top \in C^1(U_z; \mathbb{R}^{d'})$, $v = \zeta V \in C^1(U_z; \mathbb{R}^{d'})$ where $\zeta \in C_c^\infty(\Omega; \mathbb{R}^{d'})$ and that $v_\delta = \rho_\delta * v$. Let $\tilde{u} = v_\delta$ and u be the solutions to equation (2.19) and (3.2) with $f = \tilde{L}\tilde{u}$, we obtain

$$\begin{aligned} \frac{\|\tilde{u} - u\|_{H^1(\Omega; \mathbb{R}^{d'})}}{\|\tilde{u}\|_{H^1(\Omega; \mathbb{R}^{d'})}} &\geq \frac{\left\| \sum_{\beta=1}^{d'} (\chi^{\alpha_0\beta+} - \chi^{\alpha_0\beta-}) v_{\chi^{\alpha_0\beta}} \bar{A} D \tilde{u}^\beta \, d\mathcal{H}^{d-1} \right\|_{H^{-1}(\Omega; \mathbb{R}^{d'})}}{C\|\tilde{u}\|_{H^1(\Omega; \mathbb{R}^{d'})}} \\ &= \frac{\|(\chi^{\alpha_0\beta_0+} - \chi^{\alpha_0\beta_0-}) v_{\chi^{\alpha_0\beta_0}} \bar{A} D \tilde{u}^{\beta_0} \, d\mathcal{H}^{d-1}\|_{H^{-1}(\Omega; \mathbb{R}^{d'})}}{C\|\tilde{u}^{\beta_0}\|_{H^1(\Omega; \mathbb{R}^{d'})}}. \end{aligned}$$

The rest of that follows the previous one, and hence we omits it. □

Proposition 5.6 (relative deviation is large even for nearly RM-invariant data). Assumptions 2.1 and 3.1 hold with $d' \geq 1$ and that J_χ is not dense in Ω . For each $f \in L^2(\Omega; \mathbb{R}^{d'})$, we define $f_{//}$ and f_\perp to be the projections of f onto the closed spaces $\text{Ker}(T - I)$ and $(\text{Ker}(T - I))^\perp$, respectively. Then there exist constants $\varepsilon_0 > 0$ and $C > 0$ such that for any $0 < \varepsilon \leq \varepsilon_0$, we have

$$\sup_{\|f_{//}\|_{L^2(\Omega; \mathbb{R}^{d'})} = 1, \|f_\perp\|_{L^2(\Omega; \mathbb{R}^{d'})} = \varepsilon} \frac{\|\tilde{u} - u\|_{H^1(\Omega; \mathbb{R}^{d'})}}{\|\tilde{u}\|_{H^1(\Omega; \mathbb{R}^{d'})}} \geq C, \tag{5.19}$$

where u and \tilde{u} are solutions to the original equation (2.19) and modified equation (3.2), respectively, with data $f = f_{//} + f_\perp$.

We stress that the constant $C > 0$ is independent of ε .

Proof. The proof for case of equation and system are almost the same and here we provide a proof for case of equation.

Let u_1 and \tilde{u}_1 are solutions to the original equation (2.19) and modified equation (3.2), respectively, corresponding to the data $f_{//}/\|f_{//}\|_{L^2(\Omega)}$. Let u_2 and \tilde{u}_2 are solutions to the original equation (2.19) and modified equation (3.2), respectively, corresponding to the data $f_{\perp}/\|f_{\perp}\|_{L^2(\Omega)}$. Here $f_{//}$ and f_{\perp} will be determined later.

By linearity, we have

$$\tilde{u} = \tilde{u}_1 + \varepsilon\tilde{u}_2, \quad u = u_1 + \varepsilon u_2.$$

This gives rise to

$$\begin{aligned} \frac{\|\tilde{u} - u\|_{H^1(\Omega)}}{\|u\|_{H^1(\Omega)}} &= \frac{\varepsilon\|\tilde{u}_2 - u_2\|_{H^1(\Omega)}}{\|u\|_{H^1(\Omega)}} \\ &\geq \frac{\varepsilon\|\tilde{u}_2 - u_2\|_{H^1(\Omega)}}{\varepsilon\|u_2\|_{H^1(\Omega)} + \|u_1\|_{H^1(\Omega)}}. \end{aligned} \quad (5.20)$$

We then claim that we can choose $f_{//} \in \text{Ker}(T - I)$ to make $\|u_1\|_{H^1(\Omega)}$ arbitrarily small. Notice that

$$\|u_1\|_{H^1(\Omega)} = \frac{\|u_1\|_{H^1(\Omega)}}{\|u_1\|_{H^2(\Omega)}} \|u_1\|_{H^2(\Omega)} \leq C \|f_{//}\|_{L^2} \frac{\|u_1\|_{H^1(\Omega)}}{\|u_1\|_{H^2(\Omega)}},$$

where the last inequality results from Theorem 5.1. Moreover, since J_{χ} is not dense in Ω , we can choose a cube $Q_r(y)$ centered at y with side length r such that $Q_r(y) \cap J_{\chi} = \emptyset$ with r to be determined later. We define for $x = (x_1, x_2, \dots, x_d) \in Q_r(y)$

$$u_g(x) = \prod_{i=1}^d \left[\cos\left(\frac{\pi(x_i - y_i)}{r}\right) + 1 \right].$$

Then

$$\|u_g\|_{H^1(\Omega)}^2 \leq (8r)^d + d\pi^2(8r)^{d-1} \frac{1}{r}.$$

Since

$$\|u_g\|_{H^2(\Omega)}^2 \geq \|\Delta u_g\|_{L^2(\Omega)}^2 = d(3\pi r)^{d-1} \pi^4 \frac{1}{r^3},$$

we have

$$\frac{\|u_g\|_{H^1(\Omega)}}{\|u_g\|_{H^2(\Omega)}} \leq \left(\frac{2\pi^2 d 8^{d-1} r^{d-2}}{\pi^4 d (3\pi)^{d-1} r^{d-4}} \right)^{1/2} < r.$$

Let $g = \tilde{L}u_g$. It is clear that $g \in \text{Ker}(T - I)$. By setting $f// = \frac{g}{\|g\|_{L^2}}$, we have

$$\|u_1\|_{H^1(\Omega)} = \frac{\|u_1\|_{H^1(\Omega)}}{\|u_1\|_{H^2(\Omega)}} \|u_1\|_{H^2(\Omega)} = \frac{\|u_g\|_{H^1(\Omega)}}{\|u_g\|_{H^2(\Omega)}} \|u_1\|_{H^2(\Omega)} \leq Cr.$$

Choose a sufficiently small r , say $r \leq \frac{\varepsilon \|u_2\|_{H^1(\Omega)}}{4C}$, and plugin it into (5.20). We obtain

$$\frac{\|\tilde{u} - u\|_{H^1(\Omega)}}{\|u\|_{H^1(\Omega)}} > \frac{4}{5} \frac{\|\tilde{u}_2 - u_2\|_{H^1(\Omega)}}{\|u_2\|_{H^1(\Omega)}}. \tag{5.21}$$

Notice that

$$\frac{\|u\|_{H^1(\Omega)}}{\|\tilde{u}\|_{H^1(\Omega)}} = \frac{\|u_1 + \varepsilon u_2\|_{H^1(\Omega)}}{\|u_1 + \varepsilon \tilde{u}_2\|_{H^1(\Omega)}} \geq \frac{\varepsilon \|u_2\|_{H^1(\Omega)} - \|u_1\|_{H^1(\Omega)}}{\varepsilon \|\tilde{u}_2\|_{H^2(\Omega)} + \|u_1\|_{H^1(\Omega)}} \geq \frac{\varepsilon \|u_2\|_{H^1(\Omega)} - Cr}{\varepsilon \|\tilde{u}_2\|_{H^1(\Omega)} + Cr} > \frac{1}{2}.$$

This with (5.21) gives rise to

$$\frac{\|\tilde{u} - u\|_{H^1(\Omega)}}{\|\tilde{u}\|_{H^1(\Omega)}} > \frac{2}{5} \frac{\|\tilde{u}_2 - u_2\|_{H^1(\Omega)}}{\|u_2\|_{H^1(\Omega)}}.$$

The last right hand side is a constant, and hence the proof is completed. □

5.5 Implicit bias towards the solution to the modified equation

For a given function w , the population risk in the residual minimization method for solving the modified equation/system reads as

$$\tilde{R}(w) = \int_{\Omega} (\tilde{L}w - f)^2 dx + \gamma \int_{\partial\Omega} (Bw - g)^2 dx. \tag{5.22}$$

In the following theorem and proposition, we show the implicit bias of RM methods via an energetic approach. Roughly speaking, for a function close to u , it has large (modified) risk \tilde{R} ; while for any function has small (modified) risk \tilde{R} , it should be close to \tilde{u} in the sense of H^1 norm.

Theorem 5.7 (bias against the solution to the original equation). *Suppose that Assumption 2.1 and 3.1 hold with $d' \geq 1$. Let u and \tilde{u} be solutions to the original equation/system (2.19) and modified equation/system (3.2) with data $f \in X \setminus \text{Ker}(T - I)$, respectively.*

There exist constants $\varepsilon_0 > 0$ and $C_0 > 0$ such that for all $0 < \varepsilon < \varepsilon_0$ and for all $v \in B_{\varepsilon}(u)$, we have $\tilde{R}(v) \geq C_0 > 0$. Here $B_{\varepsilon}(u) = \{w \in H_0^1(\Omega; \mathbb{R}^{d'}) \cap H^2(\Omega; \mathbb{R}^{d'}) : \|w - u\|_{H^1(\Omega; \mathbb{R}^{d'})} < \varepsilon, \tilde{L}w \in X\}$.

We remark that Theorem 5.7 implies that there is $\varepsilon > 0$ such that $B_\varepsilon(u) \cap \tilde{B}_\varepsilon(\tilde{u}) = \emptyset$, where $\tilde{B}_\varepsilon(\tilde{u}) = \{\tilde{v} \in H_0^1(\Omega; \mathbb{R}^{d'}) \cap H^2(\Omega; \mathbb{R}^{d'}) : \tilde{R}(\tilde{v}) < \varepsilon\}$.

Proof. Since $f \in X \setminus \text{Ker}(T - I)$, by Theorem 5.4, there is a constant C_1 such that

$$\|u - \tilde{u}\|_{H^1(\Omega; \mathbb{R}^{d'})} \geq C_1. \quad (5.23)$$

By linearity of the modified operator \tilde{L} , we have for all $v \in H_0^1(\Omega; \mathbb{R}^{d'}) \cap H^2(\Omega; \mathbb{R}^{d'})$

$$(\tilde{L}v - \tilde{L}\tilde{u})^\alpha = (\tilde{L}v)^\alpha - f^\alpha. \quad (5.24)$$

Since $\tilde{L}v \in X$, by the definition of X and Assumption 3.1

$$\|\tilde{u} - v\|_{H^2(\Omega; \mathbb{R}^{d'})} \leq C\|f - \tilde{L}v\|_{L^2(\Omega; \mathbb{R}^{d'})}. \quad (5.25)$$

Let $\varepsilon_0 = \frac{C_1}{2}$. The for all $\varepsilon < \varepsilon_0$ and $v \in B_\varepsilon(u)$, we have

$$\|v - \tilde{u}\|_{H^2(\Omega; \mathbb{R}^{d'})} \geq \|v - \tilde{u}\|_{H^1(\Omega; \mathbb{R}^{d'})} \geq \|\tilde{u} - u\|_{H^1(\Omega; \mathbb{R}^{d'})} - \|u - v\|_{H^1(\Omega; \mathbb{R}^{d'})} > \frac{C_1}{2}.$$

This together with (5.24) implies for all $v \in B_\varepsilon(u)$

$$\sqrt{\tilde{R}(v)} \geq \|\tilde{L}v - f\|_{L^2(\Omega; \mathbb{R}^{d'})} \geq \frac{1}{C}\|\tilde{u} - v\|_{H^2(\Omega; \mathbb{R}^{d'})} > \frac{C_1}{2C}.$$

The proof is completed by setting $C_0 = \frac{C_1^2}{4C^2}$. \square

Proposition 5.1 (bias towards the solution to the modified equation/system). *Suppose that Assumption 2.1 and 3.1 hold with $d' \geq 1$. Let \tilde{u} be the solution to the modified equation (3.2) with data $f \in X$.*

(i) *Then for all $w \in H_0^1(\Omega; \mathbb{R}^{d'}) \cap H^2(\Omega; \mathbb{R}^{d'})$, there is constant $C > 0$ such that*

$$\|w - \tilde{u}\|_{H^1(\Omega; \mathbb{R}^{d'})} \leq C\sqrt{\tilde{R}(w)}. \quad (5.26)$$

(ii) *Suppose that the function $w \in H_0^1(\Omega; \mathbb{R}^{d'}) \cap H^2(\Omega; \mathbb{R}^{d'})$, the random variable X is sampled from the uniform distribution over Ω , the random variable $Y = |\Omega|(Lw(X) - f)^2$ with covariance of Y satisfies $\mathbb{V}[Y] < +\infty$. Then for any $\delta > 0$, with probability $1 - \delta$ over the choice of independent uniformly distributed data $S := \{x_i\}_{i=1}^n$ in Ω , we have*

$$\tilde{R}(w) - \tilde{R}_S(w) \leq \frac{1}{\sqrt{n}} \sqrt{\frac{\mathbb{V}[Y]}{\delta}},$$

In particular, if $\tilde{R}(w) < \varepsilon$ for some small ε , then $\|w - \tilde{u}\|_{H^1(\Omega; \mathbb{R}^{d'})} \leq C\sqrt{\varepsilon}$.

Proof. (i) is a direct consequence from Theorem 5.1. And (ii) is a direct consequence from Monte Carlo integration. \square

We remark that in Proposition 5.1, for $w \in H_0^1(\Omega; \mathbb{R}^{d'}) \cap H^2(\Omega; \mathbb{R}^{d'})$ with $\mathbb{V}[Y] < +\infty$, if $\tilde{R}(w) \leq \varepsilon$, for n sufficiently large, we have $\|w - \tilde{u}\|_{H^1(\Omega; \mathbb{R}^{d'})} \leq C\sqrt{\varepsilon}$. Moreover, the condition $\mathbb{V}[Y] < +\infty$ is equivalent to the inequality $\|(D_x^2 w - D_x^2 \tilde{u})^2\|_{L^2(\Omega; \mathbb{R}^{d'})} < +\infty$.

Remark 5.2. Theorem 5.7 and Proposition 5.1 together lead to the implicit bias of RM method in solving PDE: it will bias the numerical solution against the solution to original equation (2.19) and towards the solution to modified equation (3.2).

6 A Relaxed Residual Minimization Method for PDEs with Discontinuous Coefficients

In previous discussion, we have demonstrated through both theoretical analysis and numerical experiments that the classical PINN framework fails to accurately solve PDEs with discontinuous coefficients. The underlying reason stems from a fundamental inconsistency between the regularity of neural network approximators and the intrinsic weak regularity required by the true solution of the PDE. In particular, when the coefficient function $A(x)$ is discontinuous, the weak formulation of the PDE requires that the derivative $u_x(x, t)$ must admit suitable discontinuities to compensate for the jumps in $A(x)$. However, due to the smooth nature of commonly used activation functions, neural networks such as those in standard PINNs inherently enforce the continuity of $u_{\theta_1}(x, t)$ and its spatial derivatives. As a result, the residual minimization process fails to represent valid weak solutions and produces large systematic errors near discontinuity points.

To mitigate this failure mode, we propose a Relaxed Residual Minimization method by introducing d auxiliary neural networks $v_{\theta_2}(x, t)$, i.e. $v_{\theta_2}(x, t) = \{v_{\theta_{2,1}}(x, t), \dots, v_{\theta_{2,d}}(x, t)\}$ to explicitly approximate the flux term $A(x)u_x(x, t)$. This allows us to decouple the computation of the flux from the computation of the solution, thereby relaxing the continuity requirement on $u_x(x, t)$. The primary network $u_{\theta_1}(x, t)$ still approximates the solution, while the residual loss is modified to permit non-smoothness in the derivative of u_{θ_1} , thereby enabling the solution network to adapt to the expected jump behavior at coefficient discontinuities. This modification directly targets the structural cause of the PINN failure and ensures that the approximation better aligns with the weak solution theory.

Mathematically, we focus on heat equation defined on $\Omega \times [0, T] := \Omega_T$, where Ω is a bounded domain in spatial direction, to imply the method

$$\begin{cases} u_t - \operatorname{div}(A(x)D_x u) = f(x, t) & (x, t) \in \Omega \times [0, T], \\ u(x, 0) = g(x) & x \in \Omega, \\ u(x, t) = h(x, t) & (x, t) \in \partial\Omega \times [0, T], \end{cases} \quad (6.1)$$

we introduce two neural networks: $u_{\theta_1}(x, t)$ to approximate the exact solution of (6.1) as $u(x, t)$, and d auxiliary neural networks $\mathbf{v}_{\theta_2}(x, t)$ to approximate the flux term $A(x)D_x u(x, t)$. By noting $\theta = \{\theta_1, \theta_2\}$, then the continuous form of the relaxed residual loss to (6.1) is defined as:

$$\begin{aligned} R_D^r(\theta) &= \frac{1}{|\Omega_T|} \left(\|D_t u_{\theta_1} - \operatorname{div} \mathbf{v}_{\theta_2} - f(x, t)\|_{L^2(\Omega_T)}^2 + \|\mathbf{v}_{\theta_2} - A(x)D_x u_{\theta_1}\|_{L^2(\Omega_T)}^2 \right), \\ R_D^b(\theta) &= \frac{1}{|\partial\Omega \times [0, T]|} \|u_{\theta_1}(x, t) - h(x, t)\|_{L^2(\partial\Omega \times [0, T])}^2, \\ R_D^i(\theta) &= \frac{1}{|\Omega|} \|u_{\theta_1}(x, 0) - g(x)\|_{L^2(\Omega)}^2. \end{aligned}$$

The total loss is then given by

$$R_D^{\text{relax}}(\theta) = R_D^r(\theta) + \gamma_1 R_D^b(\theta) + \gamma_2 R_D^i(\theta), \quad (6.2)$$

where γ_1 and γ_2 are two hyper-parameters to maintain the balance of magnitudes among the components of the loss function.

Let $\{(x_i^r, t_i^r)\}_{i=1}^{N_r} \subset \Omega_T$, $\{(x_j^b, t_j^b)\}_{j=1}^{N_b} \subset \partial\Omega \times [0, T]$, and $\{x_k^i\}_{k=1}^{N_i} \subset \Omega$ be collocation points for the interior domain, boundary, and initial conditions, respectively. Then the empirical loss is given by:

$$\begin{aligned} R_S^r(\theta) &= \frac{1}{N_r} \sum_{i=1}^{N_r} |D_t u_{\theta_1}(x_i^r, t_i^r) - \operatorname{div} \mathbf{v}_{\theta_2}(x_i^r, t_i^r) - f(x_i^r, t_i^r)|^2 \\ &\quad + \frac{1}{N_r} \sum_{i=1}^{N_r} |\mathbf{v}_{\theta_2}(x_i^r, t_i^r) - A(x_i^r)D_x u_{\theta_1}(x_i^r, t_i^r)|^2, \\ R_S^b(\theta) &= \frac{1}{N_b} \sum_{j=1}^{N_b} |u_{\theta_1}(x_j^b, t_j^b) - h(x_j^b, t_j^b)|^2, \\ R_S^i(\theta) &= \frac{1}{N_i} \sum_{k=1}^{N_i} |u_{\theta_1}(x_k^i, 0) - g(x_k^i)|^2. \end{aligned}$$

The total loss is then given by

$$R_S^{\text{relax}}(\theta) = R_S^r(\theta) + \gamma_1 R_S^b(\theta) + \gamma_2 R_S^i(\theta). \quad (6.3)$$

To assess the effectiveness of the proposed relaxed residual minimization method, we present numerical results for the heat equation (2.15). Our objective is to verify whether introducing the auxiliary network $v_{\theta_2}(x, t)$ enables the numerical network $u_{\theta_1}(x, t)$ to capture the correct weak solution behavior, particularly the discontinuous features in the spatial derivative.

For the numerical setups, we choose $\gamma_1 = \gamma_2 = 1$ in the experiments. And sampling 1000 points in $\Omega_T = (-1, 1) \times [0, 2]$ as $\{(x_i^r, t_i^r)\}_{i=1}^{N_r}$, 100 points on $\Omega = (-1, 1)$ as $\{x_k^i\}_{k=1}^{N_i}$, 100 points on both $\partial\Omega \times [0, T] \{\pm 1\} \times [0, 2]$ respectively as $\{(x_j^b, t_j^b)\}_{j=1}^{N_b}$. Both $u_{\theta_1}(x, t)$ and $v_{\theta_2}(x, t)$ are residual networks with structure $2 - 256 - 256 - 256 - 1$, tanh activation, Adam optimizer with Xavier initialization.

In the following, we present the heatmaps of absolute error between numerical solution $u_{\theta_1}(x, t)$ and exact solution $u(x, t)$ together with their absolute error of spatial derivatives. Also, we choose time slices as $t = 0, 1, 2$ to see how $u_{\theta_1}(x, t)$ and $u(x, t)$ with their spatial derivatives perform.

Figure 13 compares the numerical solution $u_{\theta_1}(x, t)$ with the exact solution $u(x, t)$, as well as their corresponding spatial derivatives, in the form of absolute error heatmaps. The results clearly indicate that the proposed method successfully forces $u_{\theta_1}(x, t)$ to exhibit sharp transitions near the discontinuity in $A(x)$, thereby enabling $D_x u_{\theta_1}$ to approximate the true derivative behavior. This observation aligns with the theoretical motivation: by approximating $A(x)u_x$ directly using v_{θ_2} , the method relaxes the continuity constraint on $D_x u_{\theta_1}$, allowing the network to match the weak solution structure.

Further insights are provided in Figure 14, which shows detailed comparisons at three representative time slices $t = 0, 1, 2$. Each column corresponds to a fixed time, with the first row depicting the comparison between $u_{\theta_1}(x, t)$ and $u(x, t)$, and the second row illustrating their spatial derivatives. It is evident that across all time slices, u_{θ_1} closely matches the true solution both in value and in the behavior of its spatial derivative. In particular, the spatial derivatives exhibit appropriate jumps at the discontinuity, confirming that the method achieves first-order derivative accuracy and convergence.

These empirical findings validate the core design principle of our method: by decoupling the flux term, the relaxation framework enables neural networks to overcome the failure mode of standard PINNs and to accurately resolve PDEs with discontinuous coefficients.

We also provide a theorem to indicate the stability of the method as follows

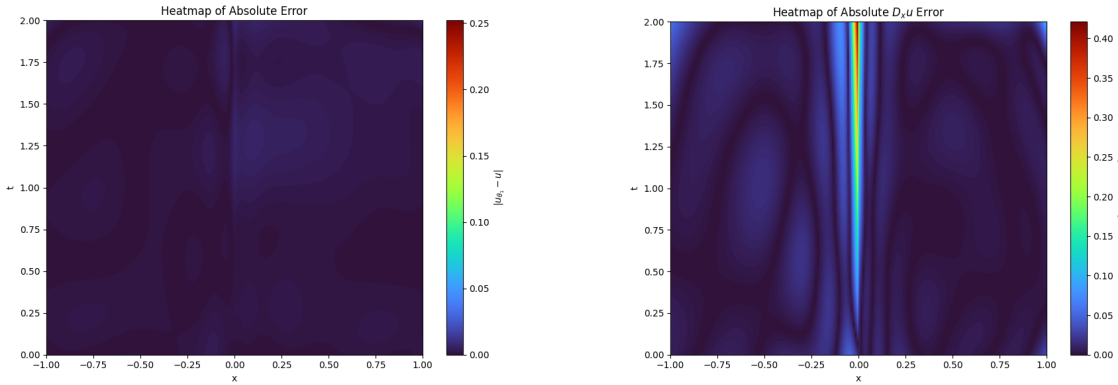


Figure 13: Heatmaps of errors. Left: Absolute error $|u_{\theta_1} - u|$. Right: Absolute derivative error $|D_x u_{\theta_1} - D_x u|$.

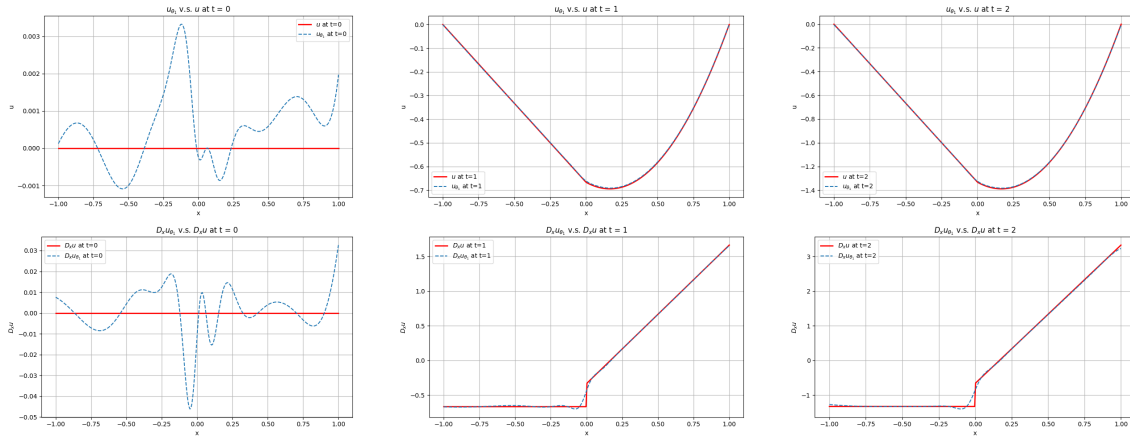


Figure 14: Comparison of solutions at time slices $t = 0, 1, 2$. Top row: Function values u_{θ_1}, u . Bottom row: Spatial derivatives $D_x u_{\theta_1}, D_x u$.

Theorem 6.1. Suppose that $u_{\theta_1}(x, 0) = g(x)$ on $x \in \Omega$, $u_{\theta_1}(x, t) = h(x, t)$ on $\partial\Omega \times [0, T]$. Then there is a constant C depends only on d, Ω, T such that

$$\|u_{\theta_1} - u\|_{L^2(H^1(\Omega); 0, T)}^2 < CR_D^{relax}(\theta) \tag{6.4}$$

Proof. By letting

$$\begin{aligned} v_\theta - AD_x u_{\theta_1} &= \varepsilon_1(x, t) \in \mathbb{R}^d \\ D_t u_{\theta_1} - \operatorname{div} v_\theta - f &= \varepsilon_2(x, t) \in \mathbb{R} \end{aligned}$$

we can immediately obtain that

$$\frac{1}{2} \frac{d}{dt} (u - u_{\theta_1})^2 + D_x (u - u_{\theta_1}) AD_x (u - u_{\theta_1}) = \varepsilon_1^\top D_x (u - u_{\theta_1}) + \varepsilon_2 (u - u_{\theta_1}) \tag{6.5}$$

by the uniform ellipticity and employing the energy estimates associated with parabolic equations, we complete the proof. \square

Remark 6.1. Although we have assumed that u_{θ_1} satisfies the initial and boundary conditions exactly, this assumption can be relaxed. In particular, under suitable regularity conditions on $\partial\Omega$, one can establish similar results without explicitly enforcing the initial-boundary compatibility, by employing standard energy estimates for parabolic equations and extension theorem about boundary defined functions.

A Notation

For the readers' convenience, we collect the frequently-used notations and list them in Table 2. Also for notation simplicity, unless specifically claimed, we abbreviate $g(x)$ as g for univariate functions. In the table, equation is the abbreviation of boundary value problem and RM is the abbreviation of residual minimization.

Table 2: List of notations.

Notation	Definition/Meaning	Refer to
$(Y, \ \cdot\ _Y)$	Banach space equipped with norm $\ \cdot\ _Y$	
$S^{d \times d}$	set of $d \times d$ symmetric real-valued matrices	
$a \odot b$	entry-wise multiplication, e.g., if $a, b \in \mathbb{R}^d$, then $c = a \odot b$ means $c_i = a_i b_i, i = \{1, \dots, d\}$	
$D_\xi \odot D_x(F)$	entry-wise differentiation, e.g., for $F(\xi, x)$ with $\xi, x \in \mathbb{R}^d, D_\xi \odot D_x(F) = (D_{\xi_1} D_{x_1} F, \dots, D_{\xi_d} D_{x_d} F)$	
f	right-hand-side of the PDE, (interior) data	
$F \circ G$	composition of functions: $(F \circ G)(x) = F(G(x))$	
$D_i[F](x), D_i F$	i -th partial derivative of F evaluated at x ; if no confusion, simply write $D_i F = D_i[F](x)$	
DF	$DF = (D_1 F, \dots, D_d F)^\top$	
J_χ, χ^\pm, v_χ	set of approximate jump points and related functions	Def. B.3

Notation	Definition/Meaning	Refer to
$D^j\chi, D^a\chi, D^c\chi$	absolutely continuous/jump/Cantor part of $D\chi$	Thm. B.1
d, d'	input/output dimension	Sec. 2.5
χ_{\min}, χ_{\max}	minimum/maximum of $\chi^{\alpha\beta}$	
$\bar{\lambda}, \bar{\Lambda}$	lower/upper bound of $\bar{A}^{\alpha\beta}$	
λ, Λ	lower/upper bound of A	
L, \tilde{L}	original/modified operator	Sec. 3.1
u, \tilde{u}	solution to original/modified equation	
$u_\theta, \tilde{u}_\theta$	RM solution to original/modified equation	
$\mu(B; \chi, \Upsilon, \varphi)$	$\mu(B; \chi, \Upsilon, \varphi) = \int_{B \cap J_\chi} (\chi^+ - \chi^-) v_\chi^\top \Upsilon[\varphi] D\varphi d\mathcal{H}^{d-1}$	Sec. 3.2
X	$X = \{\tilde{L}w : w \in H_0^1(\Omega; \mathbb{R}^{d'}) \cap H^2(\Omega; \mathbb{R}^{d'})\}$	Sec. 3.3
Tf	RM-transformed data $Tf = L\tilde{u}$	
T	RM-transformation $f \mapsto L\tilde{u}$	
$\sigma(T)$	spectrum of T	
$\text{Ker}(T - I)$	$\text{Ker}(T - I) = \text{Ker}_X(T - I) = \{f \in X : Tf = f\}$	
θ^{SV}	parameter obtained by supervised learning with target function u	Sec. 3.4
u_θ^{SV}	neural network function with parameter $\theta = \theta^{\text{SV}}$	
$u_\theta^{\text{SV} \rightarrow \text{RM}}, \tilde{u}_\theta^{\text{SV} \rightarrow \text{RM}}$	RM solution to original/modified equation with initial parameter $\theta_0 = \theta^{\text{SV}}$	
x'	$x' = (x_1, \dots, x_{d-1})$ for $x = (x_1, \dots, x_d) \in \mathbb{R}^d$	Sec. 4.1
$B_r(x)$	ball centered at x with radius r	
J_χ^\pm	$J_\chi^\pm = \{x \in J_\chi : \chi^+(x) - \chi^-(x) \gtrless 0\}$	
$U \prec \zeta \prec U'$	$\zeta \geq 0$ in \mathbb{R}^d with $\zeta = 1$ in U and $\zeta = 0$ in $\mathbb{R}^d \setminus U'$	
$\text{dist}(U, U')$	Euclidean distance between two sets U and U'	
\bar{X}	$\bar{X} = \{\tilde{L}w : w \in H_0^1(\Omega; \mathbb{C}^{d'}) \cap H^2(\Omega; \mathbb{C}^{d'})\}$	Sec. 5.3

B Functions of bounded variation

Here we list several definitions and theorems used in the main text.

Definition B.1 (function of bounded variation (BV), pp.117–118 [47]). *Let Ω be an open subset of \mathbb{R}^d and $\chi \in L^1(\Omega)$. We say that χ is a function of bounded variation on Ω if the distributional derivative of χ is representable by a finite Radon measure in Ω , that is, if*

$$\int_{\Omega} \chi D_i \varphi \, dx = - \int_{\Omega} \varphi D_i \chi \quad \forall \varphi \in C_c^\infty(\Omega), \quad i = 1, \dots, d$$

for some \mathbb{R}^d -valued measure $D\chi = (D_1\chi \dots D_d\chi)^\top$ in Ω . The vector space of all functions of bounded variation on Ω is denoted by $BV(\Omega)$.

Definition B.2 (approximate limit, rephrased from pp.160 [47]). *Let $\chi \in L^1_{\text{loc}}(\Omega)$. We say that χ has an approximate limit at $x \in \Omega$ if there exists $z \in \mathbb{R}$ such that*

$$\lim_{\rho \rightarrow 0} \frac{1}{|B_\rho(x)|} \int_{B_\rho(x)} |\chi(y) - z| \, dy = 0. \tag{B.1}$$

The set S_χ of points where this property does not hold is called the approximate discontinuity set. For any $x \in \Omega \setminus S_\chi$, z is uniquely determined by (B.1), denoted by $\chi^{\text{ap}}(x)$, and called the approximate limit of χ at x .

Definition B.3 (approximate jump points, pp.163 [47]). *Let $\chi \in L^1_{\text{loc}}(\Omega)$ and $x \in \Omega$. We say that x is an approximate jump point of χ if there exist $\chi^\pm(x) \in \mathbb{R}$ and a unit vector $\nu_\chi(x) \in S^{d-1}$ such that $\chi^+(x) \neq \chi^-(x)$ and*

$$\lim_{\rho \rightarrow 0} \frac{1}{|B_\rho^\pm(x, \nu)|} \int_{B_\rho^\pm(x, \nu)} |\chi(y) - \chi^\pm(x)| \, dy = 0, \tag{B.2}$$

where $B_\rho^\pm(x, \nu) = \{y \in B_\rho(x) : \pm \langle x - y, \nu \rangle > 0\}$. The triplet $(\chi^+(x), \chi^-(x), \nu_\chi(x))$ is uniquely determined by (B.2) up to a permutation of $(\chi^+(x), \chi^-(x))$ and a change of sign of $\nu_\chi(x)$. The set of approximate jump points is denoted by J_χ .

Theorem B.1 (structure theorem of BV function, rephrased from pp.183–185 & pp.212–213 [47]). *By Radon–Nikodym theorem, we have the representation $D\chi = D^a\chi + D^s\chi$, where $D^a\chi$ is the absolutely continuous part with respect to \mathcal{L}^d and $D^s\chi$ is the singular part with respect to \mathcal{L}^d . For any $\chi \in BV(\Omega)$, the jump part of the derivative $D^j\chi$ and the Cantor part of the derivative $D^c\chi$ are defined as*

$$D^j\chi = D^s\chi \llcorner_{J_\chi}, \quad D^c\chi = D^s\chi \llcorner_{\Omega \setminus S_\chi},$$

respectively. Then we have

$$D\chi = D^a\chi + D^j\chi + D^c\chi,$$

where $D^a\chi = \nabla\chi \mathcal{L}^d$, $\nabla\chi$ is the Radon–Nykodim density of $D^a\chi$ with respect to \mathcal{L}^d and $D^j\chi = (\chi^+ - \chi^-) \nu_\chi^\top \mathcal{H}^{d-1} \llcorner_{J_\chi}$.

Theorem B.2 (Structure theorem of approximate jump set for BV functions, pp.150 [48]). *Let Ω be a bounded open set and $\chi \in BV(\Omega)$, then there exist countably many C^1 -hypersurfaces ($(d - 1)$ -dimensional C^1 -manifolds) $\{S_k\}_{k=1}^\infty$ such that*

$$\mathcal{H}^{d-1} \left(J_\chi \setminus \bigcup_{k=1}^\infty S_k \right) = 0$$

Definition B.4 (special function of bounded variation (SBV), pp.212 [47]). *We say that $\chi \in BV(\Omega)$ is a special function of bounded variation and we write $\chi \in SBV(\Omega)$, if the Cantor part of its derivative $D^c\chi$ is zero. Thus, for $\chi \in SBV(\Omega)$, we have*

$$D\chi = D^a\chi + D^j\chi = \nabla\chi \mathcal{L}^d + (\chi^+ - \chi^-) \nu_\chi^\top \mathcal{H}^{d-1} \llcorner_{J_\chi}.$$

We further say that $\chi \in SBV^p(\Omega)$, $p \in [1, \infty]$ if and only if $\chi \in SBV(\Omega)$ and $\nabla\chi \in L^p(\Omega)$.

Corollary B.1 (property of special function of bounded variation, pp.212 [47]). *For any $\chi \in SBV(\Omega)$, we have*

$$\chi \in W^{1,1}(\Omega) \iff \mathcal{H}^{d-1}(J_\chi) = 0.$$

C Existence theorems for linear elliptic equations and systems in literature

In this appendix, we rephrase some existence theorems for linear elliptic equation and system from the literature. Theorems C.1 and C.2 focus on linear divergence and nondivergence equation, respectively, while Theorem C.3 works for linear divergence system.

Theorem C.1 (Theorem 8.3, rephrased from pp.181–182 [45]). *Let Ω be a bounded $C^{1,1}$ domain in \mathbb{R}^d , and let the operator L*

$$Lu = -\operatorname{div} \cdot (ADu) = - \sum_{i,j=1}^d D_i(a_{ij}D_ju)$$

being uniformly elliptic in Ω with coefficients $a_{ij} \in L^\infty(\Omega)$, namely there is $\lambda > 0$ satisfying $\xi^\top A \xi \geq \lambda |\xi'|^2$ for all $\xi \in \mathbb{R}^d$. Then the equation: $Lu = f$ in $\Omega, u = 0$ on $\partial\Omega$

with $f \in L^2(\Omega)$ (or $f \in H^{-1}(\Omega)$) is uniquely solvable. Furthermore, there is a constant C independent of u such that

$$\|u\|_{H^1(\Omega)} \leq C\|f\|_{L^2(\Omega)} \text{ or } (\leq C\|f\|_{H^{-1}(\Omega)}).$$

Theorem C.2 (Lemma 9.17, rephrased from pp.241–243 [45]). *Let Ω be a bounded $C^{1,1}$ domain in \mathbb{R}^d , and the operator \tilde{L}*

$$\tilde{L}u = \sum_{i,j=1}^d a_{ij}D_{ij}u + \sum_{i=1}^d b_iD_iu + cu,$$

being uniformly elliptic in Ω with coefficients $a_{ij} \in C(\bar{\Omega})$, $b_i, c \in L^\infty(\Omega)$, $c \leq 0$, with $i, j \in \{1, \dots, d\}$. If $f \in L^p(\Omega)$ for some $p \in (1, \infty)$, then the equation: $\tilde{L}u = f$ in Ω , $u = 0$ on $\partial\Omega$ has a unique solution $u \in W_0^{1,p}(\Omega) \cap W^{2,p}(\Omega)$. Furthermore, there is a constant C independent of u such that

$$\|u\|_{W^{2,p}(\Omega)} \leq C\|\tilde{L}u\|_{L^p(\Omega)}.$$

Theorem C.3 (Theorem 1.3, rephrased from pp.9–14 [46]). *Let Ω be a bounded $C^{1,1}$ domain in \mathbb{R}^d . Also define the operator L as follows*

$$(Lu)^\alpha = - \sum_{\beta=1}^{d'} \operatorname{div} \cdot (A^{\alpha\beta}(x)Du^\beta) = - \sum_{\beta=1}^{d'} \sum_{i,j=1}^d D_i(A_{ij}^{\alpha\beta} D_j u^\beta),$$

where $\alpha \in \{1, 2, \dots, d'\}$. Suppose that measurable functions $A^{\alpha\beta} \in S^{d \times d}$ are symmetric in α, β , namely $A^{\alpha\beta} = A^{\beta\alpha}$, and that the Hadamard–Legendre condition holds, namely there is $\lambda > 0$ satisfying $\sum_{\alpha,\beta=1}^{d'} (\xi^\alpha)^\top A^{\alpha\beta}(x) \xi^\beta \geq \lambda |\xi|^2$ for all $\xi^\alpha \in \mathbb{R}^d$, where $|\xi|^2 = \sum_{\alpha=1}^{d'} |\xi^\alpha|^2$.

Then the equation: $Lu = f$ in Ω , $u = 0$ on $\partial\Omega$ with $f \in L^2(\Omega; \mathbb{R}^{d'})$ (or $f \in H^{-1}(\Omega; \mathbb{R}^{d'})$) is uniquely solvable. Moreover there is a constant C independent of u such that

$$\|u\|_{H^1(\Omega; \mathbb{R}^{d'})} \leq C\|f\|_{L^2(\Omega; \mathbb{R}^{d'})} \text{ (or } \leq C\|f\|_{H^{-1}(\Omega; \mathbb{R}^{d'})}).$$

D A short proof of the failure of PINN in 1-d

To fix ideas and to understand the failure example of PINN given in Section 2.3, we provide in this appendix a succinct explanation to the failure phenomenon with one-dimensional setting $\Omega = (-1, 1)$. More general results and the complete analysis for the case of higher dimensional problem are given in the main text.

Assumption D.1 (uniform ellipticity condition and piece-wise continuous coefficients). Assume there are constants $0 < \lambda < \Lambda$ satisfying $\lambda \leq A(x) \leq \Lambda$ for all $x \in \Omega$ and

$$A(x) = \bar{a}(x) + \sum_{k=1}^{n_{\text{jump}}} a_k H(x - j_k),$$

where \bar{a} is an absolutely continuous function on Ω , weights $a_k \in \mathbb{R}$, and discontinuities $\{j_k\}_{k=1}^{n_{\text{jump}}} \subseteq \Omega$ for $n_{\text{jump}} \in \mathbb{N}^+$. Here H is the Heaviside step function.

As the general case in the main text, we introduce the modified problem:

$$\begin{cases} -(\bar{a}D_x^2 u + (D_x \bar{a})D_x u) = f & \text{in } \Omega, \\ u(\pm 1) = 0. \end{cases} \quad (\text{D.1})$$

and denote its solution as $\tilde{u} \in H_0^1(\Omega) \cap H^2(\Omega)$. The existence and regularity are guaranteed by Theorem 5.1 in the general setting.

The following proposition shows that the original operator L maps \tilde{u} to the RM-transformed data $f - \sum_{k=1}^{n_{\text{jump}}} a_k D_x \tilde{u}(j_k) \delta_{j_k}$. Thus it is clear that the latter equals f if and only if $D_x \tilde{u}$ vanishes at all jump points j_k .

Proposition D.1 (representation by RM-transformed data for 1-d linear elliptic equation). Suppose that Assumption D.1 holds and $f \in L^2$. Let \tilde{u} be the solution to problem (D.1). Then \tilde{u} is the weak solution to

$$\begin{cases} L\tilde{u} = f - \sum_{k=1}^{n_{\text{jump}}} a_k D_x \tilde{u}(j_k) \delta_{j_k} & \text{in } \Omega, \\ \tilde{u}(\pm 1) = 0, \end{cases} \quad (\text{D.2})$$

where δ_{j_k} is the Dirac measure satisfying $\langle \delta_{j_k}, \varphi \rangle = \delta_{j_k}(\varphi) = \varphi(j_k)$ for any $\varphi \in H_0^1(\Omega)$.

Proof. Without loss of generality, we assume that $j_k < j_{k'}$ if $1 \leq k < k' \leq n_{\text{jump}}$, and set $j_0 = -1$, $j_{n_{\text{jump}}+1} = 1$. The solution $\tilde{u} \in H^2(\Omega)$ implies that $D_x \tilde{u} \in C(\Omega)$ and $AD_x \tilde{u} \in H^1((j_k, j_{k+1}))$ for $k = 0, \dots, n_{\text{jump}}$. Using Lebesgue integral theorem, we have

$$\int_{j_k}^{j_{k+1}} D_x(AD_x \tilde{u}) \varphi \, dx + \int_{j_k}^{j_{k+1}} AD_x \tilde{u} D_x \varphi \, dx = AD_x \tilde{u} \varphi \Big|_{j_k^+}^{j_{k+1}^-}, \quad k = 0, \dots, n_{\text{jump}},$$

where

$$AD_x \tilde{u} \varphi \Big|_{j_k^+}^{j_{k+1}^-} = \lim_{\varepsilon \rightarrow 0} [A(j_{k+1} - \varepsilon) D_x \tilde{u}(j_{k+1} - \varepsilon) \varphi(j_{k+1} - \varepsilon) - A(j_k + \varepsilon) D_x \tilde{u}(j_k + \varepsilon) \varphi(j_k + \varepsilon)].$$

Since there is no jump discontinuity of $A(x)$ for $x \in \Omega \setminus \{j_k\}_{k=1}^{n_{\text{jump}}}$, we have $-D_x(AD_x\tilde{u}) = f$ on (j_k, j_{k+1}) and

$$\int_{j_k}^{j_{k+1}} AD_x\tilde{u}D_x\varphi \, dx = \int_{j_k}^{j_{k+1}} f\varphi \, dx + AD_x\tilde{u}\varphi \Big|_{j_k}^{j_{k+1}}, \quad \forall \varphi \in H_0^1(\Omega).$$

Thus the proof is completed by the following calculation

$$\begin{aligned} \int_{-1}^1 (AD_x\tilde{u})D_x\varphi \, dx &= \sum_{k=0}^{n_{\text{jump}}} \int_{j_k}^{j_{k+1}} AD_x\tilde{u}D_x\varphi \, dx = \sum_{k=0}^{n_{\text{jump}}} \int_{j_k}^{j_{k+1}} f\varphi \, dx + AD_x\tilde{u}\varphi \Big|_{j_k^+}^{j_{k+1}^-} \\ &= \int_{-1}^1 f\varphi \, dx - \sum_{k=1}^{n_{\text{jump}}} a_k D_x\tilde{u}(j_k) \langle \delta_{j_k}, \varphi \rangle. \end{aligned}$$

□

Next we describe the gap between u and \tilde{u} in terms of the L^2 norm. As in the main text, we will show this is non-zero.

Proposition D.2 (deviation occurs for 1-d linear elliptic equation). *Suppose that Assumption D.1 holds and $f \in L^2(\Omega)$. Let u and \tilde{u} be the solution to the problem (2.8) and (D.1), respectively. If there exists $k \in \{1, \dots, n_{\text{jump}}\}$ such that $D_x\tilde{u}(j_k) \neq 0$, then we have that:*

$$\|u - \tilde{u}\|_{L^2(\Omega)} > 0.$$

The existence and regularity are guaranteed by Theorem C.1 in a more general setting.

Proof. By Theorem D.1, we have

$$L(u - \tilde{u}) = f - L\tilde{u} = \sum_{k=1}^{n_{\text{jump}}} a_k D_x\tilde{u}(j_k) \delta_{j_k}.$$

Without loss of generality, we can choose some function $\varphi \in C_c^\infty(\Omega)$ such that $\varphi(j_k) = 1$ and $\varphi(a_{k'}) = 0$ for $k' \in \{1, \dots, n_{\text{jump}}\} \setminus \{k\}$ and $\|\varphi\|_{H^1(\Omega)} > 0$.

Since there are $0 < \lambda < \Lambda$ such that $\lambda \leq A(x) \leq \Lambda$ for all $x \in \Omega$, we have

$$\begin{aligned} \Lambda \|D_x u - D_x \tilde{u}\|_{L^2(\Omega)} \|\varphi\|_{H^1(\Omega)} &\geq \left| \int_{-1}^1 (AD_x(u - \tilde{u}))D_x\varphi \, dx \right| \\ &= \left| \int_{-1}^1 L(u - \tilde{u})\varphi \, dx \right| = |a_k D_x\tilde{u}(j_k)| > 0. \end{aligned}$$

This implies $\|u - \tilde{u}\|_{L^2(\Omega)} > 0$.

□

Acknowledgements

This work is sponsored by the National Key R&D Program of China Grant No. 2022YFA1008200 (T. L.), the National Natural Science Foundation of China Grant No. 12101401 (T. L.), Shanghai Municipal Science and Technology Key Project No. 22JC1401500 (T. L.), Shanghai Municipal of Science and Technology Major Project No. 2021SHZDZX0102, and the HPC of School of Mathematical Sciences and the Student Innovation Center, and the Siyuan-1 cluster supported by the Center for High Performance Computing at Shanghai Jiao Tong University. The authors thank Yingzhou Li and Zhi-Qin John Xu for helpful discussions.

References

- [1] W. E, J. Han and A. Jentzen, Deep learning-based numerical methods for high-dimensional parabolic partial differential equations and backward stochastic differential equations, *Commun. Math. Stat.*, 5(4):349-380, 2017.
- [2] W. E and B. Yu, The Deep Ritz method: A deep learning-based numerical algorithm for solving variational problems, *Commun. Math. Stat.*, 6(1):1-12, 2018.
- [3] J. He, L. Li, J. Xu, and C. Zheng, ReLU deep neural networks and linear finite elements, *J. Comput. Math.*, 38(3):502-527, 2020.
- [4] X. A. Li, Z. Q. J. Xu, and L. Zhang, A multi-scale DNN algorithm for nonlinear elliptic equations with multiple scales, *Commun. Comput. Phys.*, 28(5):1886-1906, 2020.
- [5] Z. Liu, W. Cai, and Z. Q. J. Xu, Multi-scale deep neural network (MscaledDNN) for solving poisson-boltzmann equation in complex domains, *Commun. Comput. Phys.*, 28(5):1970-2001, 2020.
- [6] M. Raissi, P. Perdikaris, and G. E. Karniadakis, Physics-informed neural networks: A deep learning framework for solving forward and inverse problems involving nonlinear partial differential equations, *J. Comput. Phys.*, 378:686-707, 2019.
- [7] L. Zhang, T. Luo, Y. Zhang, Z. Q. J. Xu, and Z. Ma, MOD-Net: A machine learning approach via model-operator-data network for solving PDEs, *Commun. Comput. Phys.*, 32(2):299-335, 2022.
- [8] J. Han, A. Jentzen, and W. E, Solving high-dimensional partial differential equations using deep learning, *Proc. Natl. Acad. Sci. U.S.A.*, 115(34):8505-8510, 2018.
- [9] Z. Li and K. Ito, The immersed interface method: numerical solutions of PDEs involving interfaces and irregular domains, *Society for Industrial and Applied Mathematics*, 2006.
- [10] S. Osher, R. Fedkiw, and K. Piechor, Level set methods and dynamic implicit surfaces, *Appl. Mech. Rev.*, 57(3):B15, 2004.
- [11] S. Osher and J. A. Sethian, Fronts propagating with curvature-dependent speed: Algorithms based on hamilton-jacobi formulations, *J. Comput. Phys.*, 79(1):12-49, 1988.
- [12] C. S. Peskin, Flow patterns around heart valves: a numerical method, *J. Comput. Phys.*, 10(2):252-271, 1972.
- [13] C. S. Peskin, The immersed boundary method, *Acta Numer.*, 11:479-517, 2002.

- [14] J. A. Sethian, Level set methods and fast marching methods: evolving interfaces in computational geometry, fluid mechanics, computer vision, and materials science, volume 3, Cambridge university press, 1999.
- [15] H. Lee and I. S. Kang, Neural algorithm for solving differential equations, *J. Comput. Phys.*, 91(1):110–131, 1990.
- [16] J. Sirignano and K. Spiliopoulos, DGM: A deep learning algorithm for solving partial differential equations, *J. Comput. Phys.*, 375:1339–1364, 2018
- [17] Y. Liao and P. Ming, Deep Nitsche method: Deep Ritz method with essential boundary conditions, *Commun. Comput. Phys.*, 29(5):1365–1384, 2021.
- [18] L. Lu, X. Meng, Z. Mao, and G. E. Karniadakis, DeepXDE: A deep learning library for solving differential equations, *SIAM Rev.*, 63(1):208–228, 2021.
- [19] Y. Zang, G. Bao, X. Ye, and H. Zhou, Weak adversarial networks for high-dimensional partial differential equations, *J. Comput. Phys.*, 411:109409, 2020.
- [20] S. Cai, Z. Mao, Z. Wang, M. Yin, and G. E. Karniadakis, Physics-informed neural networks (PINNs) for fluid mechanics: a review, *Acta Mech. Sin.*, 37, 01 2022.
- [21] Z. K. Lawal, H. Yassin, D. T. C. Lai, and A. Che Idris, Physics-informed neural network (PINN) evolution and beyond: A systematic literature review and bibliometric analysis, *Big Data and Cogn. Comput.*, 6(4), 2022.
- [22] S. Goswami, A. Bora, Y. Yu, and G. E. Karniadakis, Physics-informed deep neural operator networks, *Comput. Methods Eng. Sci.*, 2023.
- [23] Z. Li, N. Kovachki, K. Azizzadenesheli, B. Liu, K. Bhattacharya, A. Stuart, and A. Anandkumar, Neural operator: Graph kernel network for partial differential equations, arXiv preprint arXiv:2003.03485, 2020.
- [24] Z. Li, N. Kovachki, K. Azizzadenesheli, B. Liu, K. Bhattacharya, A. Stuart, and A. Anandkumar, Fourier neural operator for parametric partial differential equations, *Int. Conf. Learn. Represent.*, 2021.
- [25] L. Lu, P. Jin, and G. E. Karniadakis, DeepONet: Learning nonlinear operators for identifying differential equations based on the universal approximation theorem of operators, arXiv preprint arXiv:1910.03193, 2019.
- [26] G. Cybenko, Approximation by superpositions of a sigmoidal function, *Math. Control Signals Syst.*, 2(4):303–314, 1989.
- [27] Y. Jiao, Y. Lai, D. Li, X. Lu, Y. Wang, and J. Z. Yang, A rate of convergence of physics informed neural networks for the linear second order elliptic PDEs, *Commun. Comput. Phys.*, 31(4):1272–1295, 2022.
- [28] Y. Lu, J. Lu, and M. Wang, A priori generalization analysis of the deep Ritz method for solving high dimensional elliptic partial differential equations, *Conference on Learning Theory*, 3196–3241, 2021.
- [29] S. Mishra and R. Molinaro, Estimates on the generalization error of physics-informed neural networks for approximating PDEs, *IMA J. Numer. Anal.*, 43(1):1–43, 2022.
- [30] Y. Shin, J. Darbon, and G. E. Karniadakis, On the convergence of physics informed neural networks for linear second-order elliptic and parabolic type PDEs, *Commun. Comput. Phys.*, 28(5):2042–2074, 2020.

- [31] Q. Hong, J. W. Siegel, and J. Xu, A priori analysis of stable neural network solutions to numerical PDEs, arXiv preprint arXiv:2104.02903, 2022.
- [32] S. Basir, Investigating and mitigating failure modes in physics-informed neural networks (PINNs), *Commun. Comput. Phys.*, 33(5):1240–1269, 2023.
- [33] A. Krishnapriyan, A. Gholami, S. Zhe, R. Kirby, and M. W. Mahoney, Characterizing possible failure modes in physics-informed neural networks, *Adv. Neural Inf. Process. Syst.*, 34:26548–26560, 2021.
- [34] Z. Chen, J. Lu, and Y. Lu, On the representation of solutions to elliptic PDEs in Barron spaces, *Adv. Neural Inf. Process. Syst.*, 2021.
- [35] M. Münzer and C. Bard, A curriculum-training-based strategy for distributing collocation points during physics-informed neural network training, *Adv. Neural Inf. Process. Syst.*, 2022.
- [36] C. Wu, M. Zhu, Q. Tan, Y. Kartha, and L. Lu, A comprehensive study of non-adaptive and residual-based adaptive sampling for physics-informed neural networks, *Comput. Methods Appl. Mech. Eng.*, 403:115671, 2023.
- [37] Z. Cai, J. Chen, M. Liu, and X. Liu, Deep least-squares methods: An unsupervised learning-based numerical method for solving elliptic PDEs, *J. Comput. Phys.*, 420:109707, 2020.
- [38] T. Luo and Q. Zhou, On residual minimization for PDEs: Failure of PINN, modified equation, and implicit bias, arXiv preprint arXiv:2310.18201, 2023.
- [39] Y. Shin, Z. Zhang, and G. E. Karniadakis, Error estimates of residual minimization using neural networks for linear PDEs, arXiv preprint arXiv:2010.08019, 2020.
- [40] W. E, C. Ma, and L. Wu, A priori estimates of the population risk for two-layer neural networks, *Commun. Math. Sci.*, 17:1407–1425, 01 2019.
- [41] T. Luo, Z. Ma, Z. Q. J. Xu, and Y. Zhang, Theory of the frequency principle for general deep neural networks, arXiv preprint arXiv:1906.09235, 2019.
- [42] Z. Q. J. Xu, Y. Zhang, T. Luo, Y. Xiao, and Z. Ma, Frequency principle: Fourier analysis sheds light on deep neural networks, *Commun. Comput. Phys.*, 28(5):1746–1767, 2020.
- [43] Z. Q. J. Xu, Y. Zhang, and Y. Xiao, Training behavior of deep neural network in frequency domain, *Adv. Neural Inf. Process. Syst.*, pages 264–274, 2019.
- [44] Y. Zhang, T. Luo, Z. Ma, and Z. Q. J. Xu, A linear frequency principle model to understand the absence of overfitting in neural networks, *Chin. Phys. Lett.*, 38(3):038701, 2021.
- [45] D. Gilbarg and N. S. Trudinger, *Elliptic partial differential equations of second order*, Springer Berlin, Heidelberg, 2001.
- [46] L. Ambrosio, A. Carlotto, and A. Massaccesi, *Lectures on elliptic partial differential equations*, Edizioni della Normale Pisa, 2018.
- [47] L. Ambrosio, N. Fusico, and D. Pallara, *Functions of bounded variation and free discontinuity problems (Oxford Mathematical Monographs)*, *Bulletin of the London Mathematical Society*, 33(4), 2001.
- [48] F. Lin and X. Yang, *Geometric measure theory: An introduction*, International Press of Boston, Inc, 2002.
- [49] J. Lu, Z. Shen, H. Yang, and S. Zhang, Deep network approximation for smooth functions, *SIAM J. Math. Anal.*, 53(5):5465–5506, 2021.